UQAC
Université du Québec
à Chicoutimi

Development of a damage simulator for seismic vulnerability assessment of electrical installations

By

Vahid Hosseinpour

Under supervision of Prof. Ali Saeidi and co-supervision of Prof. Marie-José Nollet and Dr. Miroslav Nastev

Thesis presented to the University of Quebec at Chicoutimi with a view to obtaining the degree of Doctor of Philosophy (PhD) in engineering (Civil)

Defended on 22th November, 2023

BOARD OF EXAMINERS:

Professor Mathieu Fiset, Department of Applied Sciences at UQAC, President of the Board

Professor Mamadou Fall, Department of Civil Engineering at University of Ottawa, External Member of the Board

Doctor Rama Vara Prasad Chavali, Velagapudi Ramakrishna Siddhartha Engineeering College, External Member of the Board Professor

Ali Saeidi, Department of Applied Sciences at UQAC, Internal Member of the Board

Professor Marie-José Nollet, Department of Construction Engineering at ÉTS, Internal Member of the Board

Doctor Miroslav Nastev, Geological Survey of Canada (Quebec City), Internal Member of the Board

Québec, Canada

RÉSUMÉ

Ces dernières années, les pertes sismiques augmentent en termes d'ampleur et de fréquence, affectant ainsi gravement les sociétés et les économies. L'augmentation des pertes sismiques est principalement due à la croissance rapide des infrastructur et de la population dans les zones à risque sismique à travers le monde. Les récents séismes ont révélé la vulnérabilité des réseaux électriques aux événements sismiques. Cette thèse a pour but de développer un simulateur de dommages pour évaluer la vulnérabilité sismique des pylônes et des postes de transmission. Ce simulateur combine trois composantes majeures : l'aléa sismique comprenant les conditions locales du site, l'inventaire des pylônes, des postes exposés et leurs vulnérabilités respectives. Tout d'abord, une revue critique des méthodes existantes d'analyse des risques sismiques et des logiciels est réalisée afin d'identifier les paramètres importants dans le développement du simulateur de dommages. Les avantages et les inconvénients de chaque logiciel sont mis en évidence. Le processus de calcul débute par la sélection et le calcul des paramètres d'entrée déterministes ou probabilistes de l'aléa sismique, ainsi que l'évaluation des effets du site. Une étape crucial dans le développement de ce simulateur de dommages est l'intégration des impacts des conditions géologiques et géotechniques locales. Les valeurs de la vitesse de cisaillement (Vs) sur les 30 premiers mètres (Vs_{30}) et souvent la période fondamentale du site (T_0) sont ensuite utilisées comme des indicateurs de l'amplification potentielle. Étant donné que les incertitudes liées aux propriétés locales des sols affectent inévitablement la réponse sismique du site, une approche stochastique pour évaluer $Vs30$ et T_0 est également proposée. Cette approche tient compte des combinaisons de corrélations probabilistes de Vs-profondeur avec un modèle géologique tridimensionnel probabiliste. Des simulations avec la méthode statistique de Monte-Carlo sont également appliquées afin d'étudier l'impact des incertitudes sur le modèle de caractérisation sismique du site. L'application utilise des logiciels open-source sans aucun coût financier pour les utilisateurs. Les accélérations spectrales à la période fondamentale de vibration des pylônes de transmission et accélération maximale du sol pour les postes électriques sont considérées comme les mesures d'intensité (IMs) pour évaluer la secousse sismique transitoire. Le processus d'évaluation probabiliste intègre les incertitudes associées aux paramètres d'aléa sismique. L'incertitude épistémique est traitée à l'aide de l'approche d'arbre logique introduite dans la dernière édition du Code national du bâtiment du Canada (NBCC2020), tandis que l'incertitude aléatoire est prise en compte grâce à l'analyse statistique de Monte Carlo. La variabilité de la mesure des dommages est capturée grâce à l'application de la méthode MC aux états de dommages de la structure de la tour, alors qu'elle est soumise aux IMs appliquées. Pour démontrer l'efficacité du logiciel développé, un exemple de caractérisation du site sismique, d'évaluation de l'aléa et d'analyse de la vulnérabilité est présenté pour les pylônes et les postes de transmission électrique d'Hydro-Québec dans la région du Saguenay, au Canada. Cette étude de cas illustre l'application pratique de la méthodologie proposée.

Mots clés: Évaluation du risque sismique, pylônes de transmission électrique, logiciel d'estimation des pertes, danger probabiliste, caractérisation probabiliste du site, méthode de Monte-Carlo.

ABSTRACT

Over recent years, seismic losses are increasing in terms of magnitude and frequency, thereby severely affecting societies and economies. The increase in seismic losses is mainly due to the rapid growth of exposure and population in earthquake-prone areas worldwide. Recent earthquakes revealed the vulnerability of electric power networks to seismic events. To assess the seismic vulnerability of transmission towers and substations, a user-friendly damage simulator that combines three major components, namely, seismic hazard including local site conditions, inventory of exposed towers, substations and respective vulnerabilities, is developed in this thesis. Firstly, a critical review of existing methods for seismic risk analysis and software is conducted to determine important parameters in the development of the damage simulator. Then, the main advantages and inconveniences of each software are highlighted. The computation starts with the selection and calculation of the deterministic or probabilistic seismic hazard input parameters and the evaluation of the site effects. A major step in the development of this damage simulator is incorporating the effects of local geological and geotechnical conditions. The shear wave velocity (V_s) of the top 30 m (Vs_{30}) and often the fundamental site period (T_0) are then used as predictors of potential amplification. Recognizing that the uncertainties of local soil properties inevitably affect the seismic site response, a stochastic approach for evaluating $Vs30$ and T_0 is proposed, considering a combination of probabilistic V_s–depth correlations with a probabilistic 3D geological model. Monte Carlo (MC) simulations are applied to study the influence of the uncertainties on the seismic site characterization model. The application uses open-source software without any financial cost to users. The computation starts with the selection and calculation of the deterministic or probabilistic seismic hazard input parameters and the evaluation of the site effects. Spectral accelerations at the fundamental period of vibration of transmission towers and peak ground acceleration for substations are considered as the intensity measures (IMs) of the transitory seismic shaking. The probabilistic assessment incorporates uncertainties of the hazard parameters. The epistemic uncertainty is addressed through the logic tree approach introduced in the latest National Building Code of Canada (NBCC2020), whereas the aleatory uncertainty is captured by enabling the MC analysis option. The variability in the damage measure is captured through the application of the MC method to the damage states of the electrical installation structure as it is subjected to the applied IMs. To illustrate the effectiveness of the developed software, an example of seismic site characterization, hazard assessment, and vulnerability analysis of electric transmission installations of Hydro-Quebec in the Saguenay region, Canada, is presented.

Keywords: seismic risk assessment, electric transmission towers, loss estimation software, probabilistic hazard, probabilistic site characterization, Monte -Carlo method

TABLE OF CONTENTS

LIST OF TABLES

LIST OF FIGURES

LIST OF SYMBOLS

β_{Sds} :	total logarithmic standard deviation	k:	number of adjacent intervals
$\beta_{M\ (Sds)}$:	model variability	Nj:	number of X_i's in the j^{th} interval
β_C:	log normal standard deviation	$Sa\ (0.3s)$:	spectral acceleration for a period of 0.3 seconds
β_D:	ground motion demand spatial variability uncertainty	$Sa\ (1.0s)$:	spectral acceleration for a period of 1 seconds
$\bar{S}_{d,Sds}$:	median spectral displacement for the damage state ds	Sa_T :	spectral accelerations for selected vibration periods of interest
σ_{till}:	standard deviation of V_s for till units	T_0:	fundamental site period
$\hat{\chi}^2$:	chi-square test statistics	V_s:	shear wave velocity
h_S:	thicknesses of the sand units within the soil column	Vs_{30}:	V_s of the top 30 m
h_c :	thicknesses of the clay units within the soil column	$V_{S_{avg}}$:	average shear wave velocity
h_{till} :	thicknesses of the till units within the soil column	V_{Si} :	randomised variable of V_s in the ith block
H:	total thickness of soil column	V_{Still} :	shear wave velocities of the glacial sediments
h_i :	thickness of each soil block	V_{Srock}:	shear wave velocities of bedrock

LIST OF ABBREVIATIONS

ASCII:	American Standard Code for Information Interchange	MC:	Monte-Carlo
CAPRA:	Comprehensive Approach to Probabilistic Risk Assessment	MMI:	Modified Mercalli Intensity
CONV:	Convolution	NBCC:	National Building Code of Canada
CP:	Collapse prevention state	NEHRP:	National Earthquake Hazards Reduction Program
CPT:	Cone penetration test	NGA:	Next Generation Attenuation
CRM:	Consequence-based Risk Management	NORSAR:	Norwegian Seismic Array
CSM:	Capacity Spectrum Method	NRML:	Natural Risk Markup Language
CSV:	Comma separated version	OOFIMS:	Object-oriented Framework for Infrastructure Modelling and Simulation
DC:	Damage control	OQ:	OpenQuake Engine software
DBELA:	Displacement-based earthquake loss assessment		
DSHA:	Deterministic Seismic Hazard Assessment	PAGER:	Prompt Assessment of Global Earthquakes for Response
ER2:	Rapid Risk Evaluator	PEB:	Probabilistic event-based
EQRM:	EarthQuake Risk Model	PGA:	Peak Ground Acceleration
FEMA:	Federal Emergency Management Agency	PSHA:	Probabilistic seismic hazard analysis
GEM:	Global Earthquake Model	QGIS:	Quantum Geographic Information System
GIS:	Geographic Information System	SCPT:	Seismic Cone Penetration Test
GMPE:	Ground Motion Prediction Equation	SELENA:	Seismic Loss Estimation using a Logic Tree Approach
GUI:	Graphical User Interface	SES:	Stochastic Event Set
HAZUS:	Hazard US	SIS:	Sequential Indicator Simulation
IBC-2006:	International Building Code 2006		
ICG:	International Centre for Geohazards	SLE:	Seismic Loss Estimation
IM:	Intensity Measures	SLSJ:	Saguenay Lac Saint-John
ISDR:	Inter-segment drift ratio	UN:	United Nations
ITB:	Institut Teknologi Bandung	USGS:	United States Geological Survey
MATLAB:	Matrix Laboratory	XML:	Extensible Markup Language

DEDICATION

I dedicate this thesis to my beloved family whose unwavering support and encouragement have been vital throughout my academic journey. Their love and belief in my abilities have motivated me to overcome challenges during this research endeavor.

ACKNOWLEDGMENTS

I would like to extend my heartfelt gratitude to Prof. Ali Saeidi, my research supervisor, for his unwavering trust, continuous support, and genuine care throughout my PhD journey. Working under his supervision has been an immensely enjoyable experience, and I am truly grateful for the opportunities he has provided me.

I would also like to express warm appreciation to my co-supervisors, Prof. Marie-Jose Nollet and Dr. Mirosalv Nastev, for their valuable support and kindness. Their guidance has been instrumental in shaping both my scientific and ethical understanding, and I am thankful for the knowledge I have gained through their mentorship.

To the members of my committee, Prof. Duygu Kocaefe, Prof. Mamadou Fall, and Prof. Mathieu Fiset am Dr. Rama Vara Prasad. I am deeply grateful for their invaluable guidance and unwavering support. Their insights and expertise have greatly contributed to the development and refinement of my research.

Lastly, I would like to sincerely thank my family and friends for their endless love and unwavering support throughout my academic journey. Their presence and encouragement have been a constant source of motivation, and I am truly grateful for their belief in me.

CHAPTER 1

INTRODUCTION

1.1 STATEMENT OF THE PROBLEM

Earthquakes represent a major natural hazard that affects lives and built environment in seismic-prone areas worldwide and leads to social and economic losses. Over the past few decades, there has been a notable rise in seismic losses observed in areas susceptible to earthquakes [1]. The process of evaluating seismic risk at various levels, including urban, regional, and national, seeks to measure the potential severity and probability of negative effects [2]. This information is essential for both emergency managers and decision-makers to take appropriate actions accordingly. Predicting the negative impacts of earthquakes, known as seismic risk, involves a complex procedure that relies on systematically gathering and analyzing three input parameters: (i) hazard, (ii) existing buildings and infrastructure (exposure), and (iii) their corresponding vulnerabilities [3, 4].

In the last few decades, considerable effort has been made to create an appropriate seismic loss estimation (SLE) software that provides fairly accurate loss estimates, such as Hazard US (HAZUS) [4, 5] and its versions such as Ergo [6], Haz-Taiwan [7], SELENA [8] and HazCan [9], then InaSAFE [10], CAPRA [11], DBELA [12], OpenQuake [13], ER2 web application [14], etc. Clearly, some nations have created their own specialized versions of SLE software, while simultaneously, international initiatives like the Global Earthquake Model (GEM) are working on developing universally applicable tools [13]. The assessment involves determining the seismic hazard either by considering a specific predetermined earthquake scenario (deterministic approach) or by considering a combination of various seismic scenarios with equal probabilities of occurrence (probabilistic approach).

Most of these tools run at urban scales and consider event-based and probabilistic seismic hazard scenarios. To this end, these tools comprise algorithms to generate seismic intensity shake maps involving ground motion prediction equations (GMPEs) and local site effects. Local site effects pertain to the amplification of seismic waves within superficial geological layers [15]. If the geological conditions, such as

the presence of sediments, are unfavorable, the surface ground motion can experience significant amplification. Local site effect is generally applied to loss assessment software by considering the national building codes, e.g. NEHRP [16] for HAZUS and NBCC2015 [17] for ER2 [14], IBC-2006 and EuroCode8 in SELENA. Typically, building codes incorporate site effects by considering the shear wave velocity the top 30 meters of the ground (Vs_{30}). In case of OpenQuake engine, the site effect is considered by direct application of Vs_{30} through GMPEs. In the past decades Vs_{30} was established as the standard soil parameter which correlates with the seismic site effects [18-20]. The provisions of national building codes worldwide generally recommend to account for potential site amplification in the evaluation of the base shear force [17, 21, 22] and often in the ground motion prediction equations (GMPEs), that is, attenuation with distance, as a predictor for the intensity of seismic shaking [23]. Another key site-specific parameter is the fundamental site period (T_0) which represents the natural period of vibration of a site during an earthquake. It varies in direct proportion to the difference between the average shear wave velocity ($\mathrm{V_{Save}}$) of the surface sediments and the soil column thickness [24]. In general, thick soil layers that have higher T_0 value are more susceptible to strong earthquakes that occur at a greater distance and have a predominant low frequency content. On the other hand, regions with lower T_0 tend to amplify the energy content at higher frequencies, which is characteristic of earthquakes that occur at a closer distance[24]. However, the deterministic technique is used by many of the presented software to apply the site effect. These software packages do not account for site parameter uncertainties which have a significant influence on the quantity of the estimated hazard parameter value. Uncertainties related to the local soil properties unavoidably affect the seismic site response and hazard estimates. The typical objective of the modelling exercise should focus on describing and quantifying those uncertainties to allow better informed choices. The spatial variabilities of the soil geological and geotechnical parameters result from different sources of uncertainty [25, 26].

High-voltage electric power transmission networks are parts of the infrastructure that are vulnerable to seismic shaking and ground failures, as evidenced by recent earthquakes, e.g. the 2011 Christchurch earthquake (New Zealand) [27] and the 2023 Turkey–Syria earthquake [28]. Transmission networks consist of transmission towers that support conductive cables (conductors) and insulators, transformation substations and associated facilities. To transport power, electric towers and substations are critical for ensuring reliable electricity transmission [29]. The tower structural system can vary between lattice steel (e.g. waist-type,

double circuit, guyed-V and guyed cross-rope) and tubular structures [30]. Seismic risk assessment tools mostly calculate physical damage and the corresponding economic and social losses. Regardless of the significant advancements, current software packages do not adequately address specific challenges posed by the seismic vulnerability of the electric infrastructure. Simultaneously, a number of studies have analysed the effects of earthquakes on electric infrastructure and provided quantitative assessments of their vulnerability [31-33].

Consideration of uncertainties is a crucial point in risk analysis. Various sources of uncertainty exist in seismic loss assessment procedure (e.g. uncertainty in source characterization, ground motion prediction equations (GMPEs), building or infrastructur inventory and damage functions) [3, 34-36]. These uncertainties provide information on the expected values and likely ranges of an input parameter and then propagate to the risk results. Simplifying risk estimation, these tools are unable to consider all potential sources of uncertainties. Due to lack of sufficient knowledge and difficulties in incorporating and evaluating the potential sources of uncertainty, existing tools generally provide only the deterministic results or partially consider the uncertainties, thereby contributing to variations in the risk results.

After conducting a thorough review [3] of the features of the most widely used seismic risk software, the following drawbacks and potential solutions were identified:

- Uncertainties related to site effects, particularly geological and geotechnical variability, consistently affect hazard and risk estimations. Current seismic risk software lacks explicit integration of 3D geological modelling into risk assessment. Consequently, this simplification introduces uncertainty into damage assessment. Furthermore, the uncertainty of geotechnical parameters (e.g., shear wave velocity) should be taken into consideration in risk assessment software.
- Existing seismic risk software is typically designed for specific regions and limited to assessing the risk for a specific range of infrastructure types. For instance, software like HAZUS focuses on the seismic settings and construction practices of the US. However, these software solutions fail to account for the vulnerability of electrical installations, particularly

power transmission towers and substations. Addressing this gap is a crucial aspect of this research project.

- The majority of existing software packages risk assessment fail to consider a comprehensive range of potential sources of uncertainty. Current probabilistic approaches analyse damage using only a limited number of characteristics and scenarios. To develop a robust probabilistic technique for assessing seismic risk, accounting for various types of uncertainty in risk components is crucial. This approach includes incorporating uncertainties in site parameters, GMPEs and vulnerability functions, which are essential for a realistic probabilistic analysis.
- Regarding the technical capabilities of the damage simulators, several complications need to be considered. These challenges encompass the need for commercial software to execute the code, limited availability of comprehensive documentation, extensive reliance on hardcoded elements and time-consuming algorithms, inflexibility in accommodating user-defined input parameters, demanding preparation and formatting of user-provided input data (e.g., Open-Quake), absence of a user-friendly interface, and restrictions on the types of analyses and output parameters.

1.2 RESEARCH OBJECTIVES

The main objective of the thesis is the development of a damage simulator to assess the seismic vulnerability of electrical installations. The Hydro-Quebec installations in the City of Saguenay are used as a case study. To achieve this primary objective, several specific objectives are accomplished.

a) Developing an algorithm for probabilistic evaluation of the site parameters Vs_{30} and T_0 and respective uncertainties
b) Developing a hazard module that considers what-if event scenario shakemaps, e.g. spatial distributions of peak ground acceleration (PGA) and spectral accelerations (Sa) in selected periods determined with appropriate GMPE, and probabilistic hazard maps for different return periods

c) Selecting and adapting the existing vulnerability functions of electrical towers and substations for the Hydro-Quebec installations to implement them in the damage simulator and to quantify the uncertainties of these functions

d) Developing a deterministic damage simulator by applying deterministic what-if scenario shakemaps (spatial distributions of PGA and Sa)

e) Developing a probabilistic damage simulator considering several scenarios with different occurrence probabilities or several epicentres and different intensity values

1.3 RESEARCH METHODOLOGY

The specific methodology used to achieve the principal and specific objectives of this thesis is briefly illustrated in Fig *1-1*. To identify the components and methodology of the most efficient SLE software, a comprehensive review of literature and existing tools is conducted. This review reveals essential parameters to develop a damage simulator and also highlights the drawbacks of existing methodologies used to develop current damage simulators. Chapter 2 of this thesis presents the findings from this review.

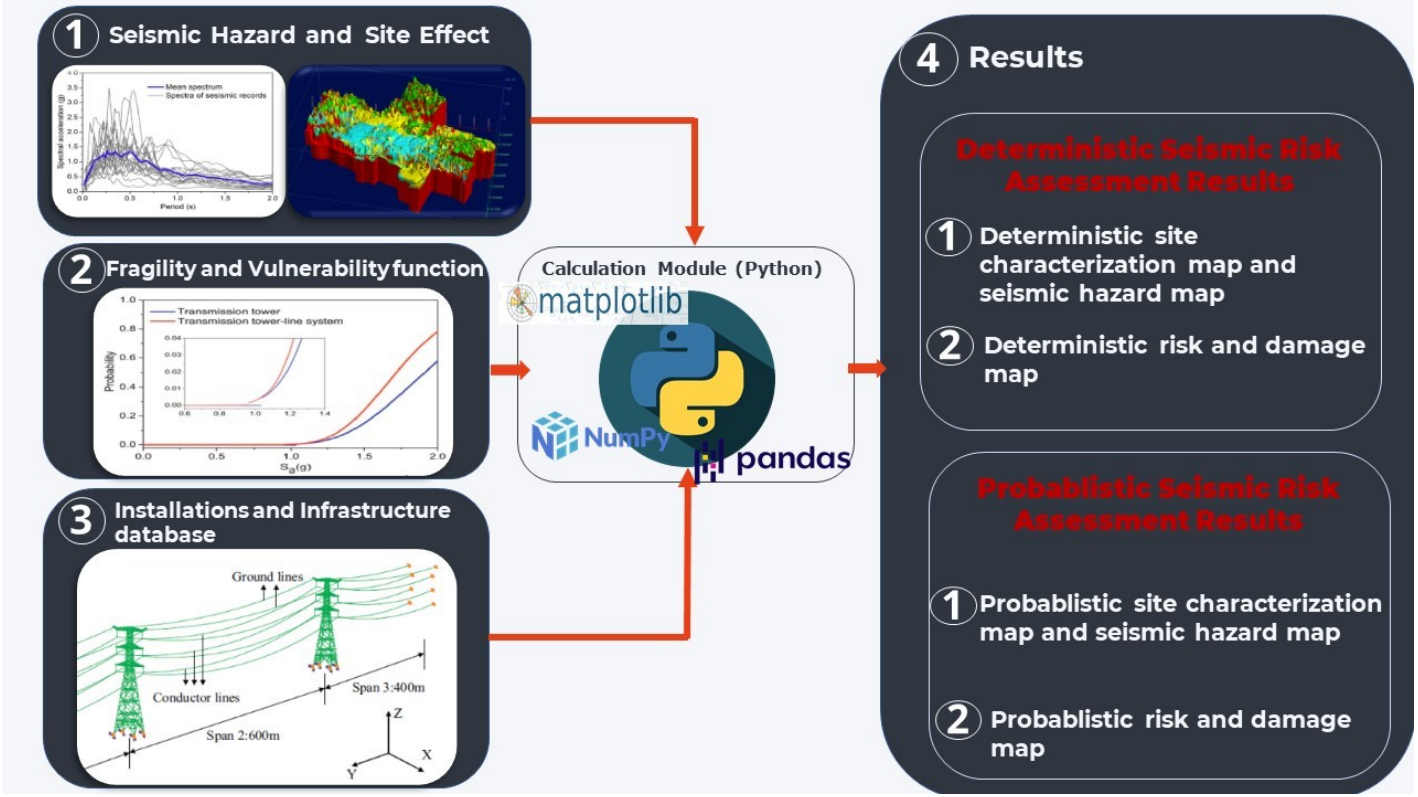

Fig 1-1. Methodology for reaching to the main and subobjectives of this thesis.

1.3.1 Programming language

As a first step, the programming language(s) to be used for the development of the damage simulator needs to be selected. The programming language should be object oriented, platform independent, web enabled and potentially distributed on the Internet. After reviewing the existing software in seismic risk evaluation [3, 37], comparing the different programming languages (e.g. Java, MATLAB, C++, Mathematica and Python) and consulting with the ER2 development team, Python is the preferred programming language for the development of the damage simulator. Python is a high-level, general-purpose programming language that emphasizes code readability with its notable use of substantial whitespace and provides constructs and object-oriented approach to help programmers write a clear, logical code for small- and large-scale projects.

1.3.2 Development of hazard module

The first step in seismic risk assessment is evaluating seismic hazard, which can be determined using probabilistic seismic hazard analysis (PSHA) or deterministic seismic hazard analysis (DSHA), and generally expressed in terms of the spatial distribution of seismic shaking intensity. The potential amplification of ground motion due to local geological and geotechnical conditions is based on the evaluation of seismic site parameters: average shear wave velocity in the top 30 m, Vs_{30} and the fundamental vibration period of the soil column on top of bedrock formations [15]. The intensity of the transitory seismic shaking is of primary focus in the present study because the simulation of induced secondary hazards site effects, such as permanent ground failure (e.g. liquefaction, landslide and lateral spread), is less accurate, time-consuming and reliant on comprehensive field measurements. The standard intensity measures (IMs) of seismic shaking are peak ground acceleration (PGA) and spectral acceleration for selected vibration periods of interest (Sa_T).

1.3.2.1 Site effect module developement

An essential phase of the project is the implementation of a 3D geological model, which can be the base for determining shear wave velocity (V_s) and the thickness of loose deposits. These parameters

are essential for calculating site parameters (i.e. Vs_{30} and T_0), which are crucial for quantifying soil amplification in demand spectra [24]. Current methods use a deterministic approach [19, 38] for considering the amplification factor and ignore the effect of variation in soil type and V_s of subsurface. The setback of using V_s in seismic site characterisation and the assessment of the potential seismic shaking at the urban and regional scales is the number of V_s measurements required to generate results with reasonable accuracy. Knowing that the uncertainties associated with the local soil properties inevitably affect the seismic site response, which otherwise cannot be properly assessed using the conventional deterministic approach, the typical objective of the modelling exercise should focus on describing and quantifying those uncertainties to enable better-informed choices. This approach emphasises the need for a well validated, robust spatial interpolation method that can consider uncertainties in the interpretation of geological units and in the V_s observations. Several methods are available in the literature to address the uncertainties of V_s. Amongst them, the stochastic modeling derives the probability distribution of the random variable from many simulations varying one or more input variables at a time and considers the effects of the coefficients of variation. In this part, a novel MC-based approach is applied to develop the Vs_{30} and T_0 spatial distribution. Fig 1-2 presents the methodology used to develop the probabilistic site parameters calculation module for the damage simulator. A more specific methodology for the development of the site effect module is discussed in Chapter 3 of this thesis.

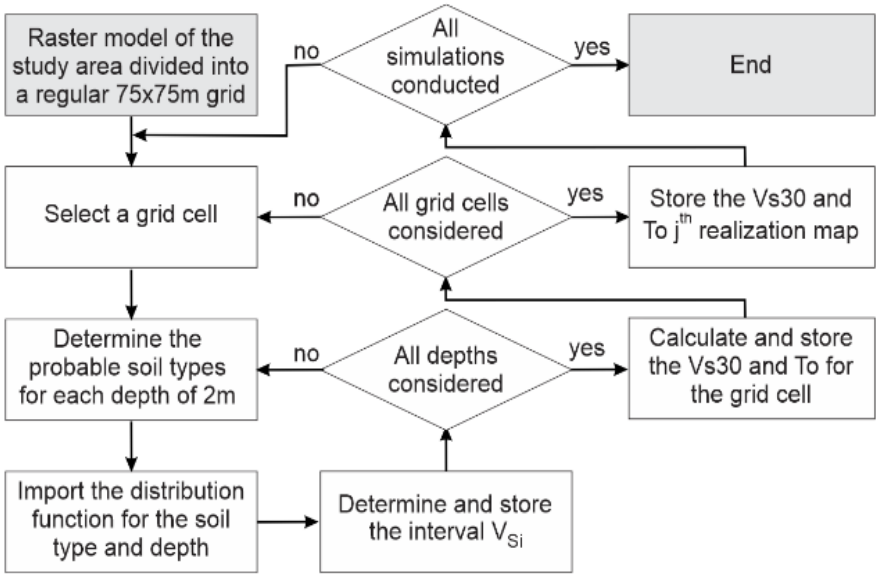

Fig 1-2. Flow chart of the Monte Carlo simulation process for site parameters calculation.

1.3.2.2 Hazard assessment

The damage to different types of infrastructure components exposed to a seismic scenario is assessed by applying the respective vulnerability functions for a given hazard intensity at that location. Two different approaches are necessary to develop the hazard module as summarized as below:

▪Deterministic scenario: A what-if event scenario is created, where a single-scenario earthquake is simulated for given magnitude, coordinates and depth of the hypocentre. To prevent creating an unrealistic scenario, these parameters must be aligned with the sixth hazard model of Canada. The seismic source is modelled as a point source and the central point on the fault where the slip occurs and from which the whole earthquake elastic energy is emitted radially. The triggered seismic waves propagate through the complex crustal structure of the earth (body waves) or near the surface (surface waves) and scatter and attenuate on their way towards the studied location. The ground motion model (GMM) introduced in the sixth hazard model of Canada [39] is applied to calculate the seismic ground motion intensity (e.g. PGA, Sa) for reference site conditions including the characteristics of the source and the path effects. Damage assessment can also be performed considering applicable GMPEs for

Eastern North America (e.g. NGA-East-13 or AA13) to evaluate the GMPE selection effect in damage assessment. Once the seismic waves arrive below the location, the vertically propagating horizontal V_ss are affected by the local site effects. This outcome is accounted for applying the respective deterministic value of the site amplification factors to the reference ground motion.

▪Probabilistic scenario: The probabilistic seismic hazard analysis (PSHA) approach quantifies the probability of exceedance (rate) of various ground-motion levels at the study areas given all possible earthquakes. The recent developed sixth-generation hazard model proposed for application in NBCC 2020 is considered. Two considerable changes are noted in the GMM: i) adoption of modern GMMs, together with a classical weighted-GMM approach replacing most of the three-branch representative suites used in NBCC2015, and ii) direct calculation of hazard on various site classes using representative Vs_{30} values, rather than the provision of hazard values on a reference site Class C site and then applying amplification factors F(T). Regarding this innovation in the latest hazard model, different scenarios for Vs_{30} values can be generated considering the distribution of Vs_{30} and the calculation hazard at the site by applying the new method. In both cases, site amplification factors are applied in accordance with the local site conditions. The results consist of representative shakemaps for PGA and Sa for different return periods.

Different uncertainties in seismic risk assessment are considered in the hazard module. Uncertainties in the 3D geological model that affect seismic microzonation (i.e. probability of occurrence of different site classes) are incorporated into the damage simulator. Furthermore, uncertainty in GMPEs provided by the latest the hazard model is incorporated into the damage simulator. In order to include all uncertainties in hazard assessment process a new multi-scenario method based on monte carlo method is developed. The flowchart of this method is present in Fig 1-3.

Detailed methodology for the development of the hazard module of the damage simulator is discussed in Chapter 4.

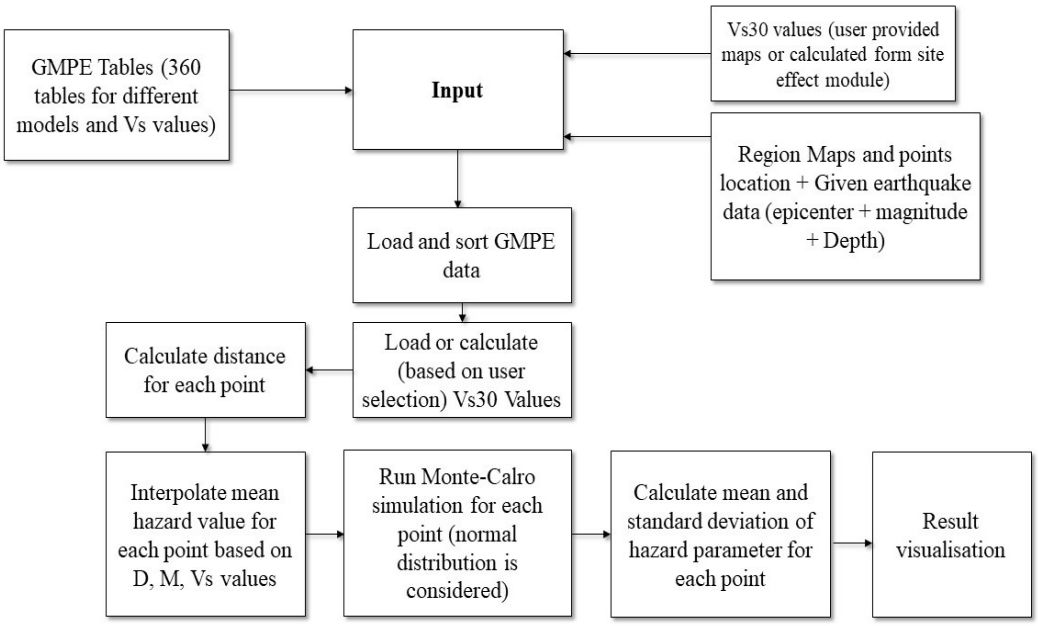

Fig 1-3. Monte Carlo approach for generation of spatial distribution of seismic IMs (Shakemaps).

1.3.3 Vulnerability analysis

The next step consists of: (1) inventory of the considered electrical installations (transmission towers and substatios) exposed to the seismic hazard scenarios (exposure), and (2) the selection of representative fragility functions [3]. Fragility functions correlate the probability of exceeding thresholds for different damage states ranging from none to complete damage with a given level of shaking intensity. They are defined as lognormal functions of damage with mean values at 50% damage and standard deviations generally in the order of 0.7–0.8. Fragility functions, which are intended mostly for use in urban and regional risk assessments, are representative for a group of structures with similar dynamic response characteristics. They are generated based on field observations of damage, analytical studies, expert judgment or a combination of these approaches, and the chosen method depends on the type, frequency and quality of available data, expertise, resources and the size of the study area.

Although a number of studies have focused on fragility functions for most common structures (e.g. buildings and bridges), there is no existing taxonomy developed specifically for the seismic fragility of electrical installations. A comprehensive literature review was conducted to select appropriate vulnerability functions representative for transmission towers in the Saguenay region [40]. Hydro-Québec data from three transmission tower types are analyzed to select fragility functions related to their diameters.

Electrical substations make part of standard electric power transmission and distribution systems that transform voltage from high to low. Herein, the fragility curves developed for HAZUS, the standard seismic risk assessment tool developed by the US Federal Emergency Management Agency[41] are used to determine the five damage states: none, slight, moderate, extensive, and complete, which can be attained during a strong seismic shaking. In case of substations, which contain many diferrent components, these damage states determine the percentage of subcomponents that suffered damage. The detailed vulnerability analysis methodology and inventory of installation are discussed in Chapter 4 of this thesis.

1.3.4 Damage computation

The damage calculation workflows within the software are composed of multiple individual calculators. Several parameters must be defined before running any of these workflows. These parameters include the geographic coordinates of the region of interest, the type of calculations being performed, the path to the input files and the specific results that must be produced. In addition, certain parameters are necessary for hazard calculations and must be specified in advance. By defining these parameters beforehand, the software can accurately and efficiently calculate seismic risks and potential damages associated with seismic events in a given region. This level of customisation and control is crucial for providing useful and reliable risk assessments for decision-making and policy planning. As such, the ability to define these parameters and run multiple workflows is a key feature of the developed software.

The damage simulator is developed in two stages. The first stage uses a deterministic approach, meaning damage is assessed for a given hazard intensity and from a vulnerability function for different types of installations. Different steps are necessary for estimating deterministic seismic damage assessment are summarized below.

1) Consideration of a scenario earthquake and estimation of related ground motion parameter by selecting a ground motion model (i.e. modern GMMs are introduced in the sixth hazard model of Canada) and a deterministic value for site amplification factor;

2) Inventory and classification of the infrastructure components according to a defined taxonomy, so elements expected to behave similarly, by sustaining similar damages when subjected to an earthquake event are grouped together;

3) Identification of an appropriate hazard-damage relationship to be used for assigning a damage level/status to each component identified and classified (step 2) as a function of the hazard estimated (step 1);

4) Estimation of the residual performance of the whole infrastructure accounting for the damages estimated at the component level;

At the second stage, a probabilistic approach is used for assessing the damage to consider a variety of seismic scenarios associated with different probabilities of occurrence as well as the uncertainties affecting the vulnerability functions for the infrastructure. Different uncertainties in seismic risk assessment are considered in the the damage simulator. Uncertainties in the 3D geological model that affect seismic micro zonation (i.e. the probability of being in different site classes) are incorporated into the damage simulator. After the development of a probabilistic seismic site effect model and propagation of uncertainties related to design parameters (Vs_{30} and T_0), the probabilistic approach for damage assessment can consider different amplification factors with related probabilities for multiscenario risk modelling.

Critical infrastructure systems, such as power, transportation and communication networks, influence the well-being of a community. These systems are often exposed to low-probability high-consequence events such as earthquakes. Interruption in any of these infrastructur affects the quality of life and can result in economic losses and casualties. Hence, after developing the damage simulator, seismic risk assessment is performed for Hydro-Quebec equipment in the SLSJ region. This risk assessment is conducted using deterministic and probabilistic scenarios. Risk and probable damage maps can be produced for Hydro-Quebec equipment in the SLSJ region. These maps can be used for planning, decision making and preparedness purposes.

1.4 ORIGINALITY AND CONTRIBUTION

The novelty of the proposed research for seismic risk assessment of electric power transmission networks is that it incorporates several rarely combined scientific models. The specific scientific contributions are related to the advancement of the seismic risk process at several levels: (i) development of probabilistic assessment of seismic site parameters, (ii) introduction of electric transmission tower amongst commonly considered infrastructure systems, (iii) improvement of the understanding of uncertainties and their interactions, and (iv) development of a damage simulator for seismic risk assessment of electric power transmission networks. Most of these research components are already available in the literature, however, they have been developed independently and have not been used in the form proposed herein.

- The innovative probabilistic evaluation of site effect parameters enables users to incorporate site uncertainties effectively into risk assessment. To compute amplified ground motion, users will dispose of a 3D geologic block model of the study area and the respective Vs_{30} values.
- The introduction of electric towers within the commonly considered assets at risk represents a step forward in comprehensive seismic risk assessment. To date, standard risk assessment software does not consider explicitly electrical facilities, particularly power transmission towers.
- Several sources of uncertainty are accounted for in risk analysis, that is uncertainty related to site parameters, predicted hazard values at bedrock level and vulnerability functions data. The applied

multisource uncertainty consideration offers a remarkable advancement in the domain because current methodologies disregard the combined effect of these uncertainties.

- The proposed damage simulator consists of two major components: the hazard module and vulnerability module. Three comprehensive database feed the modules with information on local site parameters, inventory of considered infrastructure systems, and their respective seismic vulnerabilities.
- The developed damage simulator serves as a decision-support tool for the public safety community to manage seismic risks. Providing damage predictions for a hazard scenario also helps in the identification of areas within the urban centres vulnerable to seismic hazards and provides a more accurate guidance for selecting locations for future infrastructure. In addition, the developed software provides insight into the potential hazard scenarios to which existing infrastructure may be exposed within the framework of long-term risk reduction.

1.5 THESIS OUTLINE

Three journal papers are the outcome of this thesis, and they are presented separately in Chapters 2 to 4. The general structure of the articles comprises the Abstract, Introduction, Methodology, Discussion, and Conclusion.

CHAPTER 1 describes the overall structure of the thesis by explaining the statement of the problems, the objectives of the thesis, the methodology used to achieve the principal and sub objectives, and the originality and novelty of the thesis.

CHAPTER 2 presents existing literature regarding the seismic loss estimation and existing seismic loss estimation software and discusses the pros and cons of the software and the limitations in the application of each.

CHAPTER 3 introduces the newly developed site probabilistic site effect module for the calculation of the site parameters, presents the methodology of implementing the 3D geological model

and MC method to capture geological and geotechnical uncertainties and generates the Vs_{30} and T_0 deterministic and probabilistic map for Saguenay using the developed module.

CHAPTER 4 discusses the development of the damage simulator. The hazard module is developed by integrating the site effect module presented in Chapter 3, and the recently published NBCC2020 hazard model is used to complete the hazard part. The damage calculation part is developed by implementing an MC method to incorporate uncertainties from hazard parameters and site parameters. Finally, the results from the damage simulator are presented in terms of fragility analysis and damage ratio.

CHAPTER 5 presents the most important outcomes of the present work and the recommendations for future research.

CHAPTER 2

Article 1: Seismic loss estimation software: A comprehensive review of risk assessment steps, software development and limitations

Vahid Hosseinpour [a] *, Ali Saeidi [a], Marie-José Nollet [b], Miroslav Nastev [c]

[a] Department of Applied Sciences, University of Quebec at Chicoutimi, Saguenay, G7H 2B1, QC, Canada

[b] Department of Construction Engineering, École de Technologie Supérieure, Montreal, H3C1K3, QC, Canada

[c] Geological Survey of Canada, Natural Resources Canada, Quebec City, G1K 9A9, QC, Canada

Email: vahid.hosseinpour1@uqac.ca

Published, Engineering Structures, Volume 232, 1 April 2021, 111866

https://doi.org/10.1016/j.engstruct.2021.111866

Acknowledgements:

The authors would like to thank the members of the CERM-PACES project for their cooperation to conduct the field tests and provide access to the database.

Authors contribution**:**

Vahid Hosseinpour: Conceptualization, Methodology, Formal analysis, Software, Validation, Data Curation, Visualisation, Writing – original draft. **Ali Saeidi:** Conceptualization, Funding acquisition, Validation, Project administration, Supervision, Resources, Writing - Review & Editing. **Marie-José Nollet:** Supervision, Writing - Review & Editing. **Miroslav Nastev:** Supervision, Writing - Review & Editing.

Funding:

This research was partially funded by the Natural Sciences and Engineering Research Council of Canada (NSERC) and Hydro-Quebec under project funding no. RDCPJ 521771-17 and also CRC-NSERC 950-232724.

2.1 ABSTRACT

Over recent years, seismic losses are increasing dramatically in terms of magnitude and frequency, thereby causing severe impacts on societies and economies. The increment in seismic losses is mainly due to the rapid growth of exposure and population in earthquake-prone areas worldwide. This phenomenon necessitates better understanding and accurate prediction of potential seismic risks to plan appropriate emergency response, rescue and recovery activities. The focus of the research community has shifted towards the prediction of the seismic risk, which paved way to the development of a number of modelling software. This paper presents a critical review of existing methods for seismic risk analysis and software developed by various organisations with an emphasis on their strength and limitations. First, the focus is on the essential assessment steps in seismic risk analysis, namely, hazard, exposure model and vulnerability assessment. Particular attention is paid to different approaches applied for vulnerability evaluation. The main advantages and disadvantages of each software are highlighted. Finally, a comparative analysis of major seismic risk software, such as HAZUS, Ergo, SELENA, OpenQuake and ER2, is provided. Findings of this review indicate unresolved issues in scenario loss modelling and probabilistic seismic risk assessment, such as the convergence problem in probabilistic seismic hazard analysis, selection of suitable ground motion prediction equation and consideration of epistemic uncertainty, which need to be further investigated and applied to future seismic risk assessments.

Keywords: Seismic Loss Estimation, Earthquake risk, Vulnerability, Seismic risk software, Seismic hazard

2.2 INTRODUCTION

The Earthquakes represent a major natural hazard that regularly affects lives and built environment in seismic-prone areas worldwide and leads to social and economic losses. In the last few decades, a significant increase in seismic losses has been recorded in earthquake-vulnerable areas [1]. Such increase can be attributed to several reasons, among which the increment in the exposed population and built environment, the development of super-cities in countries of the Pacific rim and the ever-rising vulnerability of modern societies and sophisticated technologies are highly important [42, 43]. Strong earthquakes (e.g., 1994 M6.7 Northridge earthquake and 2011 M9 Tohoku earthquake) result in substantial economic impacts; building

damage; casualties; and damage to essential facilities (e.g., hospitals, schools and fire and police stations), lifelines (e.g., potable water supply, gas and oil pipelines), transport networks (e.g., roads, railways and bridges), cultural heritage legacy and environment [44]. Middle-income countries and particularly those with rapidly growing cities are susceptible to devastating earthquakes [45, 46].

The seismic risk assessment process conducted at urban, regional and national scales aims to measure the magnitude of potential negative impacts and their likelihood to inform emergency managers and decision makers to act respectively. Seismic risk assessment is a complex engineering and scientific challenge because of the vibrant nexus amongst the city's environment, its residents and many interrelated networks[47]. Prediction of seismic risk requires detailed information about ground shaking intensity (hazard), exposed building and infrastructure (exposure) and respective vulnerabilities. Risk assessment results are presented by quantifying physical damage and economic and social losses and their likelihood [48, 49].

In the last few decades, considerable effort has been made to create an appropriate seismic loss estimation (SLE) software that provides fairly accurate loss estimates, such as Hazard US (HAZUS) [4, 5] and its versions such as Ergo [6], Haz-Taiwan [7], SELENA [8] and HazCan [9], then InaSAFE [10], CAPRA[11], DBELA [12], OpenQuake [13], ER2 web application [14], etc. As it can be seen, certain countries have developed their own customised versions of SLE software, whereas global projects, such as the Global Earthquake Model (GEM), are developing tools with worldwide capacity [13].

This paper aims to present a comprehensive and critical review of the existing state-of-the-art SLE software with focus on the consideration of uncertainties. The seismic risk assessment process and the standard structure of SLE software, including hazard, exposure and vulnerability modules, are discussed in detail. Special attention is paid to the different approaches for evaluation of structural vulnerability. The main advantages and disadvantages of each software are highlighted, and as such, this paper is intended to serve as a reference and guide to help risk modeller and engineers find the true value of the existing seismic risk assessment methodologies.

2.3 SEISMIC LOSS ESTIMATION COMPONENTS

Seismic hazard and risk are two fundamentally different concepts. Seismic hazard refers to a natural phenomenon that involves ground shaking generated by an earthquake, whereas seismic risk refers to the negative impacts that may occur to humans and built environment and their likelihood. The seismic risk assessment process involves quantification of three major input components, namely, seismic hazard intensity, inventory of assets at risk and respective vulnerability. Fig 2-1 shows the components of the seismic loss. The various methods used to determine each component and a number of SLE software are presented.

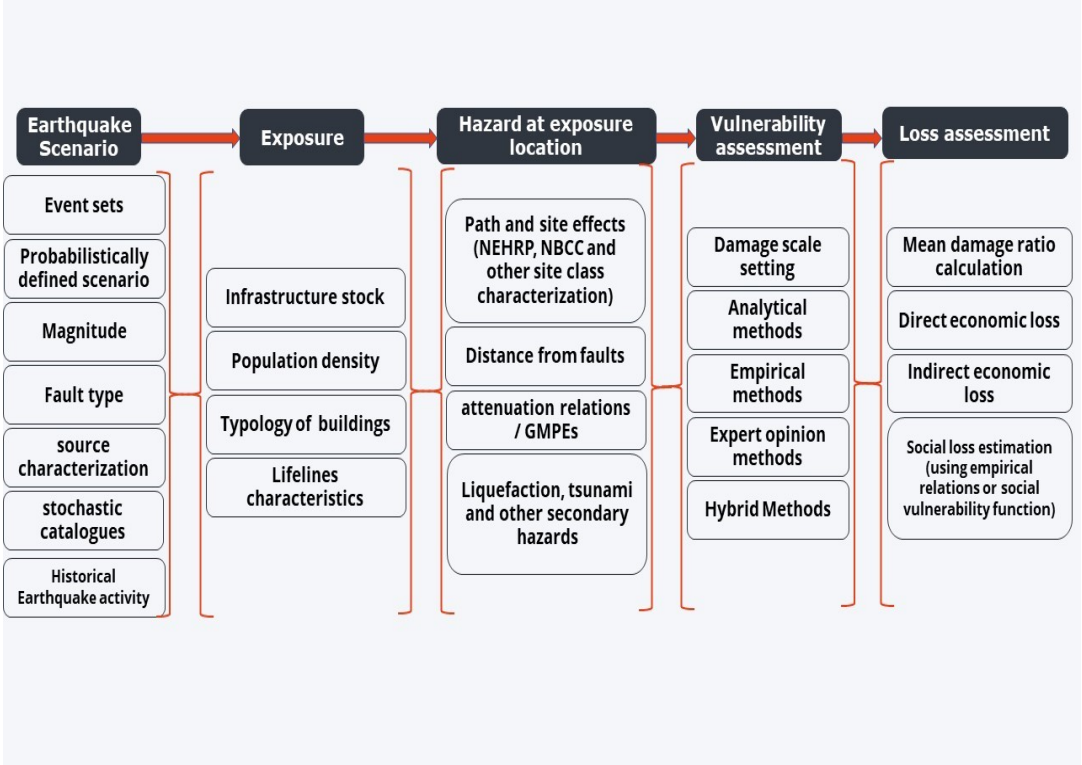

Fig 2-1. Identified Components of Seismic Loss Assessment (adapted from [50]).

2.3.1 Hazard

Seismic hazard is defined by the probability of occurrence of a ground motion of a given intensity over a specific period of time at a given location [51]. Earthquake hazards are divided into two main categories, namely, transient ground shaking and permanent ground failure (i.e. secondary effect of earthquakes). In loss assessment, the intensity of ground shaking is mainly considered because identifying and modelling the secondary hazard parameters of earthquakes is more complex and considerably less reliable [52]. The secondary hazards of earthquake include surface fault rupture, soil liquefaction, settlement, landslide and other slope instabilities, tsunami, seiche, fire, etc. In terms of ground shaking, peak ground acceleration (PGA) and 5% damped spectral accelerations at given periods, e.g., Sa(0.3s), Sa(1.0s) are generally considered as shaking intensity measures (IMs). Other risk assessment methodologies use the European Macroseismic Scale or Modified Mercalli Intensity (MMI) [53]. The procedures used to assess seismic hazard include two options:

Deterministic seismic hazard assessment (DSHA) includes a single scenario earthquake (e.g., historical event, maximum credible earthquake or user-defined event scenario)[24]. After defining the potential seismic sources that significantly impact the study area, a fixed earthquake magnitude and distance are selected. The ground motion parameters and their spatial distribution are estimated using ground motion prediction equations (GMPEs) pertinent for that region. The main steps of DSHA are presented in Fig 2-2.

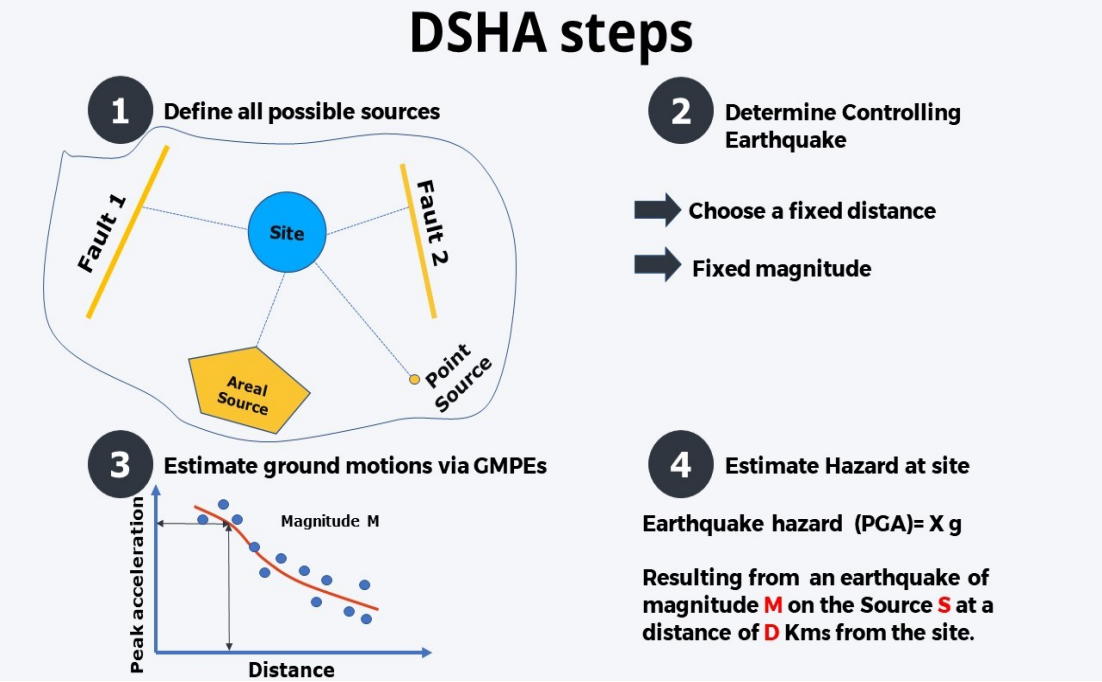

Fig 2-2. Main steps of DSHA (adapted from [24]).

Probabilistic seismic hazard analysis (PSHA) is widely used to determine the ground-motion parameters (design response spectrum) for structural analyses and engineering design. This method considers all potential seismic sources that can affect the studied location with consideration to different distance–magnitude combinations. A recurrence relationship is used to describe the magnitude-frequency (Guttenberg-Richter) relationship for each seismic source. The design response spectrum is associated with a specific annual probability of occurrence. PSHA is usually determined by the total probability theorem [54, 55]. Fig 2-3 demonstrates the PSHA process.

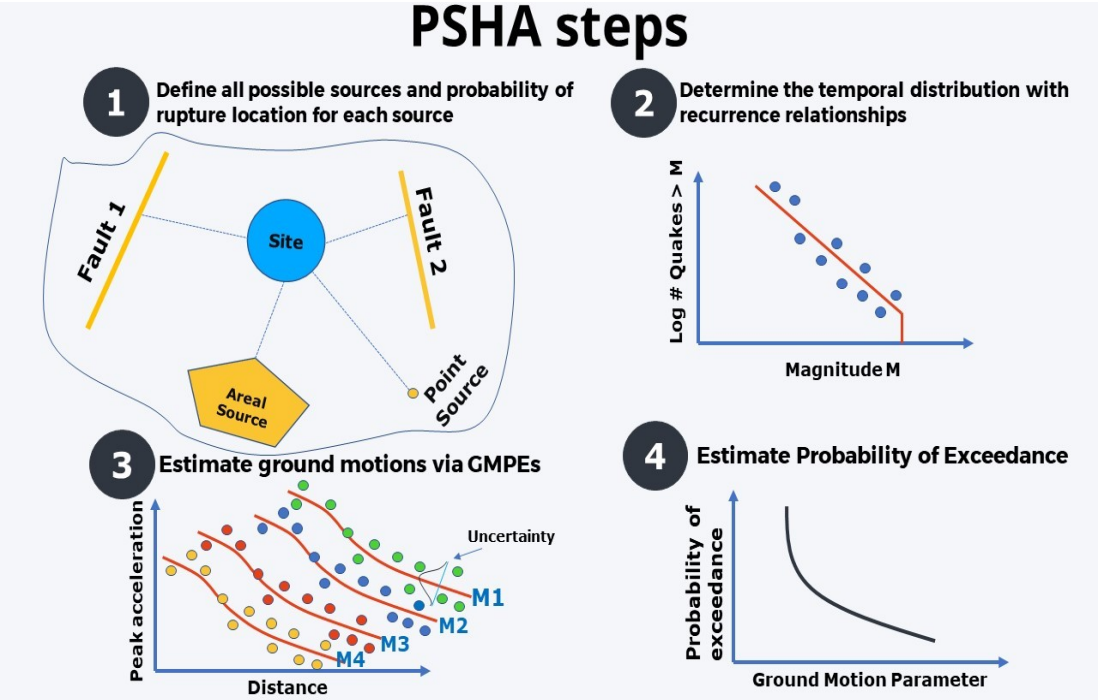

Fig 2-3. Probabilistic seismic hazard assessment process (adapted from [24]).

In both DSHA and PSHA, the most appropriate GMPEs are applied for reference site conditions (e.g., [23, 56]. The local site effects are assumed next as function of the average shear-wave velocity of the top 30 m ($Vs, 30$) to determine the potential site amplification [38, 57].

2.3.2 Exposure

The rapid growth of the population requires accurate and up-to-date characterisation of the ever-changing exposure component. The acquisition of building parameters is probably the most time-consuming, tedious and expensive part of each seismic risk assessment [58]. The fastest way to gather building information is to obtain the one that is already available (e.g. information contained in census questionnaires). A few global building inventory databases were also created during past research projects. For instance, PAGER developed a global building database from a range of national and international sources and experts opinions applying specific procedures to fill in the gaps in the datasets [53]. Some of the sources included census reports, PAGER project, descriptions from the World Housing Encyclopaedia, HAZUS database for the U.S., United Nations (UN) reports, etc. [59]. The UN's 2013 Global Assessment Report established an

exposure model to evaluate natural hazards losses at the global scale [60]. Population and housing censuses are conducted in most of the countries, and they often contain information about wall and roof materials that can be used to infer the type and height of buildings, predominant construction material [61]. Municipal archives and property tax databases offer information about the value and occupancy of the building stock, the age of development, the construction tendencies and practices at the time of development, the political history that drives the development of buildings, the timeline of design and construction codes and the reconstructions conducted after the previous damaging events [62]. The most resource-intensive method for gathering building and infrastructure information is definitely the structural survey that serves the needs of more complex seismic vulnerability assessments [63]. A potential source of information are interviews with local specialists and expert elicitation exercises that may be used to collect necessary data [64, 65].

2.3.3 Vulnerability

Physical vulnerability can be defined as the susceptibility of exposed buildings to seismic impacts (damage) determined with the likelihood of the occurrence of certain damage level caused by seismic action. Vulnerability analysis represents a powerful engineering technique for urban and regional risk assessments. Central to the vulnerability modelling is the concept of vulnerability curves that link the probability of loss at a given level of seismic motion IM, such as response spectral acceleration for given period and damping ratio. Similarly, fragility (damage) curves represent the likelihood of exceeding different limit states (e.g., physical damage state) given the intensity of the seismic motion. Depending on the specific conditions, vulnerability and fragility curves, either separately or combined, can be assumed as reliable predictors of damage for a respective group of building with similar structural characteristics and dynamic behaviour.

The development of vulnerability functions is based on one of the following fundamental approaches, namely, empirical, analytical, expert judgment or a combination of the three (hybrid methods) [2, 66, 67]. Method selection is often dependent on the quality and type of available data, expert's knowledge, available resources and the scale of the study area.

Empirical approaches use field observations from previous earthquakes to predict physical damage or economic losses for similar seismic settings. From the risk management viewpoint, empirically derived

vulnerability functions are generally the most credible since they are entirely derived from the observations of the actual performance of buildings during strong earthquake events. Empirical-based methods can be used for vulnerability assessment of various man-made structures buildings [68], pipelines [69], bridges [70], electrical power systems [29, 71], etc.

Aleatory uncertainties, such as spatial variation in ground shaking or building response, are considered inherently by the empirical methods [72]. Nonetheless, insufficient data for large and relatively rare earthquakes and different seismological and geological settings could influence the wider applicability of such results. Empirical approaches cannot consider the local structural and load bearing details of buildings specific to each region, making them hardly transferable to other regions. Moreover, existing earthquake damage databases might be inadequate or ambiguous using different limit states and building classes [73].

Analytical vulnerability assessment approaches use modelling methods to analyse the dynamic response of a given structure subjected to earthquake loading [74]. Idealising structural models to a lesser or greater extent is possible, however, they will always involve significant assumptions and simplifications that could probably lead to discrepancies in the results [73]. Analytical vulnerability modelling, which includes the use of different modelling methods, input data and assigned parameters to the model, can differ in terms of complexity. Most of the analytical methods employ the following analytical steps (
Fig 2-4).

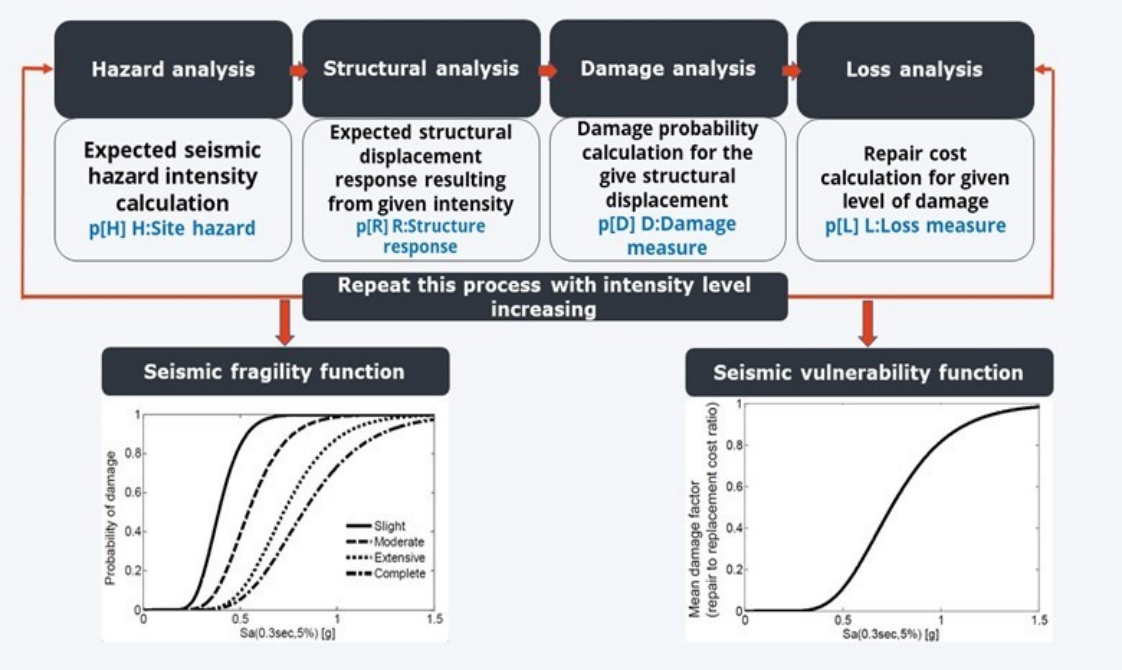

Fig 2-4. Analytical framework for estimating seismic vulnerability.

Although simple models rely on rough assumptions, their advantage lies in the fact that they are built and solved rapidly. More complex models, on the other hand, necessitate substantial computational effort and comprehensive engineering expertise to generate accurate results [75]. Analytical approaches may be grouped as follows: Capacity Spectrum Method (CSM, adaptive or not; e.g., HAZUS [76]), coefficient displacement [77], mechanics-based [78], N2 [79], and other simplified methods. In general, analytical approaches for seismic vulnerability assessments are efficient in areas with low to moderate seismic activity with scarce earthquake damage observations. Expert judgment approaches are used for eliciting, weighting and pooling the knowledge of experts [64], assumed to provide acceptable vulnerability estimations [80, 81]. The different methods available to collect experts' opinions aim to reduce potential bias [64]. The reliability of the results depends on the experience of each expert involved, mainly in terms of specific local building typologies, construction practices, detailing and materials [73]. As mentioned earlier, the hybrid approach combines analytical, empirical and/or expert opinion methods [74]. They are often used in the absence of sufficiently comprehensive data provided by one of the first three approaches [73]. Results may still be subjective, however, they may always be cross-validated against the results from one of the individual approaches [72]. Evidently, the simplest solution to acquire vulnerability functions is to select them from the

existing studies or adjust them to fit the considered scenario. Still, such approach could yield relatively imprecise results because of the absence of conformity with the studied location and/or the building type. This method can be considered a feasible option only when resources are limited or as a first screening test to attain a rough figure of the potential damages before more accurate vulnerability assessments are applied.

The physical damage predicted by the structural vulnerability analysis represents the basis for additional empirical relationships that quantify respective economic losses [41, 76, 82], casualties (e.g., injuries of different severity levels and fatalities [83]) and indirect losses, such as debris removal, business disruptions, extended transportation routes, etc. [49, 84-86].

2.4 LOSS ASSESSMENT SOFTWARE

SLE software is currently being used worldwide to provide accurate predictions of the loss estimates. Available software packages are proprietary, open access or open-source, and most of them are developed for a specific region with their own seismotectonic settings and construction practices. Table 2-1 summarises the available SLE software considered in the present study.

Table 2-1. Summary of the seismic risk assessment software packages [87, 88]

Software	Institution	Programming Language	Applicability	Open source	Hazard	Vulnerability	Graphic user interface
HAZUS-MH	FEMA	VB6, C++	U.S.	No	Deterministic Probabilistic	Analytical	Yes
HAZUS Canada (HazCan)	NRCan	VB6, C++	Canada	No	Deterministic Probabilistic	Analytical	Yes
Ergo (MAEviz)	Uni. Illinois	Java (EclipseRichClient)	US.	Yes	Deterministic Probabilistic	Analytical Empirical	Yes
OpenQuake	GEM	Python (Web-based), NRLM	Italy (Develop for Global application)	Yes	Deterministic Probabilistic	Analytical Empirical	No
SELENA	NORSAR	Matlab, C++	Norway	Yes	Deterministic Probabilistic	Analytical	Yes
CAPRA	World Bank	Visual Basic.NET	Central America	Yes	Deterministic Probabilistic	Analytical Empirical	Yes
ER2	NRCan, CSSP	Java	Canada (Quebec City)	No	Deterministic Probabilistic	Analytical	Yes
EQRM	Geoscience Australia	Python, Matlab	Australia	Yes	Deterministic Probabilistic	Analytical Empirical	No

2.4.1 HAZUS

The U.S. Federal Emergency Management Agency (FEMA) started the development of the HAZUS software in the early 1990s for calculation of seismic impacts to buildings and infrastructure, social (e.g., casualties, shelter needs) and economic losses at the census tract, county or state scales. The advanced engineering building module allows for loss assessment at the building level. Earthquake hazard is considered as transient ground shaking and permanent ground failure [89]. Today, HAZUS is a multi-hazard tool that also includes floods, hurricanes and tsunamis. The primary modules of HAZUS are shown in Fig 2-5.

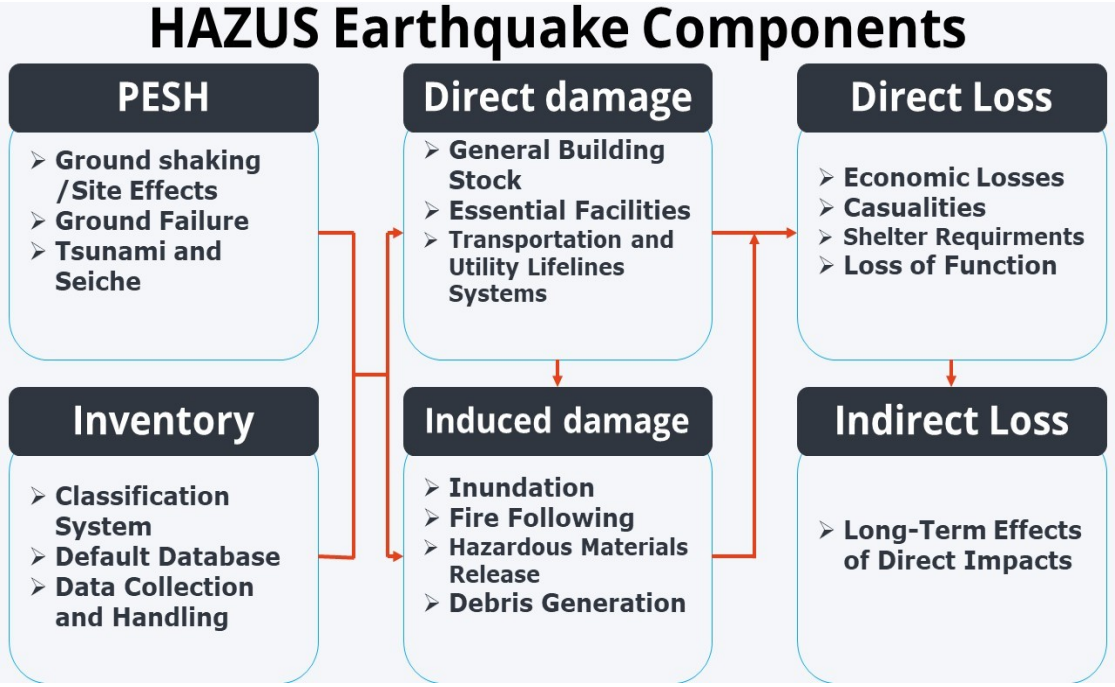

Fig 2-5. Primary components of HAZUS Earthquake.

HAZUS is developed by private companies as a closed source software accompanied by comprehensive users and technical guidelines and parameters of the applied damage functions [36]. The software uses C++ and Visual Basic algorithms and Microsoft SQL as relational database interfacing with ArcGIS to visualise damage to the building stock, lifelines and high-potential loss facilities [5, 76, 83].

Modernisation of HAZUS is ongoing with the objective to exclude any needs for commercial software on the users side. The current HAZUS v.4.2, as of May 2019, offers high-resolution shake-maps and an updated fire following earthquake module. Out-of-the-box input data with information on aggregated building stock and links to web sites with supplementary information are provided to the user. The standard building inventory consists of 15 basic categories with respect to the structural type and material, which when multiplied by building height (low: 1-3 stories, medium: 4-7 stories, and high: +8 stories) and design level (pre-code, low-code, medium-code and high-code) generates a total of 128 building types. Beside the building types, HAZUS also includes seven major occupancy categories which impact the building performance parameters and resulting social and economic losses.

The HAZUS vulnerability evaluation included in the module for direct physical damage is based on the CSM described in ATC-40 [90]. In this approach, the performance point of a given building type subjected to a specific ground-shaking scenario is determined from the intersection of the seismic demand in the acceleration–displacement domain with the capacity spectrum (pushover curve) that reflects the horizontal displacement of the structure under increased lateral load [89] (Fig 2-6).

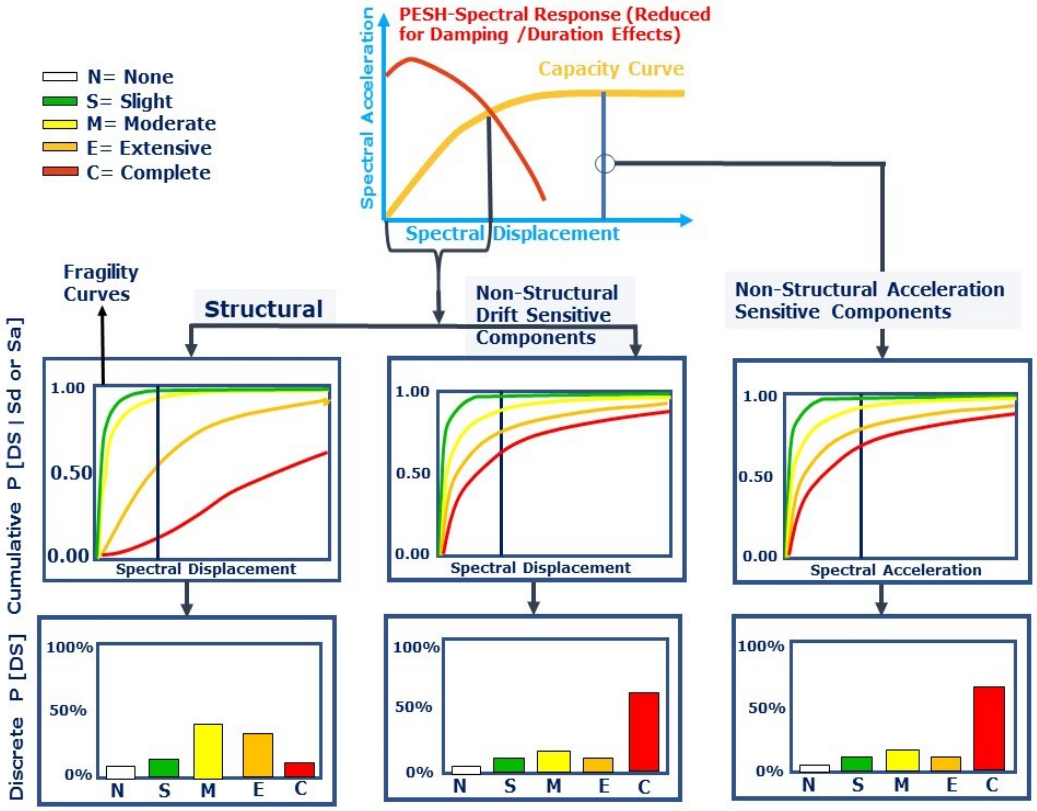

Fig 2-6. Damage assessment from ground shaking in HAZUS (adapted from [76]).

The CSM is applied for average properties of each building class and the obtained performance point provides expected building displacement (e.g., roof displacement, inter-story drift) which, when combined with the respective limit state vulnerability curves, gives the probability distributed over each of the five damage states: none, slight, moderate, extensive and complete. Depending on the building type, a collapse

state is also calculated as percentage of the probability of the complete damage. It is mainly this state that generates fatalities.

The vulnerability curves are represented with a two-parameter cumulative lognormal distribution function, with a median value and a total logarithmic standard deviation β_{Sds} which represents the damage state threshold uncertainty. $\beta_{M\,(Sds)}$ is the model variability that describes the uncertainty in the median value estimate of the structural damage state threshold. β_C is the lognormal standard deviation parameter that describes the variability of the capacity curve. β_D is the ground motion demand spatial variability uncertainty. The convolution (CONV) of the probability distributions is used to combine interdependent parameters. Moreover, they are combined with $\beta_{M(Sds)}$ using the square-root-of-the-sum-of-the-squares to obtain the total standard deviation:

$$\beta_{Sds} = \sqrt{(CONV[\beta_C, \beta_D, \bar{S}_{d,Sds}])^2 + (\beta_{M(Sds)})^2} \tag{2-1}$$

where, $\bar{S}_{d,Sds}$ is the median spectral displacement for the damage state ds. The generated median spectral displacement (or acceleration) values and the total variability for different seismic scenarios were validated against the combination of performance data from building component tests, field observations following strong earthquakes, experts' opinion and comparative judgment for each of the considered building types and damage states of concern.

The HAZUS software has been initially developed as a tool to perform DSHA and PSHA, then upgraded for seismic risk assessment. The β_D has already been considered in hazard assessment process and HAZUS upgrade led to omitting the seismic demand variation from the vulnerability curves (see eq. 2) to avoid repetition [66]. Such curves are lognormal functions with the following standard logarithmic deviation:

$$\beta_{Sds} = \sqrt{(\beta_C)^2 + (\beta_{M(Sds)})^2} \tag{2-2}$$

Computationally, CSM is a quicker than the displacement-based method and requires fewer building parameters to create the final loss estimate (i.e., building column, beam lengths and heights are not required).

However, in locations where all these details are available, CSM yields higher uncertainties than the displacement-based method [50, 66]. The static pushover analysis within CSM cannot consider certain dynamic phenomena with satisfactory precision [91]. For example, the near-field velocity pulses in the ground motion which affect the structural response are not explicitly considered [92, 93]. This drawback is addressed in FEMA-P58 [92] but it is still not considered in HAZUS.

HAZUS methodology has been applied in numerous locations worldwide for loss assessment in urban areas (e.g., Turkey [94], Norway (SELENA) [8], Taiwan (using a modified version of HAZUS called Haz-Taiwan) [7, 95], Canada (HazCan) [9, 96], Risk-UE [97, 98], EQRM [99], ER2-Earthquake [14], Ergo (ex-MAEviz), where the capacity and vulnerability curves were adapted for the local building stock.

HAZUS has a user-friendly GUI (Graphical User Interface) to input data and presents output in GIS-based platform. This software also performs loss estimation for a number of infrastructur (i.e., lifelines, essential facilities and transportation systems). It also considers damage evaluation from fires following earthquake and indirect economic losses. HAZUS has some limitations as well, such as ArcGIS license requirement (last version of HAZUS only works with ArcGIS V. 10.5.1), and difficulties in installing the software are also encountered. Although it is possible to run HAZUS, as it is, for locations outside the U.S., such applications may not give reliable loss estimation results due to different seismic and structural settings [50]. HAZUS vulnerability functions have been heavily calibrated to the huge amount of earthquake damage data [87].

2.4.2 SELENA

The International Centre for Geohazards ICG through NORSAR (Norway) and the University of Alicante (Spain) developed SELENA SLE using the logic tree approach for uncertainties [100]. A Beta version of SELENA 1.0 was released in 2007, and its latest version is the SELENA 6.5. It is coded in MATLAB and is also available as a compiled stand-alone version. SELENA relies on the principles of the CSM and uses an approach that is similar to that of HAZUS. The user provides the input data in a pre-defined ASCII format (e.g., building inventory, demography and seismic scenario), and the software calculates

respective shake maps, damage probabilities, absolute damage estimates, as well as economic losses and number of casualties.

SELENA is independent of any GIS (Geographic Information System) as opposed to many other tools [101, 102] and the numerical results can be visualised in any GIS systems. Risk Illustrator for SELENA (RISe) [103] is a Google earth-based GIS system that is primarily used in SELENA (Fig 2-7). RISe or its operation principle may be applied to other risk models, such as HAZUS or OpenQuake.

Ground-motion parameters in SELENA are calculated in three different ways: via deterministic and probabilistic analyses and with real-time data, making it convenient for planning the emergency response. SELENA can use GMPEs that include different site categories, respective amplification factors and/or corner periods to describe the input response spectra [102]. SELENA computes building damage with different vulnerability methodologies selected by the user: CSM by ATC-40 [90], the modified acceleration-displacement response spectrum method according to FEMA-440 [104], and the improved displacement coefficient method given by FEMA-440 [104].

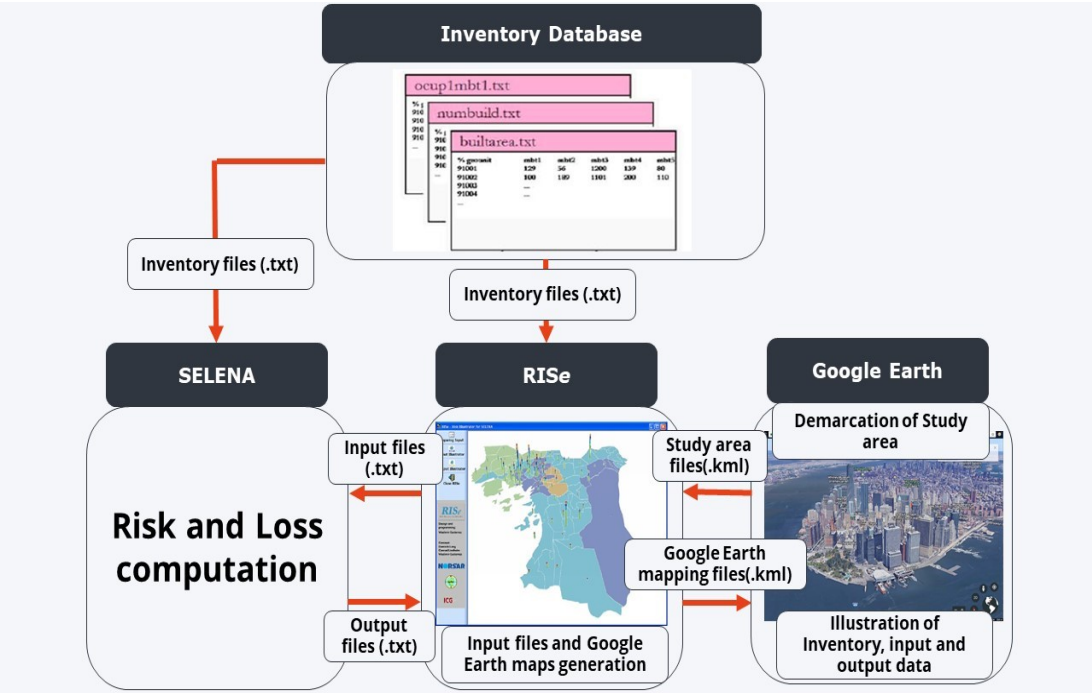

Fig 2-7. Principle integration of RISe in a seismic risk and loss assessment study (adapted from [103]).

Unlike other SLE, this method considers the logic tree approach allowing for incorporation of epistemic uncertainties related to various input parameters and provides the final results with corresponding levels of confidence [8, 105]. For the time being, the logic tree approach considers uncertainties in the earthquake source, attenuation relationships, shake maps, soil types, vulnerability and economic values of damages. SELENA also considers the effects of topography in hilly regions through a user-selectable amplification procedure [101]. Three topographic amplification approaches are considered: EN 1998 [106], the Italian building code ICMS [107], or the recently developed period-dependent topographic amplification relationship by Molina et al. [108].

2.4.3 EQRM

EQRM is an open-source SLE software developed by Geo-Science Australia for Australian seismotectonic conditions and construction practices [109]. EQRM was developed in Python and MATLAB and does not have GUI nor is integrated to a GIS system. EQRM basically applies the HAZUS methodology for damage assessment with certain differences [110, 111]:

1) CSM implementation: the full structure of the response spectrum and the soil's amplification across all the periods of interest are considered (i.e., HAZUS approach only uses periods 0.3 and 1.0 seconds).
2) HAZUS incorporates the variability of damage state thresholds, capacity curves and the ground shaking but in EQRM fragility curves only the variability of damage state is considered.
3) Uniform hazard spectra are used instead of demand curves, and MMI scale can also be used.

EQRM conducts probabilistic seismic hazard analysis and probabilistic seismic risk analysis using the event-based approach [112]. In this way, the ground shaking parameter and respective losses are first computed for each event individually, and then the results are aggregated to obtain probabilistic risk estimates [110]. This software can provide various outputs for both the hazard analyses: Seismic hazard maps, hazard exceedance curves and uniform hazard spectra, and for the risk analyses: risk exceedance curves, aggregated and disaggregated annualised losses [87, 110].

2.4.4 OpenQuake

The OpenQuake Engine is GEM's software for seismic hazard and risk assessment at different scales. The current OQ 3.7.1 version is open-source coded using the Python programming language. Natural hazard's risk Markup Language (NRML) is an XML-based language that was developed in parallel with GEM project, and OpenQuake uses this language to read input parameters and perform loss analyses [113].

OpenQuake is a transparent software used with GEM or other user-developed models to perform scenario-based or probabilistic risk analyses to generate various hazard and loss outputs. The spatial correlation of the ground motion residuals and correlation of the uncertainty in the vulnerability can also be modelled. The major calculation algorithms of the OQ engine include the scenario risk calculator, scenario damage calculator, classic PSHA-based risk, probabilistic event-based (PEB) risk (Fig 2-8) and retrofitting benefit–cost ratio [13, 114].

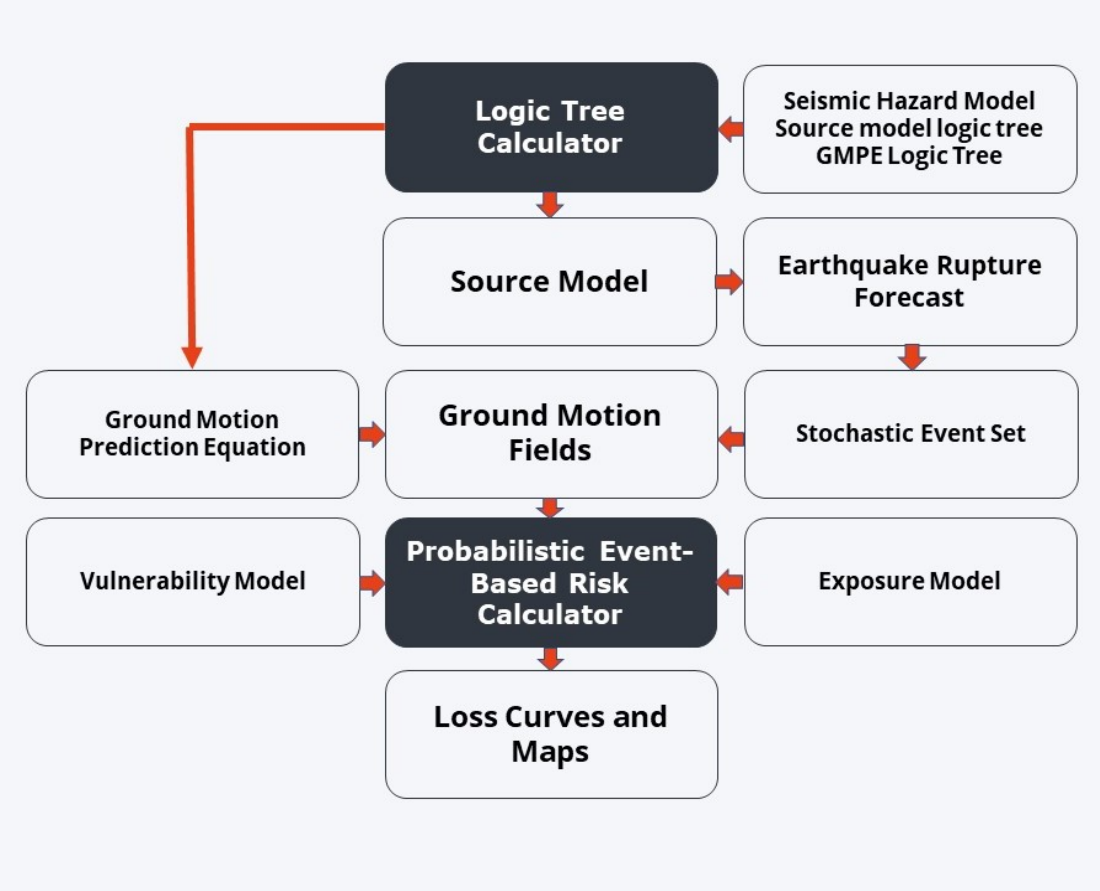

Fig 2-8. Process of the probabilistic event-based risk assessment in OpenQuake (adapted from [115]).

The PEB calculator is the most innovative module of OQ with respect to other SLE software. In PEB, Monte Carlo method is used to generate the stochastic event set (SES), which represents a potential realisation of seismicity, with a ground motion field calculated for each event contained in SES. The event-based PSHA calculator takes this large set of ground-motion fields, representative of the potential shake scenarios that the investigated area can experience over a given time period and for each site that computes the corresponding hazard curve. However, the procedure is computationally intensive and is not recommended for large study areas [114]. The main features of the OQ engine are presented in Table 2-2-2.

Table 2-2. Methodological and General characteristic of the OpenQuake engine [113, 114]

OpenQuake General and IT futures		**OpenQuake Methodological futures**	
Version	3.7.1	**PSHA Approach**	Cornell-McGuire PSHA, Monte Carlo based PSHA
Code availability	Open source, https://www.globalquakemodel.org/oq-getting-started	**Gutenberg-Richter relationship**	Yes
Programming language	Python	**Activity rate**	Computed for Mw=0
I/O format	NRML	**Earthquake rupture modeling**	Rupture finiteness in 3-D for fault and areal sources
Platform	Ubuntu, Linux, macOS, and Windows	**Type of magnitude-scaling relationship**	Magnitude-area scaling relationship of Wells & Coppersmith (1994), Thomas et al. (2010), EPRI (2011), and Strasser et al. (2010)
Number of processors	As many processors as available	**Truncation of the GMPE variability**	Yes
Documentation	User Manual	**Treatment of epistemic uncertainty**	Logic tree
GUI	No	**Outputs**	Hazard curves and maps, UHS, disaggregation for M-R-Ɛ-Location

The GEM project also developed an evaluation and selection framework of existing fragility curves for new studies [72]. It guides the user to verify the overall quality of the current fragility curves and their relevance, and to reduce inaccuracies by enhancing the selection process. The selection amongst the currently available fragility curves can be very subjective and applying the GEM framework necessitates an in-depth knowledge and data about the structural dynamic response and evaluated fragility curves.

A case study of seismic loss estimation was conducted to briefly illustrate capabilities and the actual performance of the OQ engine as a representative of sophisticated and complex to use software package. Fig

2-9 shows a diagram of input data required in each consecutive computation step. The process starts with the refined seismic hazard algorithms where the fault geometry, mechanisms and GMPE are introduced (steps 1 and 2). The inventory of assets at risk comes next with respective structural, non-structural, and content parameters and vulnerability or fragility curves (steps 3 and 4). The last step is computation of the negative impacts (step 5). The exposure dataset can also be prepared independently in a spreadsheet format and imported (step 6). In Fig 2-10 are given screen captures showing the typical input tables and QGIS visualization of the results. For this example, M7.0 scenario earthquake was run with uniform shear wave velocity across the study area (760 m/s) for local site amplification. Chiou and Youngs GMPE was applied for calculating the ground motion attenuation with distance [116]. The OQ engine can be accessed directly from QGIS [117], which is an open source GIS platform. The user first provides input data using the Input Preparation toolkit (Fig 2-10-1). Follows the selection of different types of calculation, e.g., Event based calculation, Scenario seismic risk and hazard assessment calculation (Fig 2-10-2). At the end, the user downloads outputs from each calculation step, e.g., Average asset loss, ground motion fields and calculation reports (Fig 2-10-3) the results are visualized using QGIS (Fig 2-10-4).

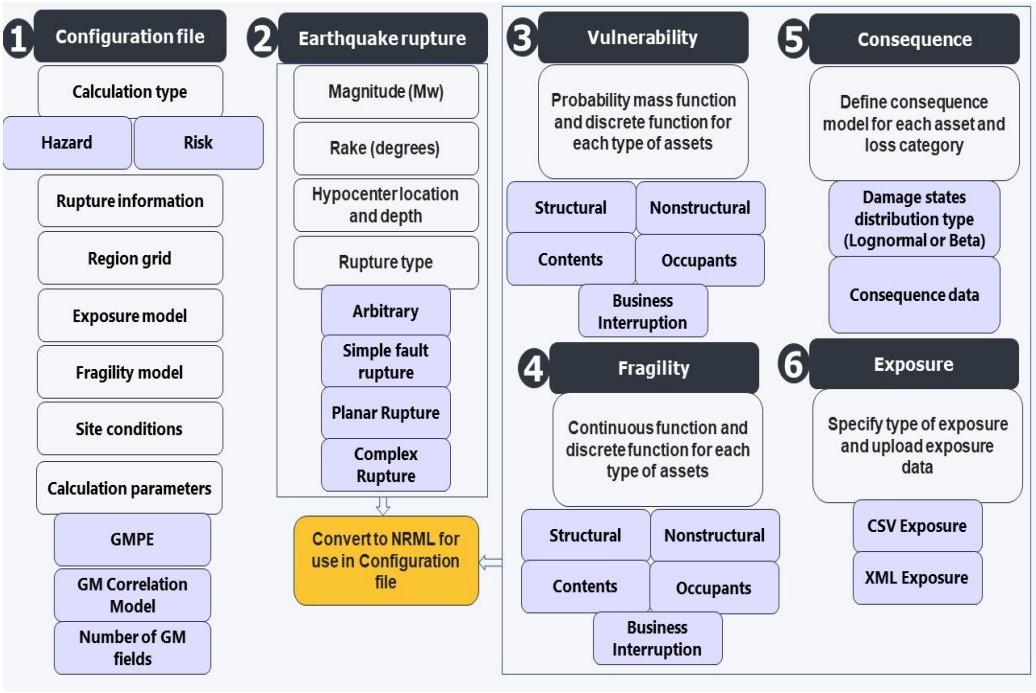

Fig 2-9. Data requirements to run OpenQuake.

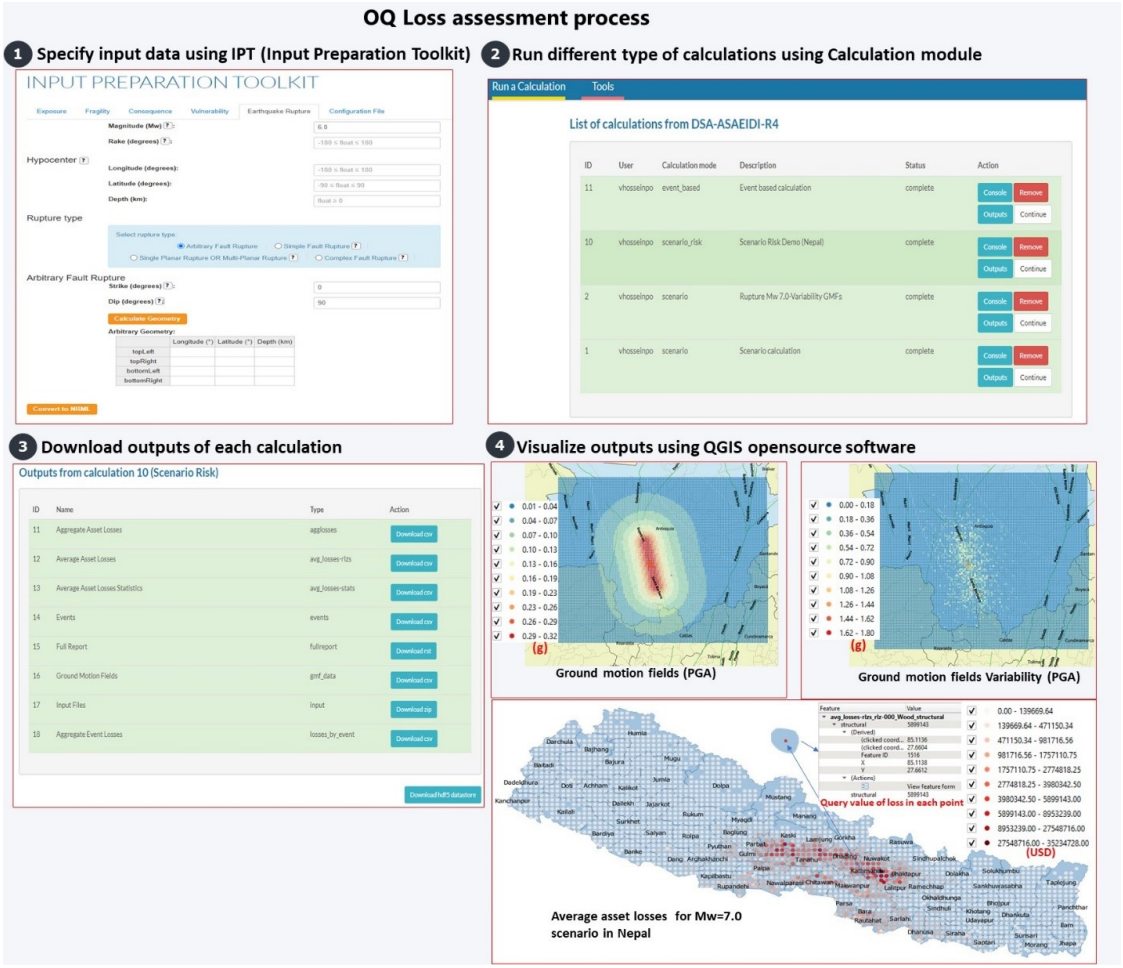

Fig 2-10. OpenQuake loss estimation process and visualization of loss results.

2.4.5 ER2-Earthquake

ER2-Earthquake (Rapid Risk Evaluator) is another HAZUS-based risk assessment software that is currently being developed by Natural Resources Canada [14, 118]. So far, this software is the only web-based user-friendly software that can be applied by both expert and non-expert users. ER2 is developed using Java (vulnerability assessment applet) and Python (web-based interface) programming languages. Seismic risk assessment can be carried out for scenario earthquake or for probabilistic scenarios over a range of return periods between 100 and 10,000 years.

An innovation regarding the standard HAZUS methodology is that ER2 introduces a non-iterative algorithm instead of the standard CSM for the computation of the performance point [119]. The efficient inverse procedure starts from the performance point (structural response) and then determines the respective seismic scenario that caused it. The performance point is specified with an effective damping ratio and a pair of spectral displacement-spectral acceleration values. This seismic demand is correlated to the 5% damped input spectrum determined with the IMs, e.g. Sa(0.3s) and Sa(1.0s), from the respective seismic scenario (magnitude, distance, local site conditions, GMPE). For the considered building type, the spectral displacement of the performance point is associated with the set of the respective HAZUS displacement-based fragility functions and the probability of being in each of the five potential damage states is obtained. In the last step, probabilities of the damage states are linked to the IMs of the input spectrum. The procedure commences with low spectral acceleration values yielding elastic response (displacement) on the capacity curve. The spectral acceleration is gradually increased until a reasonably high displacement is attained in a fully plastic state of the capacity curve. The results from numerous scenarios are stored in a database for each building type [14, 120], substituting the tedious iterations for the performance point quantification with simple queries to pick-up rapidly the appropriate pre-computed scenario. The development process for the forward (HAZUS) and backward (ER2) method is presented in Fig 2-11. The new log-normal vulnerability curves express directly the probability of physical damage as function of the shaking IMs for each building type [14, 120].

Fig 2-12 shows a comparative example of building damage state computation with HAZUS AEBM [83] and with ER2. The results are computed for M6.0 earthquake scenario with Boore and Atkinson GMPE [121] for: 128 North American building types, 5 soil categories for local site amplification and 2 epicentral distances from the point source. Taking into account the five potential damage states, there are a total of 6,400 damage state results in Fig 2-12. It can be observed that the damage states predictions with ER2 are practically identical to those of HAZUS [14]. Additional advantages of ER2 are the relatively short runtime, usually less than a minute for an urban centre of about 1M inhabitants, and there are no requirements for user provided input data except the few parameters of the seismic scenario. These characteristics make ER2 easily accessible option, particularly for regions with low to moderate seismic activity, where its results can be used as a first-hand information for high level planning purposes or for shakeout type operational drills.

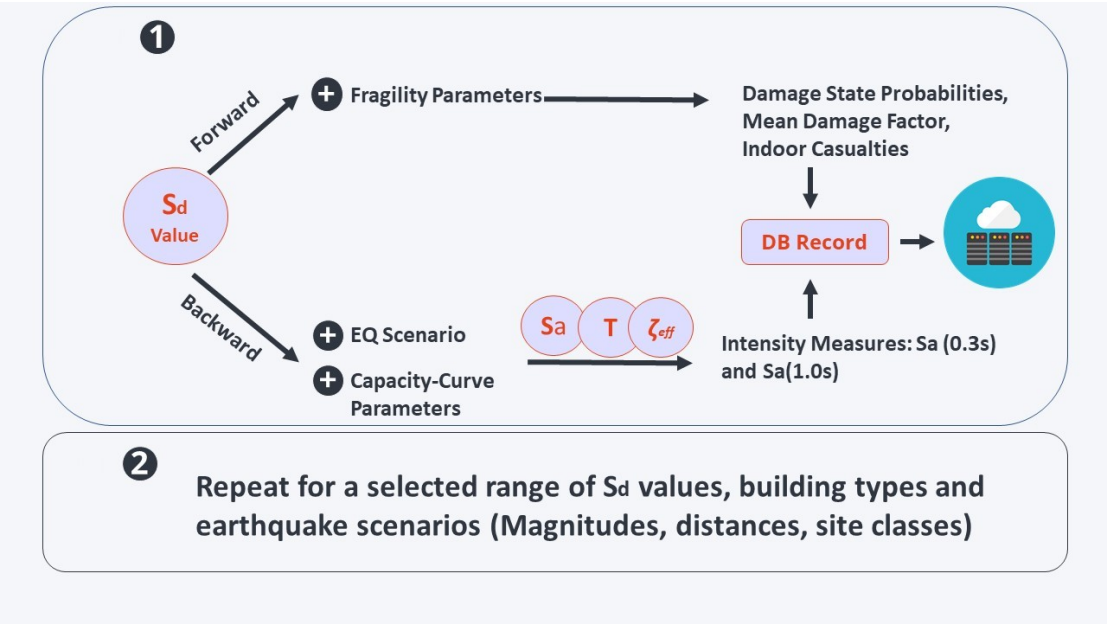

Fig 2-11. Forward (HAZUS) and backward (ER2) methods for computation of building damage states.

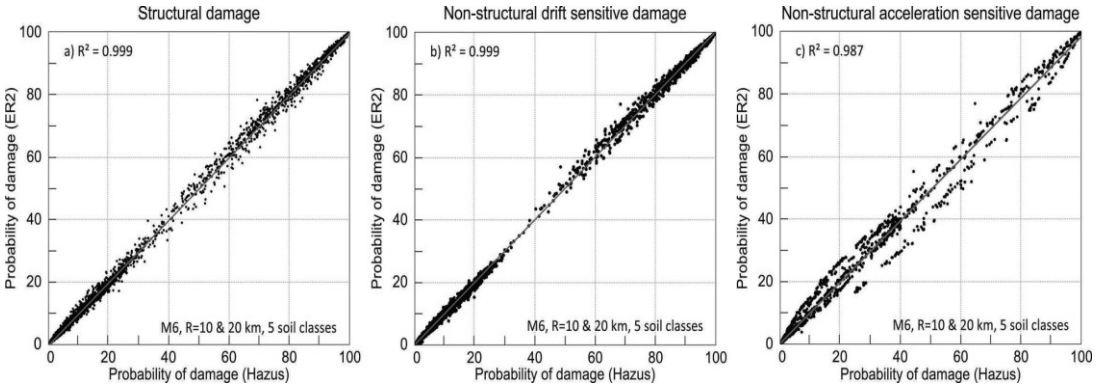

Fig 2-12. Comparison of damage state results between ER2 and HAZUS for 128 building types (adapted from. [14]).

The screen captures of the ER2 execution process accompanied with intuitive step-by-step prompts and instructions are presented in Fig 2-13. For this particular scenario, an earthquake with M7.0, 5 km depth and Atkinson and Adams GMPE [23] was considered. The user first specifies the epicenter within the study region and selects the type of the scenario, what-if event or probabilistic scenario with given return period

(Fig 2-13-1), and then provides the required parameters in the scroll down menus (Figure 13-2). The aggregated loss results are presented at the census tract level (Fig 2-13-3 and 2-13-4).

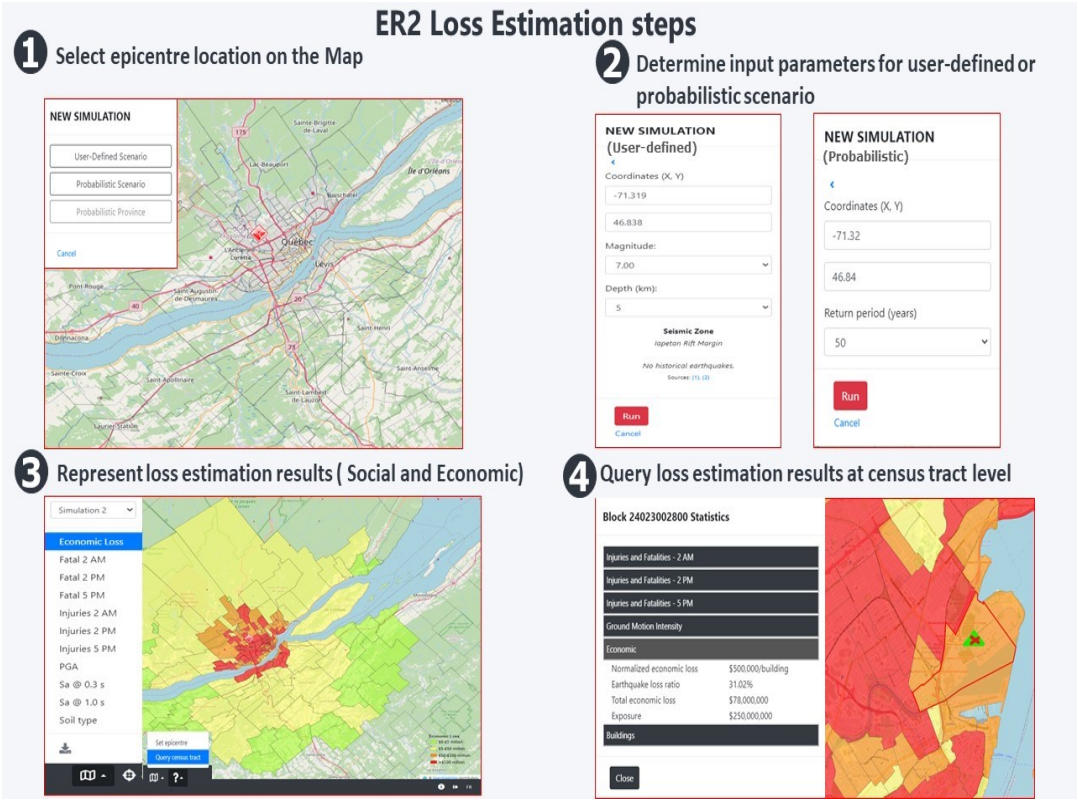

Fig 2-13. Schematic presentation of the consecutive steps when running ER2 for M7and 5 km depth seismic scenario.

2.4.6 CAPRA-Earthquake

CAPRA is another risk assessment platform released in 2008 with the support of the World Bank [122]. This platform is an open-source software programmed in Visual Basic language, and its GUI is relatively easy to understand. This software has different modules for risk assessment: the Strong Motion Analyst deals with processing of strong motion signals and seismological data, Seismic Microzonation Studio focuses on the dynamic soil response in 3D geological environments, and CRISIS 2015 is the PSHA module [123, 124].

The main module is CAPRA-GIS (V 2.4.0), which calculates losses caused by different natural hazards, including earthquakes. CAPRA-GIS performs loss assessment once the required input files (i.e. hazard, exposure and vulnerability files) are imported to this module. The seismic hazard analysis is first conducted by CRISIS 2015 [125], and the results are imported to CAPRA-GIS in *.ame file format for further loss assessments. The hazard model includes a collection of stochastic scenarios related to specific annual frequency of occurrence, spatial distribution of intensity and variability across the region of interest. A new CAPRA module called CAPRA-EQ is currently being developed and will have the capability to conduct stochastic seismic hazard modelling to be used in risk analyses, reduction and management [122].

The damage assessment relies on the vulnerability functions developed for each building type that are provided to the CAPRA-GIS. The development of vulnerability functions is carried out using the CAPRA module ERN-Vulnerabilidad, which is developed by ERN Co. This module considers different methods to generate vulnerability functions and allows the user to define their own functions. The uncertainty in vulnerability functions is considered by adjusting the variance ensuring zero variance for no seismic demand and for infinite demand, considering that the predictable damage is zero for no seismic demand and complete for infinite demand level. The parameters used for adjusting the variance are determined by experts' judgment [126]. CAPRA provides the following outputs over a set of buildings or for a single building: loss exceedance curve, probable maximum loss and average annual loss.

2.4.7 ERGO (MAEviz, mHARP, Hazturk)

Ergo (formerly named MAEviz and mHARP) is also a HAZUS-based loss estimation software developed by Mid-America Earthquake Centre (MAE) and the National Centre for Supercomputing Applications at the University of Illinois [127]. Ergo was developed primarily to perform seismic risk assessment in central U.S. states. Ergo is coded using the JAVA programming language as an open-source software with a user-friendly GUI. The software has also in-built GIS system to represent the input and output data without the need for any commercial package.

The open-source Eclipse Rich Client Platform allows Ergo developers to add new plug-ins to the software. For example, plug-ins were developed to support different types of analysis, base geometries, datasets, data mapping, GIS schemas, locations, metadata, repository types and units [128]. Ergo's visual-based interface uses a combination of the Sakai open source web portal; NEESgrid application platform used for communicating with researchers; and Scientific Annotation Middleware, which enables users to add their own hazard data. In terms of hazard module, Ergo can consider liquefaction and ground shaking. The Ergo catalogue box contains default earthquake scenarios and probabilistic hazard maps whilst users can upload their own hazard within the GUI.

Ergo implements the so-called consequence-based risk management (CRM) [129] using a graphical, menu-driven system to generate damage estimates from scientific and engineering principles and data [126]. CRM is a framework for execution of loss assessment and potential mitigation alternatives aiming at reducing predicted losses to an acceptable level. The CRM paradigm provides philosophical as well as practical framework for assessment of the dynamic inter-disciplinary relationships amongst causes, effects and effect mitigation measures for disaster management. [128].

Ergo has already been integrated into HAZTurk, Turkey's seismic risk assessment platform [130], EQvis European platform [131], and was used for the SYNER-G project, which added a large fragility function manager system [29].

2.4.8 InaSAFE

InaSAFE is a free and open-source software developed by the Indonesia National Disaster Agency and the Australian Government through the Australia–Indonesia Facility for Disaster Reduction in collaboration with the World Bank–Global Facility for Disaster Reduction and Recovery [10]. InaSAFE is a plugin for QGIS, a free and open-source GIS platform intended to help disaster managers to better understand the possible impacts of specific disaster events [132]. The software includes shelter need measurement tools that calculate the amount of food, drinking water, family kits and washroom requirements based on the number of displaced people estimated from the exceedance of an imposed limit for a specific level of damage [133].

MMI is used as the hazard IM and calculated outside the InaSAFE software. Subsequently, it is imported to generate impact functions and loss calculation. InaSAFE calculates economic losses based on floor area and building value. The number of fatalities is calculated using the model developed by Institut Teknologi Bandung (ITB) [134] based on a Bayesian approach and the PAGER fatality model [135]. ITB is based on the limited number of observed fatality rates during four previous fatal events and seems to over-predict the fatality rates at MMI higher than VIII. However, the associated uncertainty for the proposed model has not been addressed [10].

2.4.9 Object-oriented Framework for Infrastructure Modelling and Simulation (OOFIMS)

OOFIMS SLE software has been developed as a part of the SYNER-G project [29] to evaluate the seismic vulnerability of an urban area, including buildings, life lines and transportations systems. OOFIMS is coded in MATALB by utilising the object-oriented programming paradigm. It is an open-source software [136] recently extended to include multiple hazards, such as flood and volcanic hazards. OOFIMS V.4.4 was released in August 2018. In its latest version, Boore and Atkinson GMPE [121] and HAZUS fragility models are included for water supply systems.

OOFIMS can be applied to analyse the vulnerability of interconnected infrastructure systems [137] and portfolios of building. The seismic vulnerability of natural gas transition infrastructure, water supply systems,

electrical power network and transportation systems can also be modelled with this software. The OOFIMS framework has been applied to transportation and electric networks [138] and gas distribution systems in Italy [139].

2.5 DISCUSSION

The considered SLE software has many positive features, such as the implementation of GUI and the possibility for on-screen visualisation of input and output parameters (e.g., Ergo), open-source codes (e.g., SELENA, EQRM, Ergo, ER2), web-based online software free of any charge for use of commercial software (e.g., OpenQuake, ER2), use of logic tree to model epistemic uncertainty (e.g., SELENA), comprehensive user and technical manuals (e.g., SELENA, HAZUS) and the possibility for users to provide their own input data and determine the type of analysis (e.g., user-defined regions, vulnerability functions and hazard parameters).

However, certain limitations have also been observed in terms of the application of the SLE software, including the absence of detailed technical documentation, the need of significant coding, lack of flexibility for user-provided input, wide-range of pre-processing, formatting and input data preparation, lack of GUI, restrictions on the type of analyses and outputs, and most of all the requirement for a high level of expertise for application of majority of the software and the need for licenses to run proprietary software.

Several data acquisition methods have been reviewed in the Exposure section. The most effective method for a given study area can be determined followed by the comparison of the cost of data acquisition against the obtained level accuracy precision of the final datasets, as well as the ability of each of the methods to collect the most important or the ‘more useful’ data.

Different approaches and methods for seismic vulnerability assessment were highlighted. The input data vary considerably based on the seismic vulnerability assessments method, simplified methods that apply data that mostly affect the seismic vulnerability to more complex ones that requires comprehensive information on the buildings and infrastructur characteristics. Given the assessment of seismic vulnerability of a large study area, attaining the level of detail required by the more complex methods could be an important

challenge. Consequently, simplified methods are generally applied. Nonetheless, several methods are focused on specific buildings, infrastructure classes or locations, thereby limiting their wider applicability.

The PSHA can be computationally laborious and its use in regional SLE is potentially less effective. The other more efficient option is to represent the seismic hazard with a large number of earthquake scenarios consistent with the regional seismicity in magnitude, location and associated frequency [140, 141]. OpenQuake and EQRM perform event-based PSHA and analyses, and these processes should be applied to other risk assessment software. For convergence in event-based risk assessment for the rate of exceedance above 10^(−3) at a single location, SES with 200,000 years is generated to achieve reliable results [141]. PSHA-based loss curves overestimate the losses because the aleatory variability in the ground-motion prediction at each site is treated as being entirely inter-event variability where in fact a large component of the variability is intra-event [140, 142, 143].

Problems in scenario loss modelling and probabilistic seismic risk assessment, such as the number of simulations needed to obtain reliable results and convergence in probabilistic event-based loss assessment, effects of selection of GMPEs, assessment of aleatory uncertainty in ground motion and vulnerability and consideration of fault geometry, are encountered [141, 144-146].

HAZUS does not explicitly include uncertainty. The obtained results represent the expected values of losses and do not include uncertainty ranges that would help better understand the potential variability of the results. To some extent, the user can examine the variability of the model by performing a sensitivity analysis. In addition, HAZUS does not consider the epistemic uncertainty that arises from the lack of information. For the time being, this problem is addressed by the logic tree approach only in SELENA [8]. Damage states and loss levels of building structural components defined with qualitative variables (e.g., slight damage state) are not accurate enough and generate high uncertainty in the loss assessment process. Ergo does not support probabilistic assessment. Moreover, it only calculates damages caused by earthquakes, but a user can use USGS probabilistic seismic shake maps as input.

2.6 CONCLUSION

A detailed state-of-the-art review of existing SLE software is presented in this paper. First, the framework and structure of seismic loss assessment were investigated and explained briefly. The review summarises applied seismic risk methodologies and software components helping identify their advantages and limitations and gives directions for future development of risk methods and software.

Various software for seismic loss assessment are developed and applied worldwide, and most of them have the same or similar methodology as the one employed by HAZUS. For example, ER2 was inspired from HAZUS and is applied in Canadian condition; SELENA is another HAZUS based tool that considers epistemic uncertainty and topography effect on seismic risk assessment.

Deterministic scenario earthquake and probabilistic seismic hazard are the two types of earthquakes shaking hazards included in all of the considered SLE software. Most of the software perform their own hazard analyses with the exception of Ergo, Insafe and ER2 that rely on importing respective PSHA shake maps. All of the SLE software have their own embedded inventory datasets or consider it as an input parameter, with OpenQuake intending to provide a global coverage for buildings. Analytical, empirical and expert opinion methods are the three common approaches for providing vulnerability indices and functions used in the analyses. In most SLE software, analytical vulnerability based on the standard CSM is used (e.g., HAZUS and other HAZUS-based software) since no to scarce damage observations exist to calibrate the vulnerability functions in most of the study areas. Therefore, direct implementation of a given SLE in regions other than the one for which it was developed is not recommended due to the different seismotectonic and construction settings.

Various sources of uncertainty exist in the seismic loss assessment procedure (e.g., uncertainty in source characterisation, GMPEs, building inventory, fragility and vulnerability functions). These uncertainties provide information on the expected values and likely ranges for a given input parameter and then propagate to the risk results. However, due to lack of data and difficulties in incorporating and evaluating all potential sources of uncertainty, existing tools generally provide the average results or only partially consider the uncertainties, thereby resulting in variations in risk results. For example, OpenQuake considers uncertainties

in the seismic hazard (e.g., intra and inter-event uncertainties), SELENA applies the logic-tree model to evaluate the uncertainties, and the probabilistic vulnerability functions implicitly consider uncertainty in the physical damage.

Increased demand for online seismic risk assessment tools equipped with GUI that can be accessed via internet and run by users with moderate knowledge and expertise in earthquake engineering and GIS has been observed. OpenQuake and the user-friendly ER2 are pioneers in such online SLE software. These software represent an excellent example for the development of the next generation of SLE tools. Other practical observation was the option for user provided input data and selection of the type of analysis (e.g., user-defined regions, vulnerability functions and hazard parameters), which is currently possible in OpenQuake. Important and practical point would also be the availability of comprehensive user's and technical manuals (e.g., SELENA, HAZUS), which allow users to understand assumptions and simplifications in each step of the loss assessment process.

CHAPTER 3

Article 2: Development of a probabilistic seismic microzonation software considering geological and geotechnical uncertainties

Vahid Hosseinpour [a] *, Ali Saeidi [a], Mohammad Salsabili [a,] Miroslav Nastev [b], Marie-José Nollet [c]

[a] Department of Applied Sciences, Université du Québec à Chicoutimi, Saguenay, G7H 2B1, Saguenay, QC, Canada

[b]Geological Survey of Canada, Natural Resources Canada, G1K 9A9, Quebec City, QC, Canada

[c]Department of Construction Engineering, École de Technologie Supérieure, H3C1K3, Montreal, QC, Canada

*Email: vahid.hosseinpour1@uqac.ca

Revision submitted to Georisk journal, https://www.tandfonline.com/toc/ngrk20/current

Acknowledgements:

The authors would like to thank the members of the CERM-PACES project for their cooperation to conduct the field tests and provide access to the database.

Authors contribution**:**

Vahid Hosseinpour: Conceptualization, Methodology, Formal analysis, Software, Validation, Data Curation, Visualisation, Writing – original draft. **Ali Saeidi:** Conceptualization, Methodology, Funding acquisition, Validation, Project administration, Supervision, Resources, Writing - Review & Editing. **Mohammad Salsabili:** Investigation, field tests. **Miroslav Nastev:** Supervision, Writing - Review & Editing. **Marie-José Nollet:** Supervision, Writing - Review & Editing.

Funding:

This research was partially funded by the Natural Sciences and Engineering Research Council of Canada (NSERC) and Hydro-Quebec under project funding no. RDCPJ 521771-17 and also CRC-NSERC 950-232724.

3.1 ABSTRACT

Modern seismic risk assessment software includes seismic hazard analysis algorithms or relies on precomputed hazard maps. In both cases, a major step is incorporating the impacts of the local geological and geotechnical conditions. The common practice to address this phenomenon, often referred to as site effect, is to use shear wave velocity (V_s)–depth correlation(s) and a deterministic geological model as proxy for the V_s mapping. The V_s of the top 30 m (Vs_{30}) and often the fundamental site period (T_0) are then used as predictors of the potential amplification. Recognizing that local soil properties uncertainties inevitably affect the seismic site response, a stochastic approach for evaluating Vs_{30} and T_0 is proposed herein, considering a combination of probabilistic V_s–depth correlations with a probabilistic 3D geological model. Monte Carlo simulations are applied to study the impact of the uncertainties on the seismic site characterization model. The generated stochastic maps consist of Vs_{30} and T_0 realizations accompanied with the spatial distribution of uncertainty. These results show the spatial extent and level of uncertainty and indicate where further fieldwork is needed to improve predictions. The developed methodology is also being used in a under develop risk assessment software's hazard module.

Keywords: Seismic site characterization, uncertainty integration, Monte Carlo simulation, Shear wave velocity, Hazard assessment.

3.2 INTRODUCTION

Extreme earthquake events are the natural hazard with the potential for the greatest physical, economic, and social losses in Canada, and are known as earthquake risk. Due to significant population and exposure growth in earthquake-prone areas, such as British Columbia and the Ontario/Quebec region, the risk of earthquakes is increasing in certain regions of Canada. Although earthquakes cannot be prevented, a number of strategies can be carried out to prepare for and reduce their negative impacts. The first of which is increasing the knowledge of the seismic hazard and decreasing the vulnerability of structures.

In order to analyse seismic hazard as a component of earthquake risk, it is crucial to account for the effects of overlying geological layers and geotechnical conditions. The duration, amplitude and frequency

content of incoming waves can be affected by the local site conditions, and this phenomenon is known as site effect [15]. In the past decades, the shear wave velocity (V_s) of the top 30 m, Vs_{30}, was established as the standard soil parameter which correlates with the seismic site effects [18-20]. The provisions of national building codes worldwide generally recommend to account for potential site amplification in the evaluation of the base shear force [17, 21, 22] and often in the ground motion prediction equations (GMPEs), that is, attenuation with distance, as a predictor for the intensity of seismic shaking [23]. Another key site-specific parameter is the fundamental site period (T_0). It varies in direct proportion to the difference between the average shear wave velocity ($\mathrm{V_{Save}}$) of the surface sediments and the soil column thickness [24]. In general, thick soil layers that have higher T_0 value are more susceptible to strong earthquakes that occur at a greater distance and have a predominant low frequency content. On the other hand, regions with lower T_0 tend to amplify the energy content at higher frequencies, which is characteristic of earthquakes that occur at a closer distance[24]. At the moment, studies are being conducted in order to explicitly take T_0 into account while determining the potential amplification [147-149].

In parallel, geophysical, geological and geotechnical engineers, engineering seismologists and other experts exerted effort to create seismic risk assessment software for predicting loss estimates, e.g. HAZUS [76] and its derivatives (Ergo [6], Haz-Taiwan [7], SELENA [102] and HazCan), InaSAFE, CAPRA, DBELA, OpenQuake [114], ER2 [14] and so on [3, 37]. Most of these tools run at urban scales and consider event-based and probabilistic seismic hazard scenarios. To this end, these tools comprise algorithms to generate seismic intensity shake maps involving GMPEs and local site effects. The latter parameter is generally applied to loss assessment software by considering the national building codes, e.g. NEHRP [16] for HAZUS and NBCC2015 [17] for ER2 [14], IBC-2006 [150] and EuroCode8 [21] in SELENA. In case of OpenQuake engine, the site effect is considered by direct application of $Vs30$ through GMPEs. However, the deterministic technique is used by many of the presented software to apply the site effect. These software packages do not account for site parameter uncertainties which have a significant influence on the quantity of the estimated hazard parameter value. Uncertainties related to the local soil properties unavoidably affect the seismic site response and hazard estimates. The typical objective of the modelling exercise should focus on describing and quantifying those uncertainties to allow better informed choices. The spatial variabilities of the

soil geological and geotechnical parameters result from different sources of uncertainty. They may be broken down into the two primary categories of aleatory uncertainty [25, 26] and epistemic uncertainty [151, 152].

Only a few works have explored the uncertainty of Vs_{30} for urban-scale seismic site microzonation analyses, particularly in Eastern Canada [38, 153-156]. For Montreal region, Rosset et al. [154] calculated the magnitude and the variance of Vs_{30} with respect to different soil units and 3D geological stratigraphies. The conditional second-moment analysis concluded that the combination of a four-layer surficial geology model with T_0 field measurements yields lowest uncertainty. In the consecutive study, a procedure proposed based on conditional second-moment analysis to estimate Vs_{30} and its uncertainty [153]. They used these estimations to generate probability maps for soil classification and calculate the expected values and variance of amplification factors and 3D deterministic geological models developed based on interpretation of the available geological data and V_s and T_0 measurements in the Ottawa–Quebec and Chicoutimi regions, respectively [38, 155]. Generic V_s-depth regression analyses were conducted in post-glacial sediments incorporating uniform uncertainty with depth [155]. Their results confirmed similar Vs_{30} standard deviation values averaged across the study area of about 30%. The above eastern Canadian studies concluded that analyses considering soil uncertainty produced results different than when deterministic properties were assumed. They all used deterministic geological models inadequate to capture the observed heterogeneity and uncertainties in the occurrence of surficial soil units. This is particularly true in the vertical direction, where the particle size distribution of the layered post-glacial sediments (clays, silts, sands and gravels mainly of marine and alluvial origin) is known to be irregular and associated to relatively thin layers. In addition, the standard regression V_s-depth analyses considered normally distributed population error around the mean response value yielding uniform standard deviation with depth. Knowing that not only the geological and geotechnical parameters but also their uncertainties vary with depth, such over-simplification may actually increase the degree of uncertainty in the final seismic site response.

A number of methods are available in the literature to address the uncertainties of the shear wave velocity. Among them, the stochastic modelling derives the probability distribution of the random variable from a large number of simulations, varying one or more input variables at a time and taking into account the impacts of the coefficients of variation. For example, in a seismic site response analysis, Bazzurro et. al. [157]

applied the MC simulation to evaluate the effects of the input ground shaking parameter and sediments parameters on the nonlinear amplification function. Sun et al. [158] proposed an original statistical model to randomise the layered stratigraphy and respective shear wave velocities assuming a lognormal distribution of V_s. Toro [159] performed a MC-based site response analysis to assess the outcome of V_s uncertainty on the predicted ground motion parameter.

The objective of the present study is to develop a probabilistic site effect assessment algorithm considering uncertainties in geological model (probability of occurrence of a given soil type) and geotechnical parameters. A Monte-Carlo based (MC-based) approach was applied to quantify both uncertainty types with particular focus on the effect of randomised V_s values on seismic microzonation classes in terms of $Vs30$. The Saguenay-Lac-St-Jean region in eastern Quebec province (Canada) was chosen as the research region owing to the highly heterogenous Quaternary sediments of variable thickness. The geological uncertainty was determined from an existing probabilistic 3D geological block model with categorical soil variables (sand, clay, gravel and till). The V_s data, measured with SCPT, were analysed on the basis of soil category (sand, clay, gravel or till) and measurement depth. The conventional regression functions for V_s data were developed for each soil type. The best fit probability distribution functions for each soil category and each 2 m depth were selected using the chi-square test and Q-Q plot. The MC simulations were conducted taking independent samples of respective V_s variables within the pre-determined distributions. The final probabilistic seismic microzonation maps include $Vs30$ and T_0 realizations and their spatial distribution of the uncertainties. The mean $Vs30$ and T_0 field and the spatial distribution of the uncertainty were developed using Monte Carlo method.

3.3 METHODOLOGY

The setback of using V_s in seismic site characterisation and the assessment of the potential seismic shaking at urban and regional scales is the number of V_s measurements required to generate results with reasonable accuracy. The uncertainties associated with the local soil properties inevitably affect the seismic site response, which is otherwise unable to be properly assessed using the conventional deterministic approach. Hence, the typical objective of the modelling exercise should focus on describing and quantifying

those uncertainties to allow better informed choices. This emphasises the need for a well validated and robust spatial interpolation method that can consider uncertainties in the interpretation of geological units and in observations of V_s.

In the present study, a novel MC-based approach was applied to develop the $Vs30$ spatial distribution. In order to implement the methodology that was suggested, the following steps were taken into account:

3.3.1 3D geological model implementation

The probabilistic 3D geological of subsurface sediments model was created based on the knowledge developed in the previous study [160]. To this end, various surface and subsurface data were gathered including 3,524 data acquired from borehole logs from the provincial water well database (https://www.environnement.gouv.qc.ca/eau/souterraines/sih/) and exploratory and geotechnical drilling records. This information was complemented with data derived from interpretations of 26 geological cross-sections, 1033 bedrock outcrops and veneer till polygons from the surficial geological map. Next, a 3D volume was created to reproduce the depth and thickness of each soil type (till, clay, sand and gravel) using the digital elevation model (DEM). For this purpose, the till interface with the underlying bedrock formations and the superimposed post-glacial units, the till thickness map and the total thickness of unconsolidated sediments must be created. The volume between the ground surface and the bedrock interface was modelled with a grid of 155 800 2D 75 × 75 m grid cells at the surface and 1 061 200 3D block elements of 75 × 75 × 2 m extending all the way to the bedrock interface. The glacial sediments were assumed to constitute a single continuous soil layer. For the discontinuous post-glacial sediments (clay, sand and gravel) the probability of occurrence was determined based on the simulations with the sequential indicator simulation method (SIS) [160]. Fig 3-1 shows one of the SIS realizations of the 3D geological model.

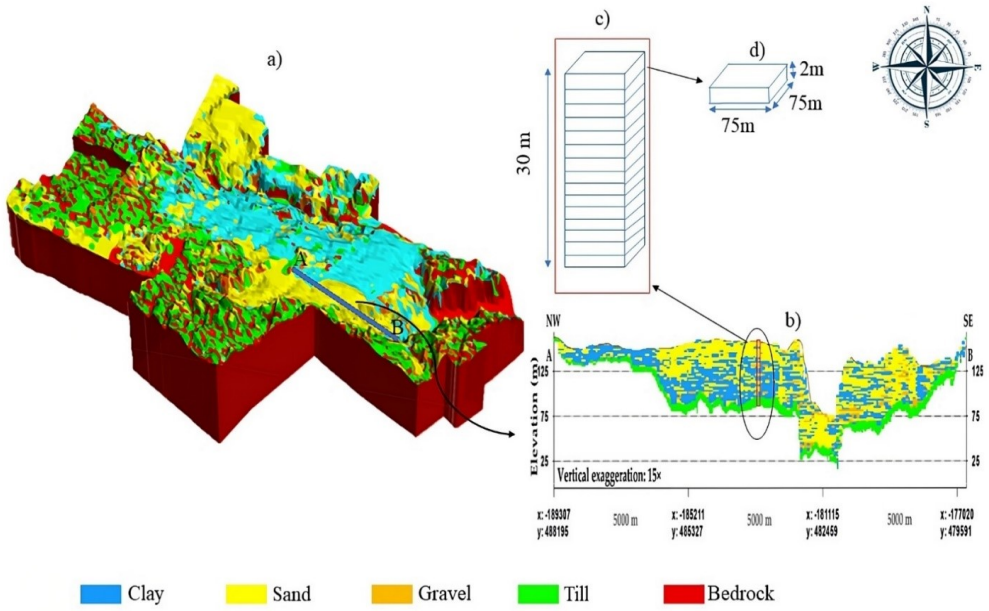

Fig 3-1. 3D geological model with an example of a cross section with block elements (Modified from: [160]).

3.3.2 Shear wave velocity measurement and V_s-depth regression development

The intensity of the seismic shaking at the ground surface is governed in part by V_s of the topsoil layers, with building codes recommending higher amplification factors of the shaking at sites with lower V_s. This important geotechnical parameter defines the shear modulus and the soil behaviour at small strain amplitudes (elastic behaviour). Higher V_s values are observed in stiffer/denser soils and rock. It can be measured or inferred from laboratory or in situ tests, e.g., cone penetration test (CPT), seismic cone penetration (SCPT), standard penetration test (SPT) and so on.

In this study, the V_s database of postglacial sediments was compiled from field measurements at 16 locations (Fig 3-6) [161]. SCPT tests were conducted within the study area by the authors with a complete set of measurements. In total, there are 733 V_s observations in fine sediments and 277 in coarse sediments. The SCPTu soundings were conducted utilizing a standard type 2 piezocone with the following specifications: a

60° apex angle, a conical tip with a base area of 10 cm², and a sleeve area of 150 cm², with the filter positioned at the shoulder. All SCPTu soundings were executed at a penetration rate of 2 cm/s. High-resolution CPTu data were gathered at intervals of 1 cm, and Vs values were recorded at each 50 cm depth interval. The V_s-depth data are compared in Fig 3-2 together with regression analysis [158, 162]. Sand units display comparatively higher V_s than clays, but the values seem to be overlapping with apparent discrepancies well within the potential variabilities causing from field measurement, methods of data interpretation, geological information and geological modelling. Both groups exhibit a large amount of scatter in their V_s data due to the heterogeneity in the grain-size distribution as well as the compactness of the grains. In practice, when the number of measured data is limited, the above simplified assumption of uniform variance with depth can actually increase the uncertainty in the Vs_{30} results.

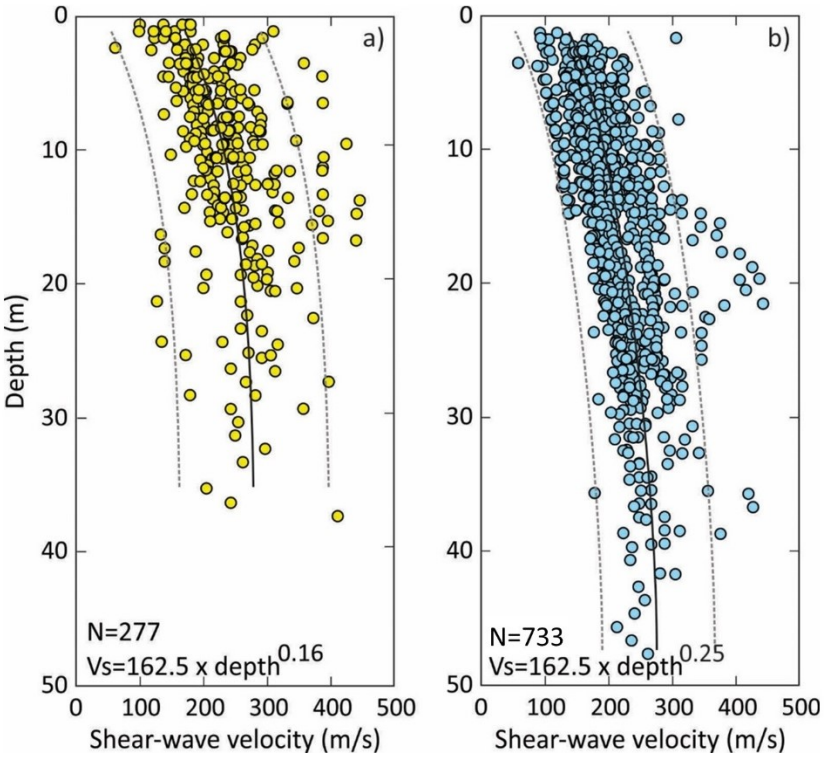

Fig 3-2. V_s data for: a) coarse sediments (sand and gravel), b) fine sediments (clay and silt). Bold black lines illustrate conventional regression functions; dashed red lines show 95% confidence intervals.

As no SCPTu measurements could be conducted in the glacial sediments, a representative regional V_s-till value of 580 ±175 m/s was assumed as proposed by Motazedian et al. [163]. The σ_{till} value is used in the next chapters which discuss the proposed probabilistic approach. Similarly, a regional V_s value of 2500 m/s was assigned to the bedrock formations [38].

3.3.3 Distribution fitting to the V_s data

Fig 3-3 represents the method employed for determining the V_s distributions for different soil types. It is assumed herein that the distribution of V_s measurements at different depths is not uniform and vary with respect to the encountered geological and geotechnical heterogeneities and the number of field measurements. First, V_s data respective to the sandy and clayey soil units were extracted from the database and separated into 2 m sections, coincident to the geological 2 m-thick model blocks. The histogram bin count was then determined, and ten widely used probability distribution functions, suggested in the Python's SciPy library [164], were fitted to the V_s data: normal, lognormal, beta, gamma, Pearson, inverse Gaussian, exponential, Weibull, triangular and the uniform distribution functions. To choose the distribution that best represents the data probability density, the distribution fitting performance was assessed with the Chi-square statistics and Q-Q plots [165].

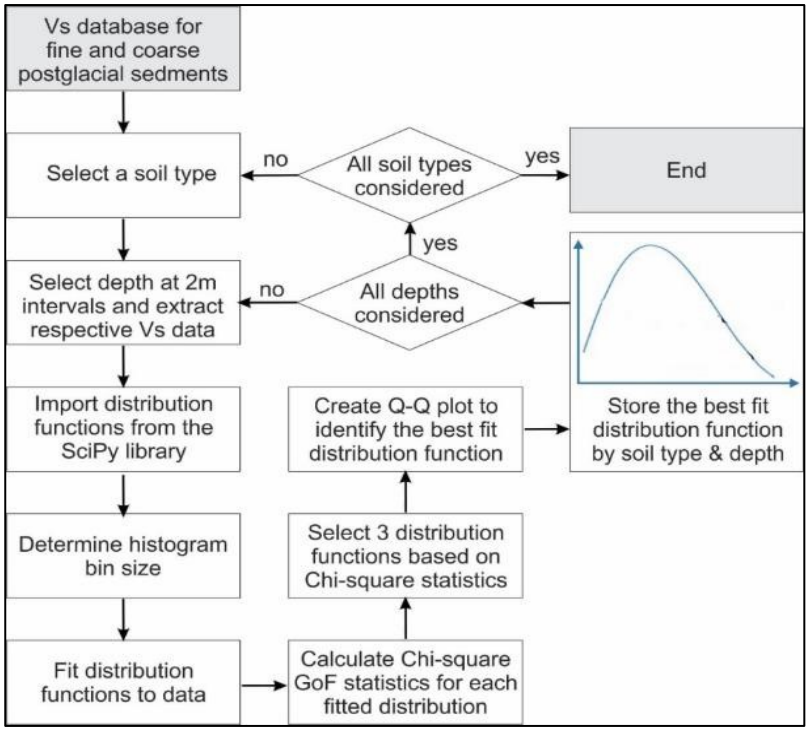

Fig 3-3. Algorithm for fitting of the interval V_s distribution function.

The chi-square test provides a standardised comparison between the data histogram and the density function of the fitted distribution. In order to calculate the chi-square test statistics in the discrete case, the range of the fitted distribution was split into *k* contiguous intervals $[a_0, a_1)$, $[a_1, a_2)$, …, $[a_{k-1}, a_k)$ and the following equation was applied:

$$\hat{\chi}^2 = \sum_{j=1}^{k} \frac{(N_j - np_j)^2}{np_j} \tag{3-1}$$

where k is the number of adjacent intervals, N_j is the number of X_i's in the j^{th} interval $[a_{j-1}, a_j)$. Note that $\sum_{j=1}^{k} N_j = n$, p_j is the expected proportion of X_i's that would fall in the j^{th} interval if sampling from the fitted distribution.

The selection of the V_s probability distribution function with depth was automated. The chi-square statistics was computed for each probability distribution, and the distributions were sorted according to the

chi-square value in decreasing order. A Q-Q plot was created for the three first distributions to identify the best fit distribution for each soil type–depth pair.

3.3.4 Monte Carlo approach for site parameters calculation

Once the probabilistic 3D geological model and interval V_s distribution functions were determined according to the soil type and depth, MC simulations were conducted to evaluate the Vs_{30} spatial and vertical variability considering the uncertainty of the soil geological and geotechnical parameters. The flow chart of the developed MC-based approach is given in Fig 3-4.

The vertical stratigraphy was simulated for each of the grid cells by sampling the soil type at 2 m depth. Simultaneously, the respective best-fit V_s probability distribution function was retrieved for the given soil type and depth, and the V_s value was randomly generated. The number of random variables was determined based on the thickness of the geological units column. The V_s estimates were sampled from related distribution based on soil type and depth of block.

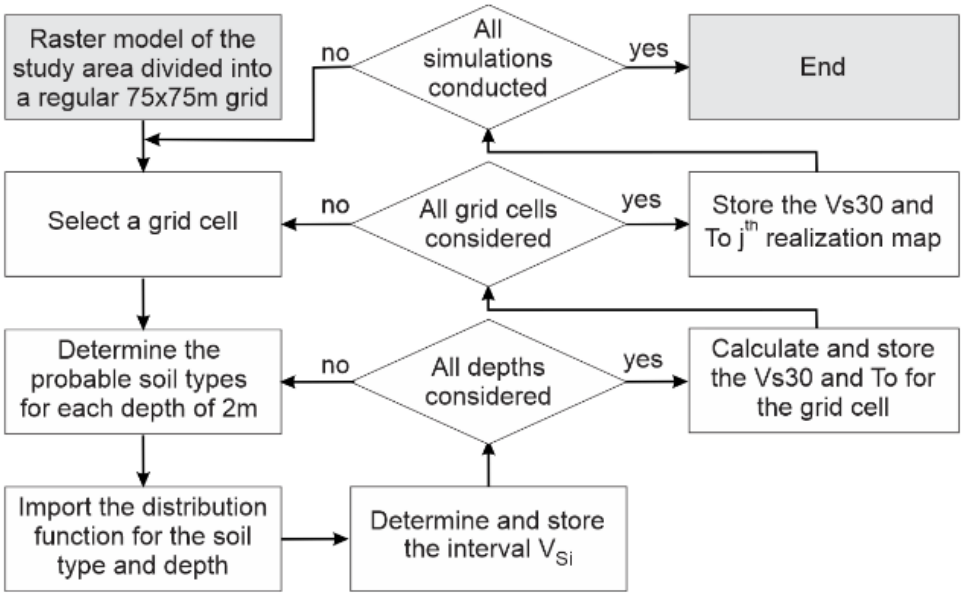

Fig 3-4. Flow chart of the Monte Carlo simulation process for Vs30 and T0 calculation.

The random generation of V_s values was repeated 15 times (for each soil block) or until the bedrock unit was reached. The Vs_{30} value was then calculated using the following equation [24]:

$$Vs_{30} = \frac{30}{\sum \frac{h_i}{V_{Si}} + \frac{(30 - (h_{till} + \sum hi))}{V_{Srock}}} \quad (3\text{-}2)$$

Where h_i is the thickness of each soil block (2 m in this case), V_{Si} is the randomised variable of V_s in the ith block, and V_{Still} and V_{Srock} are the shear wave velocities of the glacial sediments and bedrock assumed as uniform across the study area.

To calculate probabilistic T_0 values, the average V_s was first calculated using Equation 3. The T_0 values for each point of the grid cell was then calculated using Equation 3-4.

$$V_{S_{avg}} = \frac{H}{\sum \frac{h_i}{V_{Si}}} \quad (3\text{-}3)$$

Where H is the total thickness of the surficial sediments from the ground surface to the bedrock interval, h_i represent the thickness of each respective soil block (2 m in this case) and V_{Si} is the randomised variable of V_s in the ith block.

$$T_n = \frac{4H}{V_{Savg}(1 + 2n)} \quad (3\text{-}4)$$

Where V_{Save} is the average V_s down to the bedrock computed with Equation 3, n=1 for the fundamental vibration period and n≥1 indicates higher harmonics. Equations 3-2, 3-3 and 3-4 are valid for a stratigraphic profile where all three major geological units were encountered (post-glacial and glacial sediments and bedrock). The respective variables were removed from the denominator when one or two of the units were missing.

In each simulation, the above process was repeated for each grid cell, and a Vs_{30} map realization was generated. The MC simulations were run until the stability of the shear wave velocity values. To determine the stop condition, i.e. the maximum number of simulations, four example raster cells were selected on the basis of the different geological profiles encountered in the top 30 m: #1 contains glacial and post-glacial sediments in the top 30 m, #2 include all the geological units, whereas #3 and #4 include post-glacial sediments only. Fig 3-5 shows the variation of the predicted average Vs_{30} in the raster cells with the number of simulations.

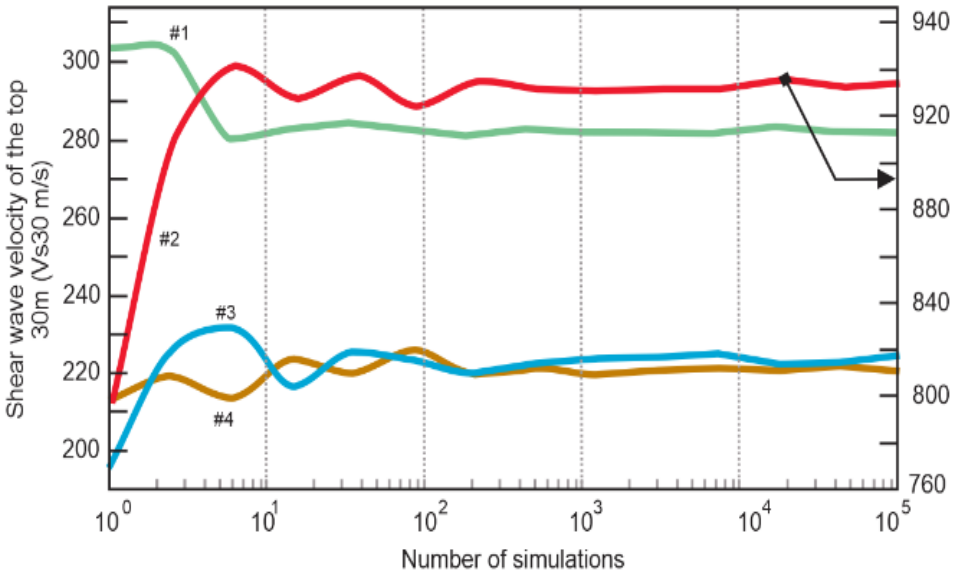

Fig 3-5. Convergence of the mean Vs30 with the increasing number of realizations (The right-hand vertical axis is valid for the grid-cell #2)

As is apparent from Fig 3-5, the stability of the response variable Vs_{30} is attained already after a few hundred simulations regardless of the stratigraphy. This is important observation since a potential relationship between the number of simulations and the stratigraphy could introduce an unwanted bias or to unnecessary increase the CPU time spent. It was therefore decided to limit the number of MC simulations of the seismic site parameters to 1000 as a more conservative option. In each MC simulation, the above process was repeated for each of the 155 800 raster cells. Following each simulation, the realizations of Vs_{30} and T_0, computed as functions of the Vs_{avg} with mentioned equations, were stored in the temporary database. At the

end of the 1000 simulations, the standard deviations maps Vs_{30} and T_0 were created as quantitative measures of the considered geological and geotechnical uncertainties.

3.4 STUDY AREA

Saguenay city (Fig 3-6) is the central municipality in the Saguenay–Lac-Saint-Jean region, Eastern Quebec (Canada), located approximately 200 km north from Quebec City. It has 147 100 inhabitents and a land area of 1 136 km^2 split into three major localities: Chicoutimi, Jonquiere, and La-Baie. The study area is characterised by a moderate local seismic hazard, whereas on the regional scale, it is affected by the Charlevoix–Kamouraska seismic zone about 75 km southward, which is the most active area in Eastern Canada [166]. The strongest recorded earthquake in the region is the 1988 M5.9 Saguenay earthquake, the strongest earthquake in eastern North America in the twentieth century. The negative impacts were frequently reported to local brick masonry structures, and several embankment failures also occurred. In addition, non-structural damage was done to the former Montreal East City Hall in Montreal, 350 km from the epicentre, and the ground shaking was felt as far as Toronto and Boston, both at a distance of about 800 km [167].

3.4.1 Local geology

The bedrock in the Saguenay makes part of the Grenville Province of the Canadian Shield, composed of crystalline Precambrian rocks [168]. The different soil units can be divided into two main categories, glacial deposits and post-glacial sediments [169-171]. The bedrock at the base of the geological column is covered with glacial deposits (till), practically ubiquitous in the region. The overlying post-glacial deposits can further be classified with respect to their grain-size composition into three major units: gravel, clay and sands.

Till was generated by glacial abrasion of parent bedrock and was deposited mostly during the final advance of the Laurentian glacier, around 20,000 years ago. This poorly sorted mix of debris material is compact and semi consolidated with irregular thickness ranging from a few metres to ten metres in certain places. In the highlands, the <1 m thick till deposits is discontinuous and alternated with rock outcrops [170]. Gravely sediments are mainly of glaciofluvial and sometimes of alluvial origin. They consist of a mixture of

gravel, sand, and less frequently of lenses of till and even boulders transported during high discharge periods. This unit appears occasionally, often in combination with till or sandy units. Clays are known as Laflamme marine clays and constitute the dominant soil type in the study region in terms of volume. They are mostly comprised of fine silty materials, silty clay and clayey silt. In average up to 10 m thick, these sediments can be reach a maximum thickness of more than 100 m in the lowlands. Sands consist mostly of shallow sheets of coarse glacio-marine sediments and alluvial sands.

Other unconsolidated sediments of much lesser extent can also be found in the study area, such as less than 2–3 m-thick sequences of floodplain sediments, bog sediments and colluvium. For the purpose of this study, they are regrouped into sand, clay and/or gravely material based on the grain-size distribution. Fig 3-6 shows maps of unconsolidated surficial deposits together with the estimated thickness. The relatively shallow glacial deposits in the highlands and thicker marine clays in the lowlands are the most common soil types at the ground surface.

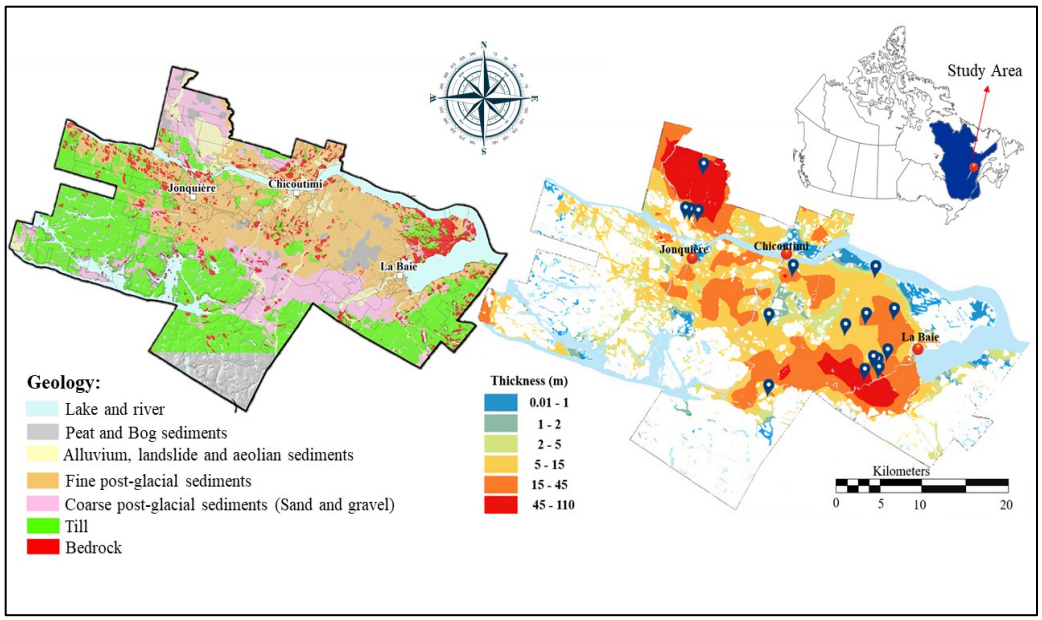

Fig 3-6. Study area: (a) surficial geology map, and (b) total thickness of unconsolidated sediments. Black dots indicate locations of the SCPT test sites discussed in the next chapter (Modified from: [160]).

3.5 SIMULATION RESULTS AND VALIDATION

The approach proposed above for incorporating the geological and geotechnical uncertainties into site characterization analysis was applied for specific site. The average site parameter value was obtained by calculating the mean value of Vs_{30} and T_0 values obtained from for 1000 realizations. The influence of uncertainty in V_s was investigated by determining the distributions for soils in different depths and application of MC method. The most representative results of the stochastic site parameters evaluation are presented and discussed in this section, including: (1) results from conventional assessment of site parameters, (2) fitted distribution for measured V_s values, (3) probabilistic Vs_{30} and T_0 map and seismic microzonation variability map and (4) comparison map with conventional deterministic method.

3.5.1 Conventional assessment of site parameters

Both seismic site parameters Vs_{30} and T_0 are functions of V_s. The common practice to assess their spatial distributions is to use site specific V_s –depth correlations for each soil unit considered in the deterministic geological model applied as a proxy for the spatial distribution of V_s.

The interval V_s–depth correlations were determined for the post-glacial sand and clay soil types (Fig 3-2), whereas for glacial sediments, the uniform value was applied across the study area. In each grid cell of the 3D geological model, the respective V_s values were assigned to the encountered vertical stratigraphy, and a final travel-time weighted average V_s was calculated following Equation 3-5 (modified from Equation 3-3):

$$\mathrm{V_{S}}_{avg} = \frac{\mathrm{H}}{\sum_1^{\mathrm{m}} \frac{\mathrm{h_{si}}}{\mathrm{V_{Ssi}}} + \sum_1^{\mathrm{n}} \frac{\mathrm{h_{cj}}}{\mathrm{V_{Scj}}} + \sum_1^{\mathrm{p}} \frac{\mathrm{h_{tk}}}{\mathrm{V_{Still}}}} \tag{3-5}$$

Where H is the total thickness of the surficial sediments from the ground surface to the bedrock interval; hs_i, hc_j and h_{tk} represent the thickness of each respective soil block (2 m in this case); i, j and k are indexes of summation; stopping points m, n and p represent the number of blocks for each soil unit in the soil column;

V_{Ssi} and V_{Sci} are the shear wave velocities of the sand and clay soil units at depths $2i$ and $2j$, respectively and $V_{Still} = 580$ m/s.

Similarly, Vs_{30} was computed for the first 30 m, which may also include part of the underlying bedrock as stated with Equation 6 (modified from Equation 3-2):

$$Vs_{30} = \frac{30}{\sum_1^m \frac{h_i}{V_{Ssi}} + \sum_1^n \frac{h_j}{V_{Scj}} + \sum_1^p \frac{h_{till}}{V_{Still}} + \frac{(30 - (h_S + h_C + h_{till}))}{V_{Srock}}} \quad (3\text{-}6)$$

Where h_s, h_c and h_{till} are the respective thicknesses of the sand, clay and till units within the soil column and V_{Srock}=2500 m/s is assumed uniform across the study area. Equations 3-1 and 3-2 are valid for a stratigraphic profile where all three major geological units are encountered (post-glacial and glacial sediments and bedrock). The respective variables were removed from the denominator when some of the considered units were missing.

To compute approximate T_0, equation 3-4 modified as following and applied to 3D block model:

$$T_n = \frac{4(h_S + h_C + h_{till})}{V_{Savg}(1 + 2n)} \quad (3\text{-}7)$$

Where Vs_{avg} is the average shear wave velocity calculated with Equation 3, $n = 0$ for the T_0, and h_s, h_c and h_{till} are the respective thicknesses of the sand, clay and till units within the soil column. The spatial distributions of Vs_{30} and T_0 are given in Fig 3-7.

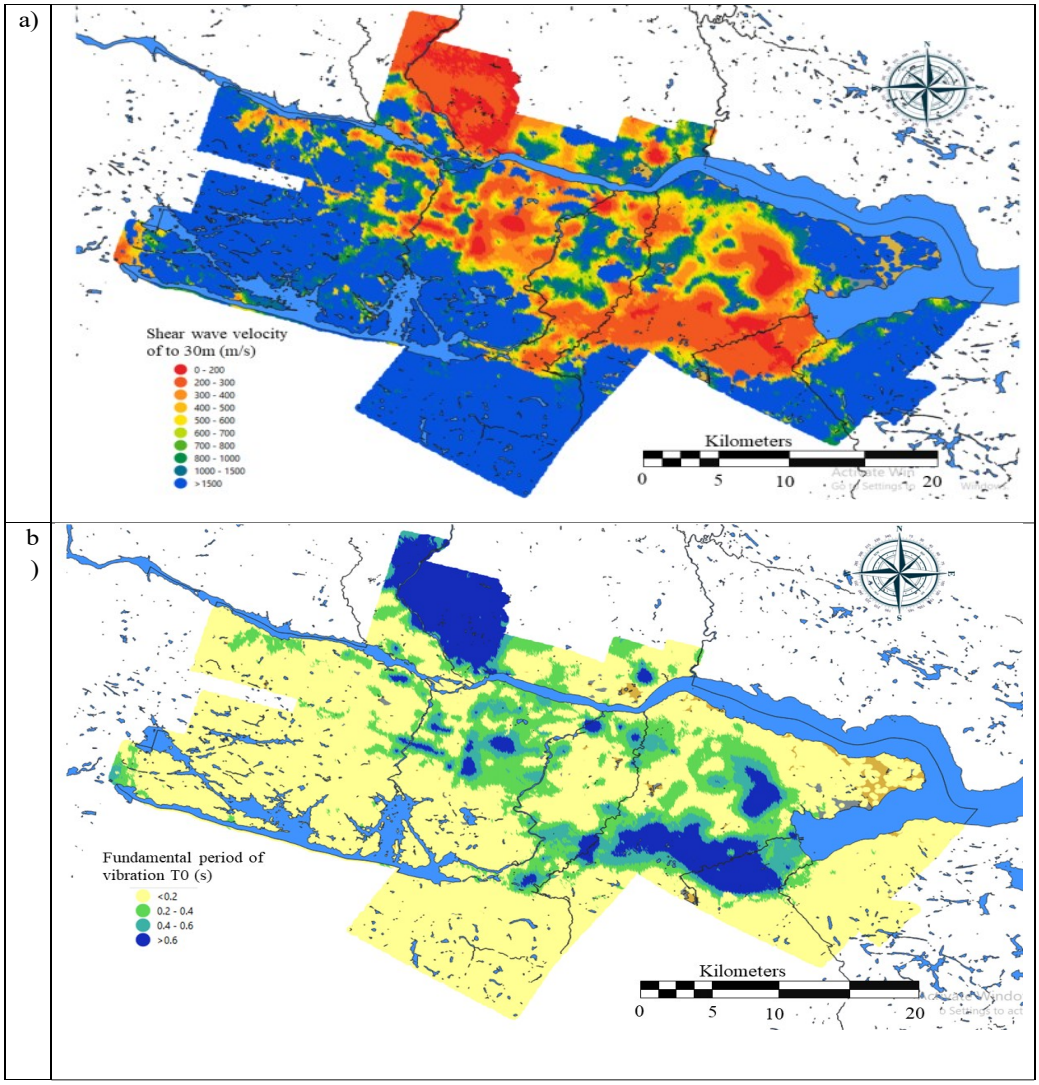

Fig 3-7. Vs_{30} and To maps based on the deterministic 3D geological model and conventional V_s-depth regression models.

3.5.2 V_s-depth probability distributions

Table 3-1 shows distribution types obtained from the combination of the Chi-square method and Q-Q plot. Distribution type and parameter depends on soil type-depth condition. For the clay shear wave velocity data, the selected distribution functions in frequency order are gamma, inverse Gaussian, and beta distribution. For the sand and gravel data, the three most selected distributions are normal, beta and uniform distribution. Fig 3-8 represents the distribution shapes used for variability incorporation of clay and coarse soil types V_s. The distribution of shear wave velocity is not the same for all the data, and it changes by increment of the depth. Consequently, considering same distribution types and parameters for all data (as commonly used in previous studies) could cause uncertainty in seismic hazard assessment.

Table 3-1. Final distribution types and equations used for random variable generation and Vs_{30} model development.

Z(m)	Clay V_s data distributions		Sand V_s data distribution	
0 - 2 m	Inverse gaussian	$f(x) = \sqrt{\frac{1.126}{2\pi x^3}}\, e^{-\frac{1.126(x-122.1)^2}{2x122.1^2}}$	Normal	$f(x) = \frac{1}{51.14\sqrt{2\pi}} e^{-\frac{1}{2}\left(\frac{x-167.29}{51.14}\right)^2}$
2 -4 m	Pearson 3	Skewness parameter = -0.514	Normal	$f(x) = \frac{1}{46.42\sqrt{2\pi}} e^{-\frac{1}{2}\left(\frac{x-195}{46.42}\right)^2}$
4 - 6 m	Beta	$\frac{\Gamma(6.55+7.22)x^{6.55-1}(1-x)^{7.22-1}}{\Gamma(6.55)\Gamma(7.22)}$	Normal	$f(x) = \frac{1}{32.79\sqrt{2\pi}} e^{-\frac{1}{2}\left(\frac{x-200.7}{32.79}\right)^2}$
6 - 8 m	Beta	$\frac{\Gamma(1.4+2.18)x^{1.4-1}(1-x)^{2.18-1}}{\Gamma(1.4)\Gamma(2.18)}$	Inverse gaussian	$f(x) = \sqrt{\frac{0.057}{2\pi x^3}}\, e^{-\frac{0.057(x-224.9)^2}{2x224.9^2}}$
8 - 10 m	Gamma	$f(x, 19.7) = \frac{x^{19.7-1}e^{-x}}{\Gamma(19.7)}$	Beta	$\frac{\Gamma(1.24+2.48)x^{1.24-1}(1-x)^{2.48-1}}{\Gamma(1.24)\Gamma(2.48)}$
10 - 12 m	Normal	$f(x) = \frac{1}{40\sqrt{2\pi}} e^{-\frac{1}{2}\left(\frac{x-193.86}{40}\right)^2}$	Gamma	$f(x, 7.07) = \frac{x^{7.07-1}e^{-x}}{\Gamma(7.07)}$
12 - 14 m	Beta	$\frac{\Gamma(2.27+3.39)x^{2.27-1}(1-x)^{3.39-1}}{\Gamma(2.27)\Gamma(3.39)}$	Gamma	$f(x, 1.88) = \frac{x^{1.88-1}e^{-x}}{\Gamma(1.88)}$
14 - 16 m	Gamma	$f(x, 3.64) = \frac{x^{3.64-1}e^{-x}}{\Gamma(3.64)}$	Beta	$\frac{\Gamma(0.82+0.98)x^{0.82-1}(1-x)^{0.98-1}}{\Gamma(0.82)\Gamma(0.98)}$
16 - 18 m	Inverse gaussian	$f(x) = \sqrt{\frac{0.64}{2\pi x^3}}\, e^{-\frac{0.64(x-223.64)^2}{2x223.64^2}}$	Normal	$f(x) = \frac{1}{80.94\sqrt{2\pi}} e^{-\frac{1}{2}\left(\frac{x-251.27}{80.94}\right)^2}$
18 - 20 m	I-nverse gaussian	$f(x) = \sqrt{\frac{0.598}{2\pi x^3}}\, e^{-\frac{0.598(x-235.38)^2}{2x235.38^2}}$	Normal	$f(x) = \frac{1}{53.03\sqrt{2\pi}} e^{-\frac{1}{2}\left(\frac{x-258}{53.03}\right)^2}$
20 - 22 m	Gamma	$f(x, 1.32) = \frac{x^{1.32-1}e^{-x}}{\Gamma(1.32)}$	Beta	$\frac{\Gamma(0.72+0.3)x^{0.72-1}(1-x)^{0.3-1}}{\Gamma(0.72)\Gamma(0.3)}$
22 - 24 m	Pearson 3	Skewness parameter = 0.82	Uniform	μ= 258.0, σ=33.0
24 -26 m	Inverse gaussian	$f(x) = \sqrt{\frac{0.276}{2\pi x^3}}\, e^{-\frac{0.276(x-247.42)^2}{2x247.42^2}}$	Normal	$f(x) = \frac{1}{71.93\sqrt{2\pi}} e^{-\frac{1}{2}\left(\frac{x-227.83}{71.93}\right)^2}$
26 - 28 m	Gamma	$f(x, 2.74) = \frac{x^{2.74-1}e^{-x}}{\Gamma(2.74)}$	Uniform	μ= 242.0, σ=70.0
28 - 30	Uniform	μ= 184, σ=115	Uniform	μ=178.0, σ=103.0

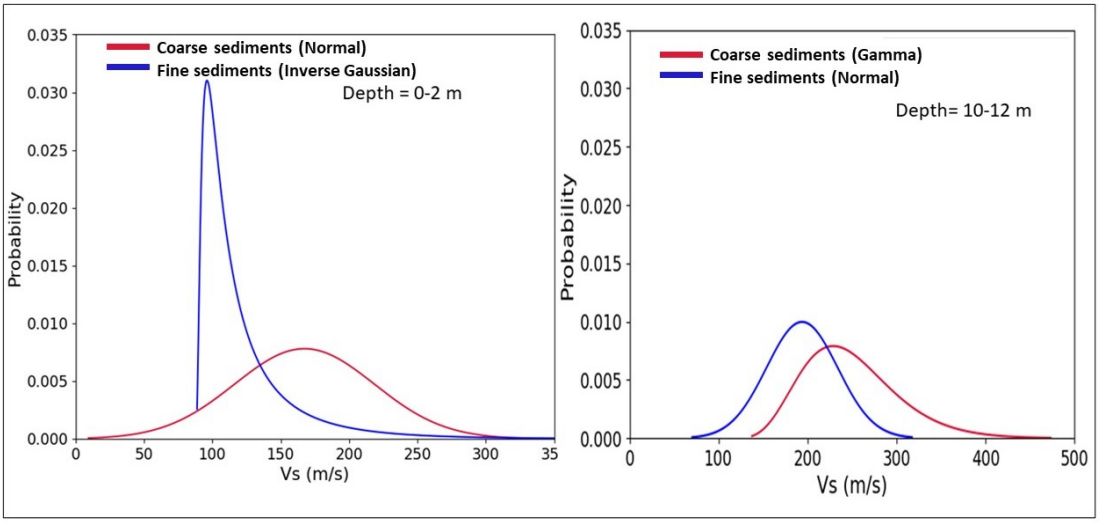

Fig 3-8. Probability distribution functions used in the V_s simulations for clayey soil and sandy soil (See Appendix for other distributions figures)

Fig 3-9 shows an example of Q-Q plot analysis which was performed for clay soil type V_s data at depths between 12 and 14 m. For this particular depth, five probability distributions were selected first by chi-square, among which the beta distribution shows superior performance. As for the other four distributions, they all exhibit outliers at beginning and end of the range. The same process was repeated for each of the soil type–depth pairs. As a result, 30 Q-Q plot analyses were performed to obtain the final V_s–depth distributions.

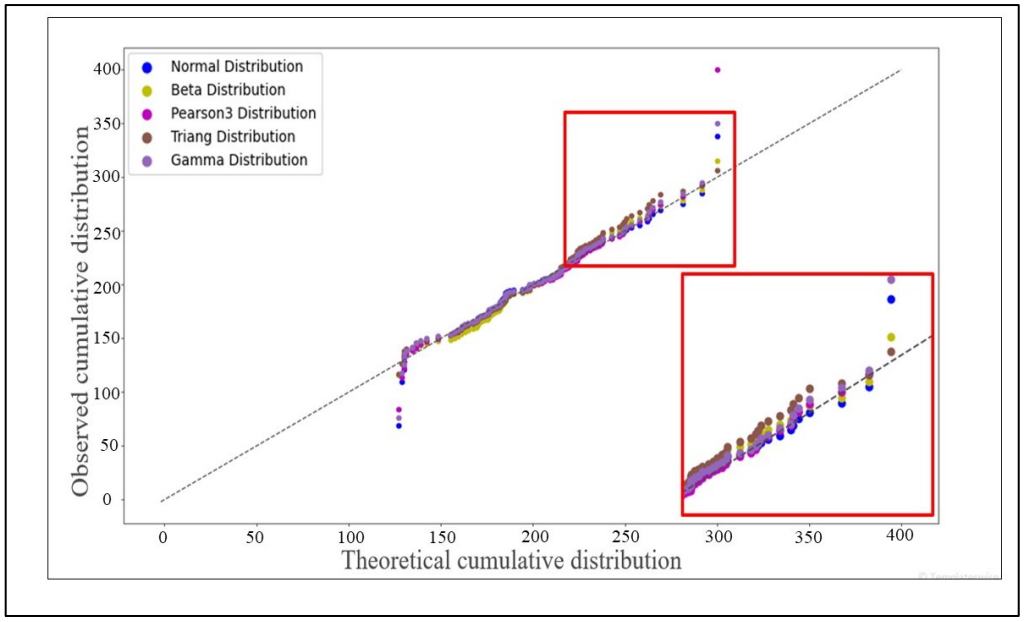

Fig 3-9. Example of Q_Q plot analysis for clay shear wave velocity data.

3.5.3 Probabilistic Vs_{30} and T0 map

In order to conduct additional research into the efficiency of the suggested strategy for Vs_{30} mapping, representative V_s values were selected with random sampling from respective probability distributions for each soil depth. As previously stated, the postglacial layer often comprises of sands covering silty clay or silty clay up to the surface. The geological units complexity and inherent natural variability add uncertainty that cannot be adequately represented by the regional 3D model. Previously mentioned as well, a novel 3D geological block model is used to reduce uncertainties related to the geological units. Moreover, the observed dispersion in measured V_s contributes to an increase in uncertainty levels, often available down to the first strong impendence contrast with glacial till, or with bedrock. As a result, in order to propose an accurate and robust Vs_{30} mapping process, a MC based approach was applied to capture the V_s uncertainty. The representative results of the stochastic evaluation of Vs_{30} and respective uncertainties for 1000 realizations are depicted in Fig 3-10.

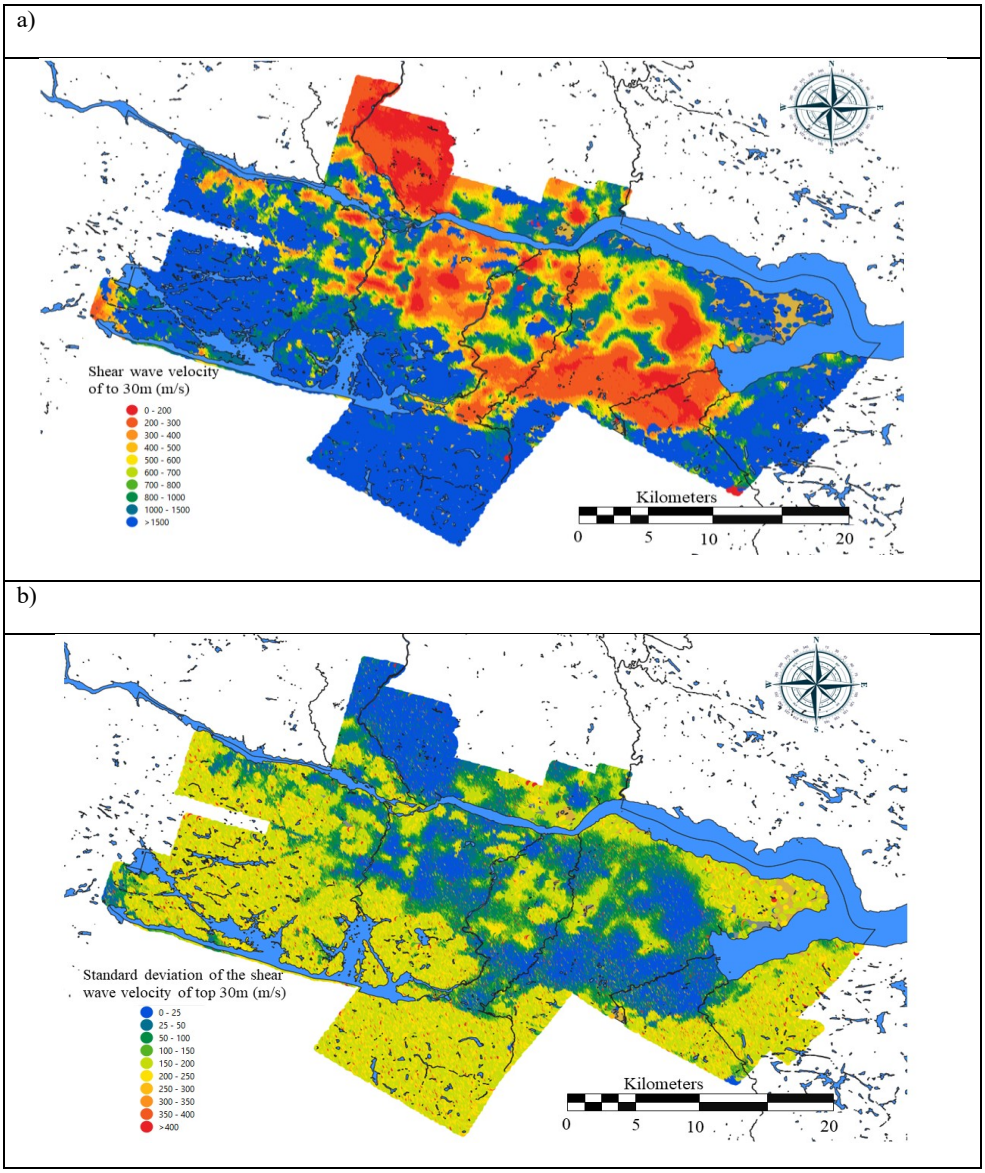

Fig 3-10. Spatial distribution of a) Average Vs_{30} values obtained from 1000 realisations and b) Standard deviation of Vs_{30}.

The $Vs30$ map represents average field conditions, although it is highly unlikely that Vs_{30} in each grid cell attains the 50% probability of occurrence at the same time. As it is probabilistic in nature, it is accompanied with the uncertainty expressed by the spatial distribution of the standard deviation of Vs_{30}, σ_{VS30}, (see Fig 3-10.b). The Vs_{30} spatial distribution follow approximately the discrepancy patterns of the surficial geological units and their thicknesses are shown in Fig 3-6. By comparing the thickness map (Fig 3-

6) and the standard deviation map (Fig 3-10.b), lower uncertainty is observed in grid-cells with higher sediment thickness, rock outcrops and areas covered with till sediments. On the contrary, higher uncertainty is observed in grid cells with lower sediment thickness at the edge of the rock outcrops and partially in areas with average sediment thickness between 5 and 15 m. Rapid transitions from relatively low (Vs_{30}<200 m/s) to high $Vs30$ at rock units outcrops (Vs_{30}>2500 m/s) seen between neighbouring cells as well. In addition to the seismic amplification due to layered soil conditions with decreasing V_s towards the ground surface, these transitional areas are exposed to another site effect, the so called `basin edge effect', where the amplitudes of incoming seismic waves increase because of the decreasing depths towards the edge of the sedimentation sequence.

Fig 3-11 is a scatter plot of the whole set of Vs_{30} values together with the accompanying standard deviation values. The highest uncertainty is attributed to Vs_{30} values in the range between 180 and 400 m/s. These stratigraphic profiles include generally softer post-glacial soil sediments with relatively higher thickness. Lower uncertainties are displayed for higher Vs_{30} values, Vs_{30} ≥760 m/s, where the soil sediment thickness is low.

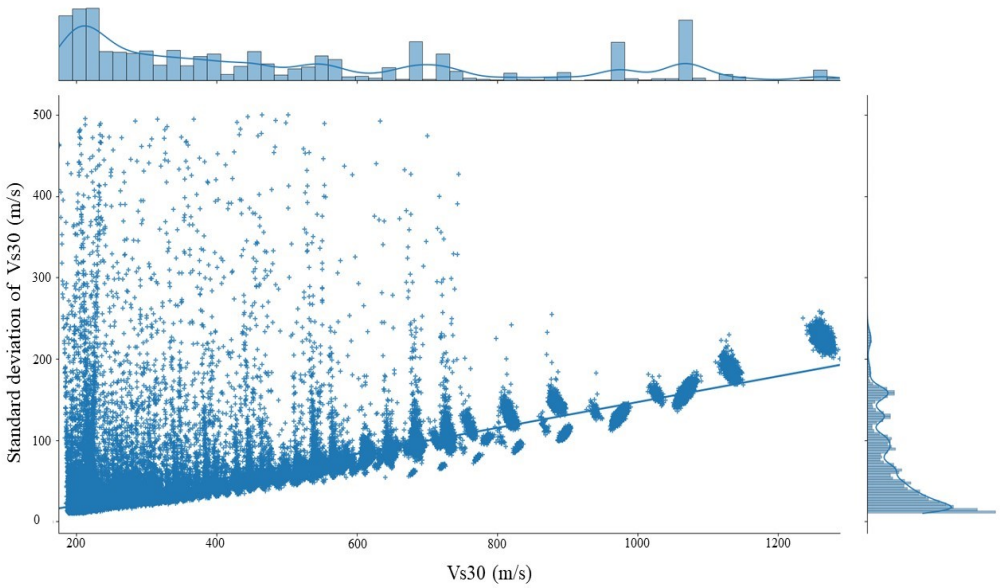

Fig 3-11. Standard deviation of the shear-wave velocity of the top 30 m versus Vs_{30} results from Monte-Carlo method

The spatial distribution map of T_0 is presented in Fig 3-12.a, and T_0 uncertainty distribution is given in Fig 3-12.b. In most cases, longer T_0 correspond to lower shear wave velocity. These zones are covered with thick geological units which are generally susceptible to far strong earthquakes with dominant low frequencies. On the contrary, areas with lower T_0 related to superficial sediments amplify mainly closer earthquakes with destructive energy content. In addition to this, non-linear stress strains can lead to a gradual increase in T_0 when intense ground shaking is occurring. It is therefore preferable to include local T_0 when developing a design plan for new structures or retrofitting existing ones.

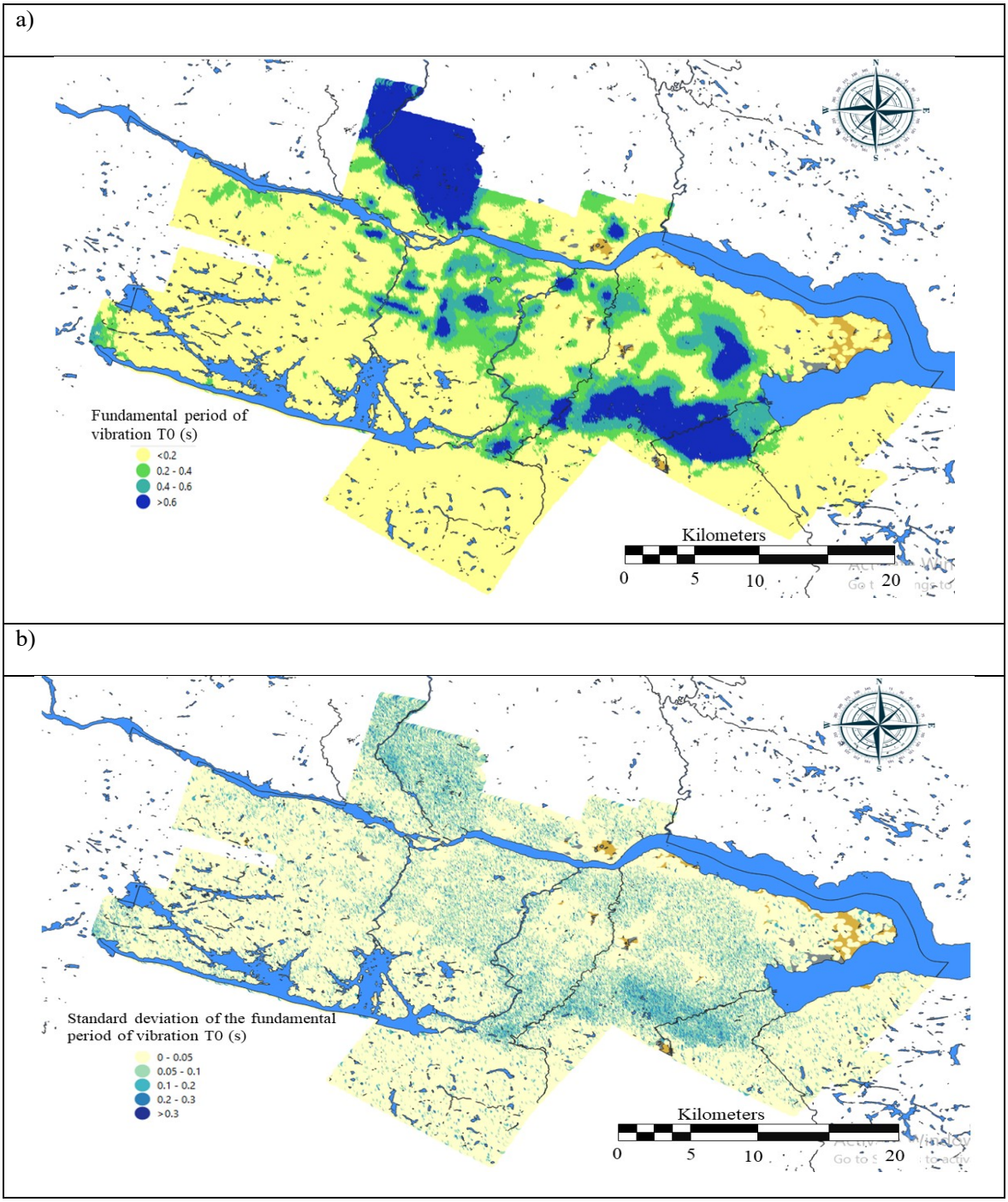

Fig 3-12. Spatial distribution of a) average T_0 values obtained from 1000 realisations and b) standard deviation of T_0.

When the thickness map (Fig 3-6) and the standard deviation map (Fig 3-12.b) are compared, grid cells with higher sediment thickness and especially in area with T_0 greater than 0.6 s have lower uncertainty. In contrast, uncertainty is more in grid cells with less sediment thickness and partially in regions with medium sediment thickness.

3.5.4 Validation and comparison of the results

To evaluate the efficiency of the proposed method and conduct the validation of the site characterization model developed in this study, two Vs_{30} map were developed. The first model was developed by assigning the mean value of distributions selected for MC method (*Table 3-1*) to geological model (Fig 3-1). The first model was compared against a deterministic Vs_{30} map created for this purpose based on experts' opinion of 3D geological model (Fig 3-1) and the conventional regression method for V_s–depth variation. To this end, the developed V_s regression equations, given in Fig 3-2 were assigned to each block elements of the 3D geological model, and a single Vs_{30} value was calculated for each grid cell. Fig 3-13 shows the distribution mean and conventional Vs_{30} maps for the study area.

The comparison between the two approaches with respect to the discrepancy between the estimated $Vs30$ values is presented in Fig 3-14. Considerable difference is noted in the Vs_{30} values computed by the two methods. The maximum difference value is observed in border of regions with high and low $Vs30$. Additionally, the difference between two methods relatively is correlated with the thickness of the sediments.

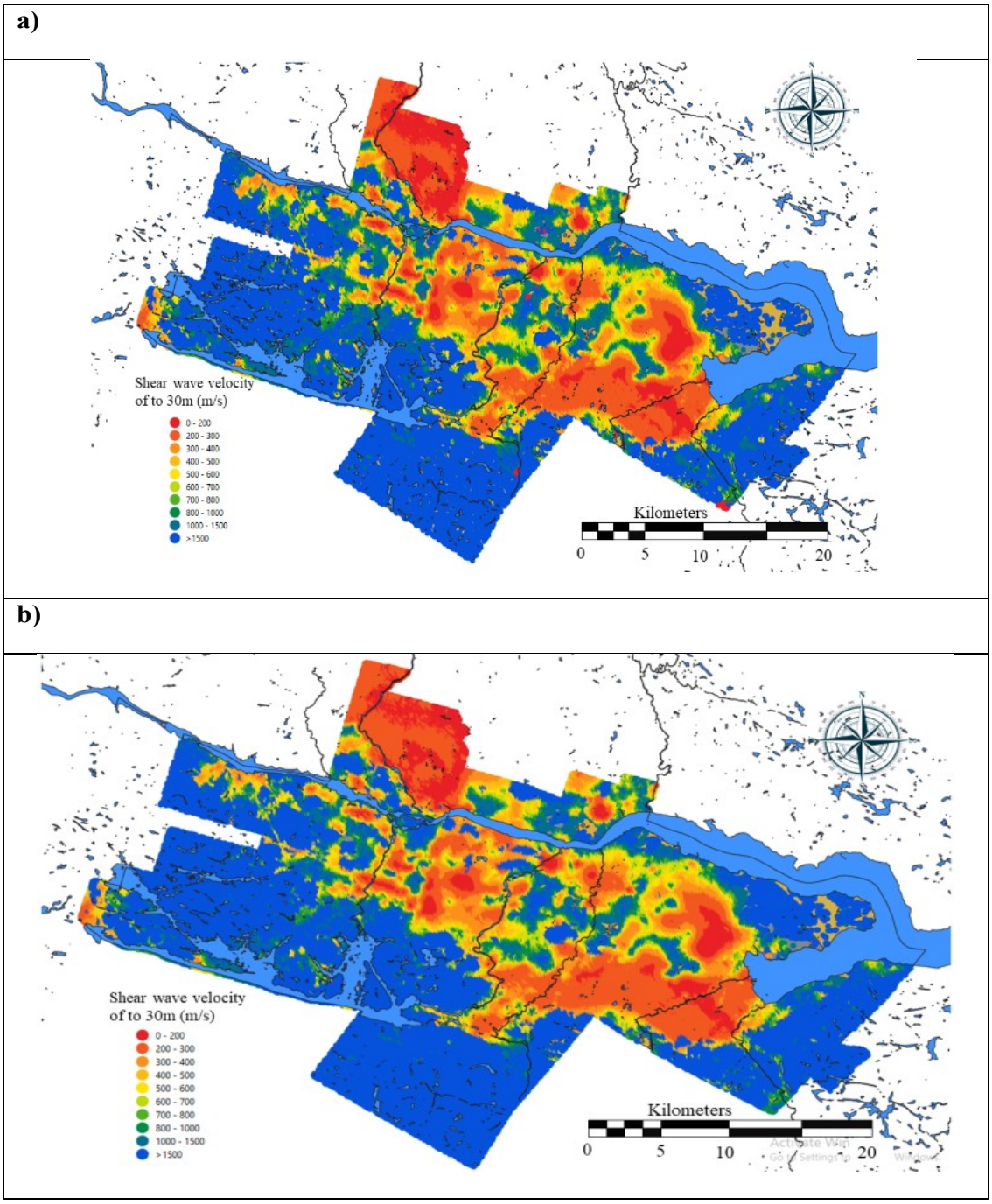

Fig 3-13. Vs_{30} maps for the Saguenay region: a) mean values, b) map based on the deterministic 3D geological model and conventional regression method with consistent V_s–depth variation.

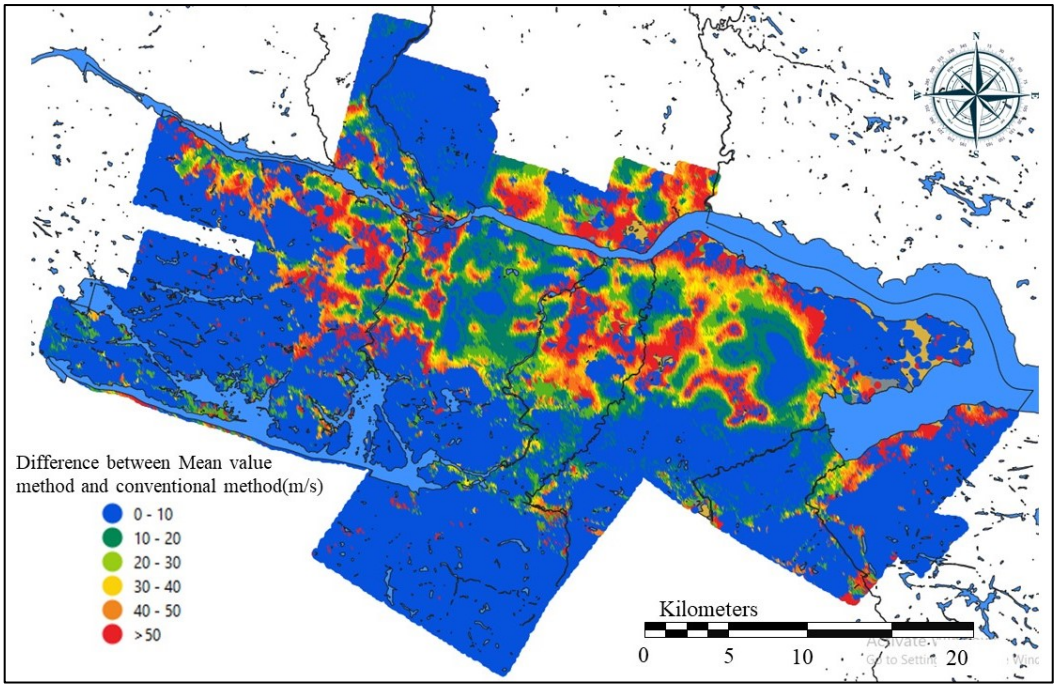

Fig 3-14. Discrepancy between two methods for Vs_{30} determination

The higher differences exist in areas with deeper soil sediments and relatively low Vs_{30}. For Vs_{30} values above 800 m/s, the results are identical because uniform V_s value is considered for bedrock in both methods. As discussed above, these differences are due to the consideration of the best fit probability distribution function for each 2 m depth in the present study (Fig 3-13.a) and the consistent V_s–depth distribution function by the conventional method (Fig 3-13.b). More importantly, the former approach tends to honour the observed variability of the V_s distribution functions with depth which reflects the specific sedimentation and erosion that took place during the geological age of the local soils. By contrast, the latter approach implicitly involves additional uncertainty constraining the variable distribution of the V_s values in the Vs_{30} calculation. For further validation, the developed model and ER2 software was compared (i.e., which is developed for Eastern Canada setting in terms of NBCC 2015 site classes).

Fig 3-15 presents the seismic site classes for the MC-based method (Fig 3-15.a) and ER2-Earthquake software (Fig 3-15.b) for Saguenay region. ER2 assigns only one soil type (Class D) to estimate the hazard and risk values. However, in the MC-based method, all of the site classes proposed in NBCC 2015 can be seen. By comparing the two maps, the following conclusion can be reached: in most regions, the site classes

differ from class D, and assigning a constant value to all regions can lead to significant uncertainty in hazard and risk estimates.

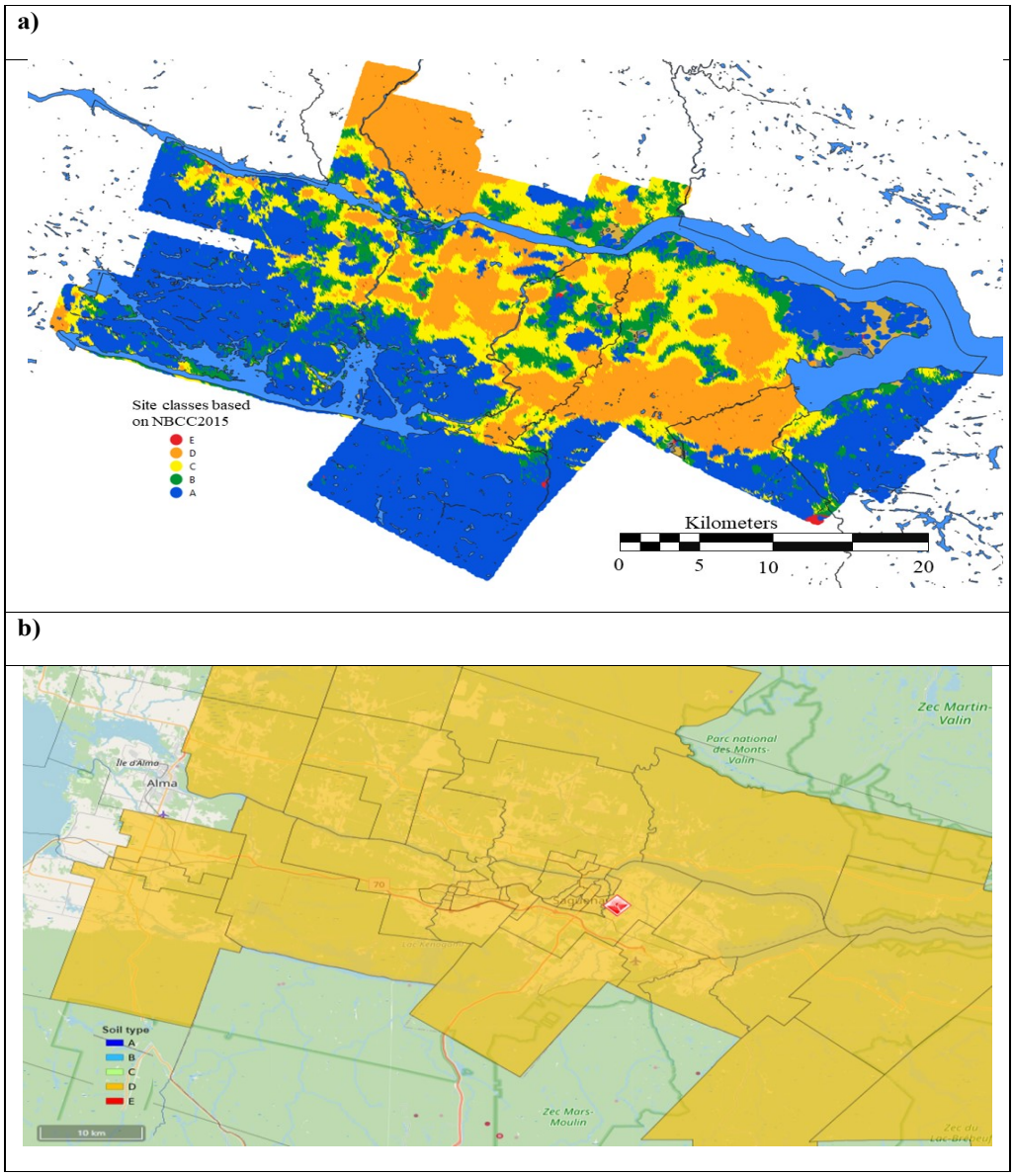

Fig 3-15. Seismic microzonation site classes according to NBCC 2015: a) MC-based approach b) ER2 software assumptions.

3.6 CONCLUSION

A probabilistic seismic site effect code was developed based on MC simulation and was applied in Saguenay City, Canada. The code tracks uncertainty in the geological model (probability of occurrence of a given soil type) and in the geotechnical model (probability of occurrence of V_s value given the occurrence of the soil type). The novelty of this approach is recognising that the V_s–depth probability distribution and variability are not consistent with depth, but rather irregular. The major assumption is that the soil stiffness properties, of which V_s is taken as a reference, are functions of the specific sedimentation and erosion that took place during the geological age of the local soils and of the location within the local stratigraphy. This is accounted for by site-specific V_s variability profiles for each of the considered soil types (clayey and sandy soils) and each 2 m depth.

The study region was first modelled with a grid of 155 800 2D 75 × 75 m grid cells at the surface. Additionally, 1 061 200 3D block elements of 75 × 75 × 2 m were included, extending all the way to the bedrock interface. A statistical model based on chi-square and Q-Q plot was developed to determine, for each 2 m depth, the respective best fit V_s distribution functions among the considered 10 different distribution functions. The randomised V_s values were generated by applying MC simulations with the pre-determined distribution functions for each block element of the previously developed probabilistic 3D geological model. A total of 1000 V_s simulations were conducted, as the convergence of the results had already been observed. The final seismic microzonation results consist of the VS_{30} map, the V_s of the first 30 m, VS_{30} uncertainty map, T_0 map and T_0 uncertainty map.

Validation was conducted against the conventional regression method with consistent V_s –depth variation. The observed differences between the two approaches are due to the consideration of the best fit probability distribution function for each 2 m depth in the present study, as opposed to the consistent V_s–depth distribution function in the conventional method. The former approach proposed herein tends to honour the observed variability of the V_s distribution with depth and minimises the eventual uncertainty related to the V_s assessment. By contrast, the conventional approach implicitly involves additional uncertainty constraining

the variable distribution of the V_s values. The developed model was compared with the ER2 software in terms of NBCC 2015 site classes for further validation.

The developed code may be utilised as a probabilistic module for incorporating site effects in seismic hazard and risk assessments. The uncertainty in a 3D geological model and V_s may be applied using this strategy which can lead to more accurate hazard assessment results.

3.7 APPINDEX: DISTRIBUTIONS FITTED AT DIFFERENT DEPTH ACCORDING TO SOIL TYPE

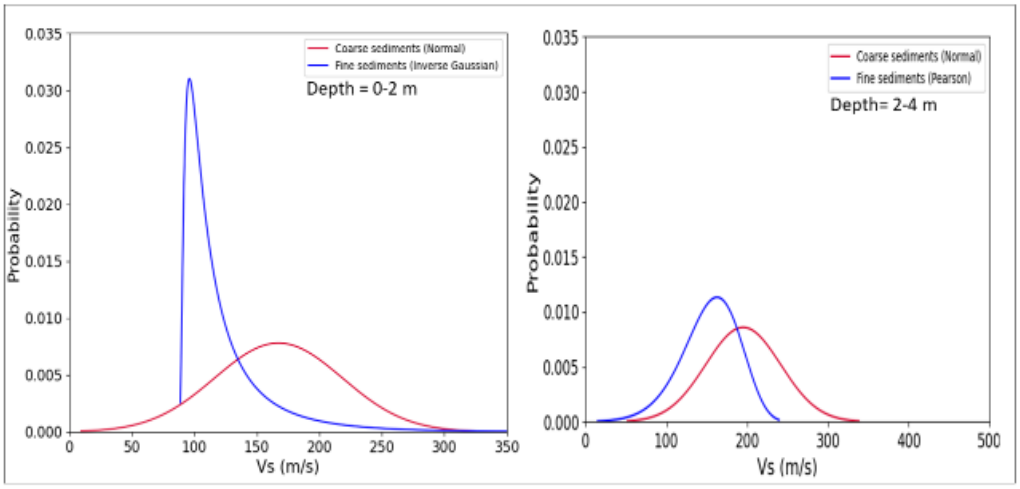

Fig 3-16. Distributions fitted to the coarse and fine sediments in 0-2 m and 2-4 m depth

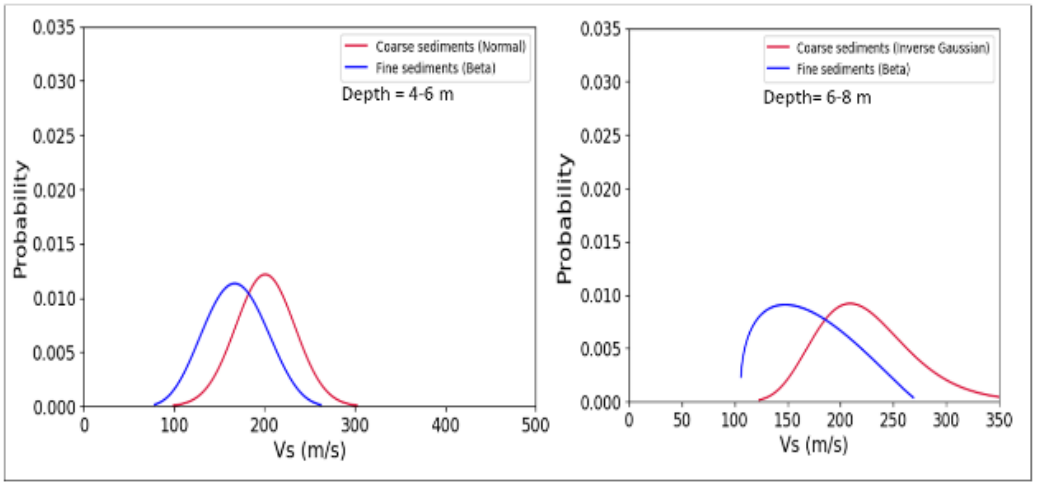

Fig 3-17. Distributions fitted to the coarse and fine sediments in 4-6 m and 6-8 m depth

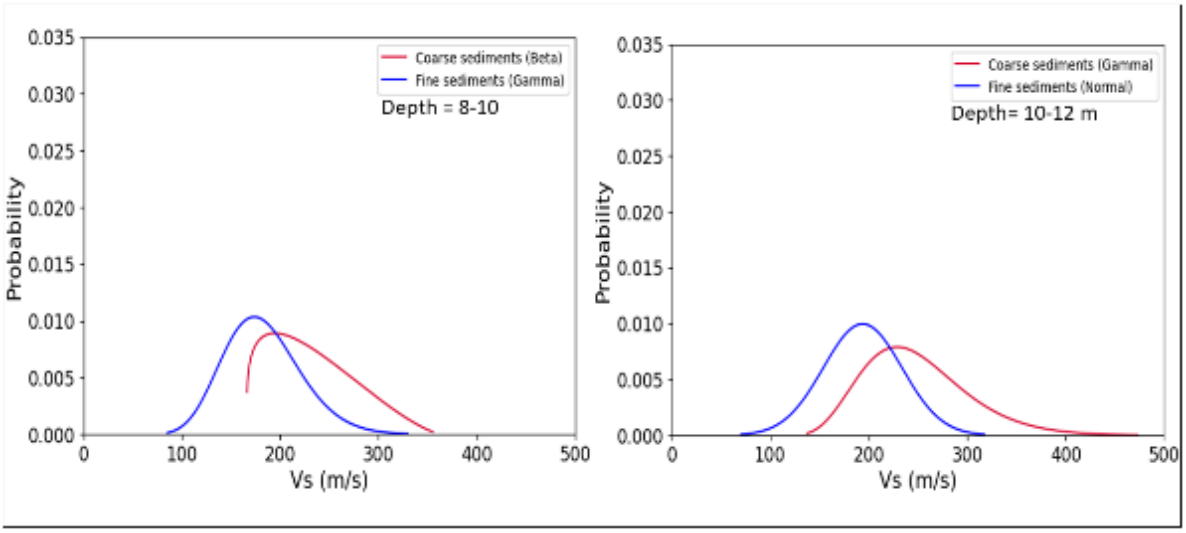

Fig 3-18. Distributions fitted to the coarse and fine sediments in 8-10 m and 10-12 m depth

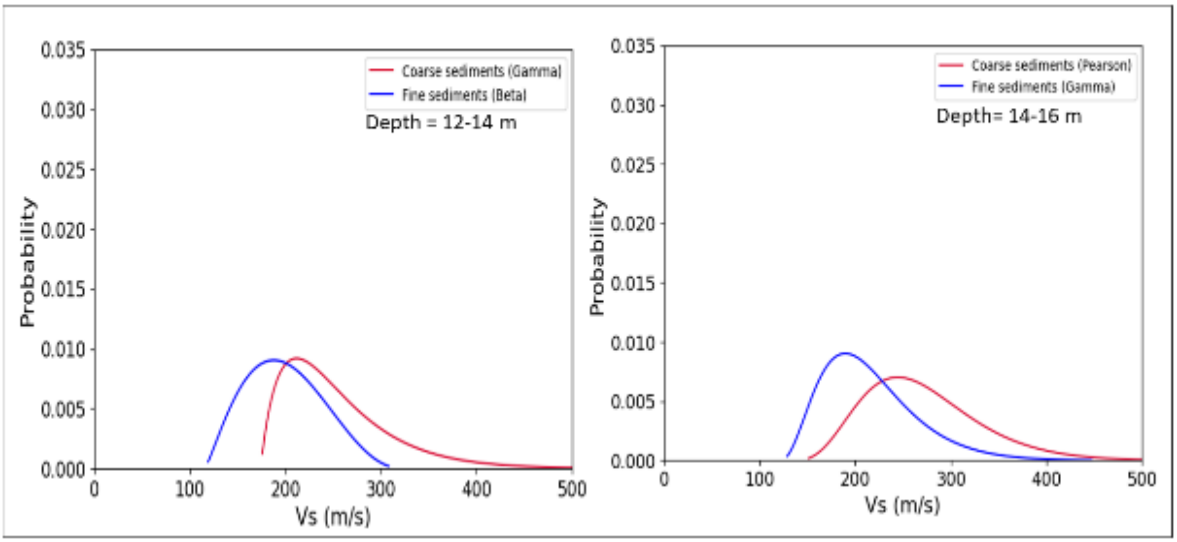

Fig 3-19. Distributions fitted to the coarse and fine sediments in 12-14 m and 14-16 m depth

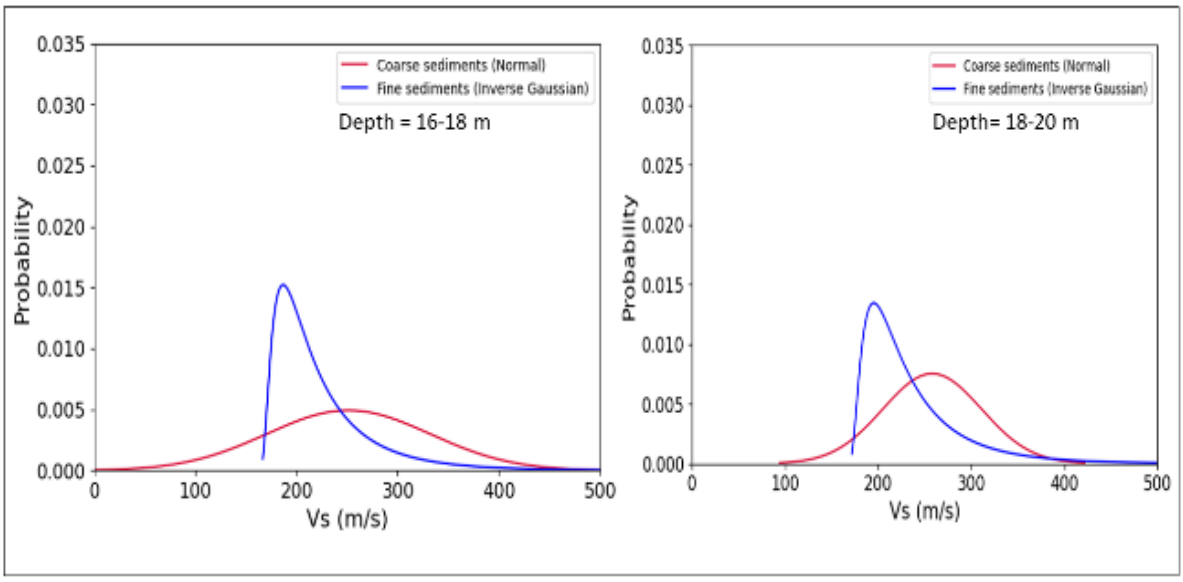

Fig 3-20. Distributions fitted to the coarse and fine sediments in 16-18 m and 18-20 m depth

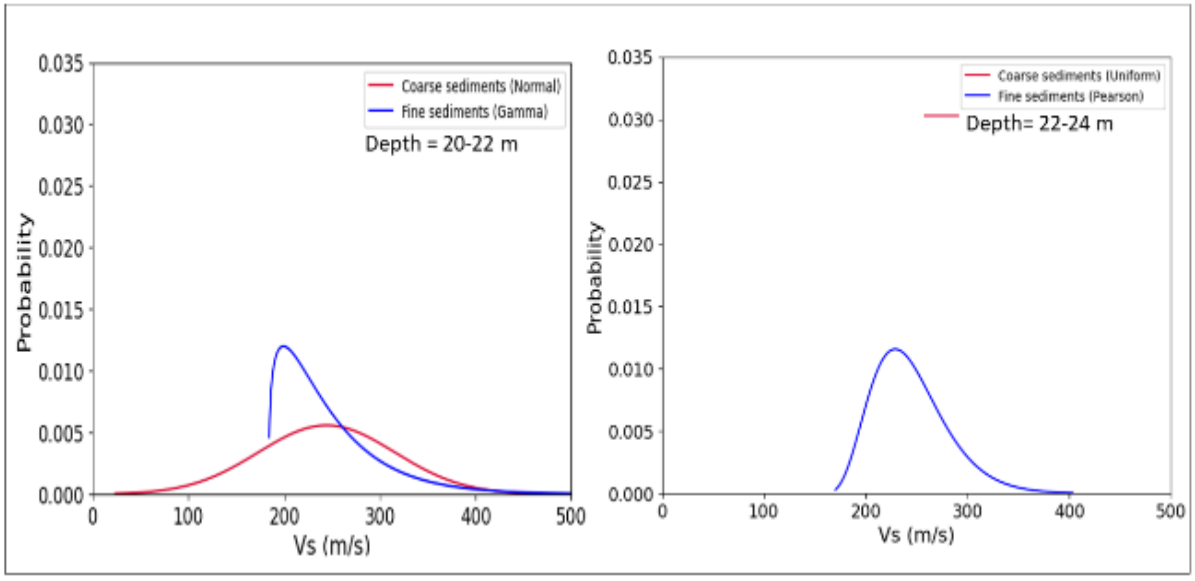

Fig 3-21. Distributions fitted to the coarse and fine sediments in 20-22 m and 22-24 m depth

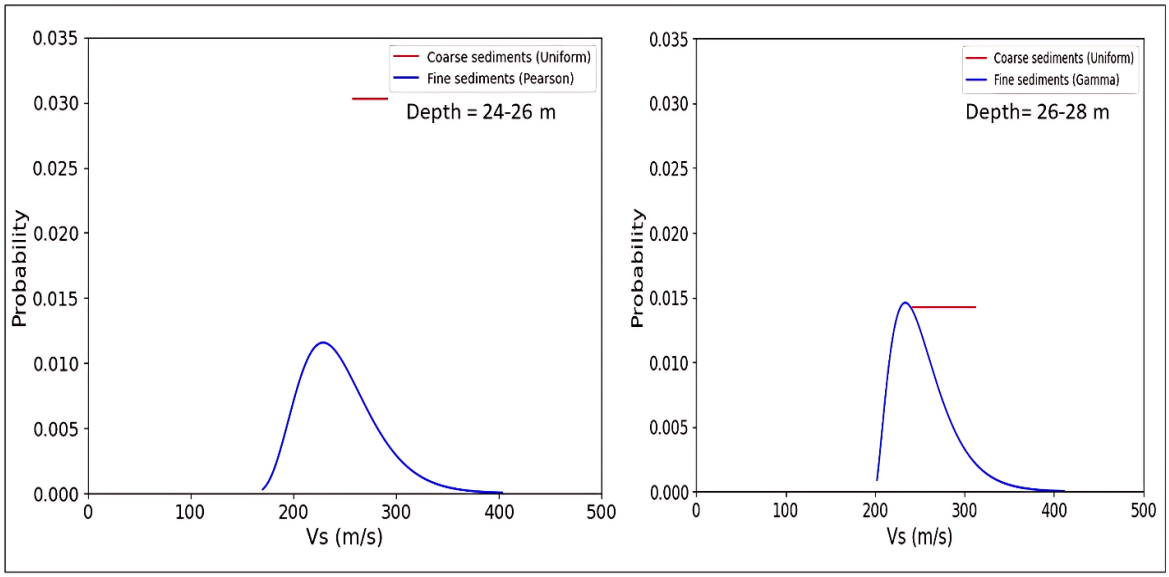

Fig 3-22. Distributions fitted to the coarse and fine sediments in 24-26 m and 26-28 m depth

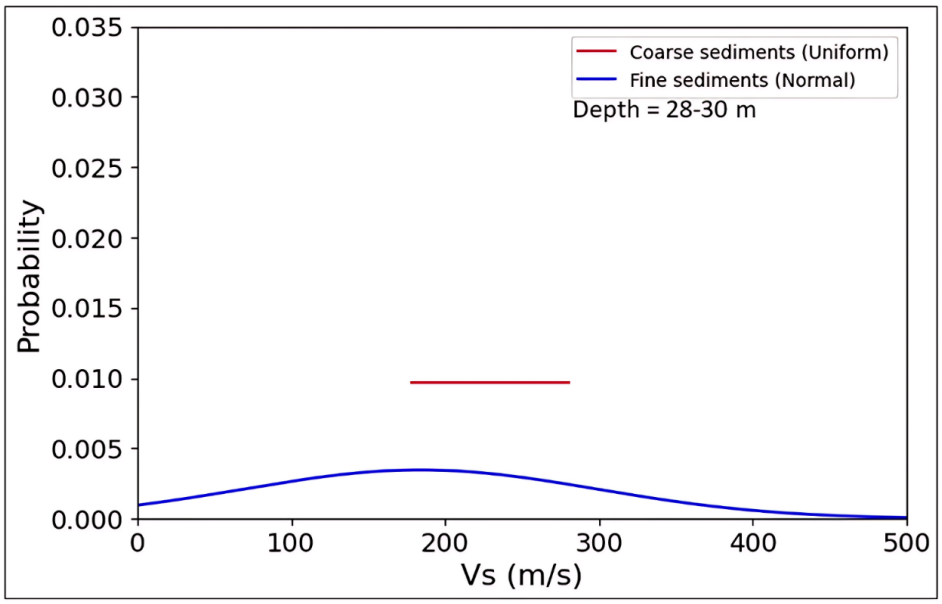

Fig 3-23. Distributions fitted to the coarse and fine sediments in 28-30 m

CHAPTER 4

Article 3: Development of a damage simulator for probabilistic assessment of seismic vulnerability of electrical installations

Vahid Hosseinpour [a *], Ali Saeidi [a], Miroslav Nastev [b], Marie-José Nollet [c]

[a] *Department of Applied Sciences, Université du Québec à Chicoutimi, Saguenay, G7H 2B1, Saguenay, QC, Canada*

[b] *Geological Survey of Canada, Natural Resources Canada, G1K 9A9, Quebec City, QC, Canada*

[c] *Department of Construction Engineering, École de Technologie Supérieure, H3C1K3, Montreal, QC, Canada*

*Email: vahid.hosseinpour1@uqac.ca

Submitted to : International Journal of Disaster Risk Reduction,
https://www.sciencedirect.com/journal/international-journal-of-disaster-risk-reduction

Acknowledgements:

The authors would like to thank the members of the CERM-PACES project for their cooperation to conduct the field tests and provide access to the databas.

Authors contribution**:**

Vahid Hosseinpour: Conceptualization, Methodology, Formal analysis, Software, Validation, Data Curation, Visualisation, Writing – original draft. **Ali Saeidi:** Conceptualization, Funding acquisition, Validation, Project administration, Supervision, Resources, Writing - Review & Editing. **Miroslav Nastev:** Supervision, Writing - Review & Editing. **Marie-José Nollet:** Supervision, Writing - Review & Editing.

Funding:

This research was partially funded by the Natural Sciences and Engineering Research Council of Canada (NSERC) and Hydro-Quebec under project funding no. RDCPJ 521771-17 and also CRC-NSERC 950-232724.

4.1 ABSTRACT

Recent earthquakes have revealed the vulnerability of electric power networks to seismic events. To assess their vulnerability to seismic shaking, a user-friendly damage simulator is developed. It consists of three major components: seismic hazard, vulnerability of the exposed transmission towers and substations and damage calculation. The application uses open-source software without any financial cost to the users. The computation starts with selection and calculation of probabilistic and/or user defined seismic hazard scenarios including the local site effects. Spectral accelerations at the fundamental vibration period of the transmission towers and the ground accelerations for the substations are considered as intensity measures (IMs) of the transitory seismic shaking. The probabilistic damage assessment incorporates uncertainties in the site parameters, the epistemic uncertainty is considered through the logic tree approach introduced in the latest seismic hazard of the National Building Code of Canada, aleatory uncertainty is captured with the Monte Carlo analysis option, whereas the inherent uncertainty related to the structural dynamic response and damage assessment is accounted for with a set of fragility curves describing different damage states. An example of the seismic site characterisation, hazard assessment and vulnerability analysis of the Hydro-Quebec electrical installations in the Saguenay region, Canada, is presented to illustrate the capacity of the developed software. Results indicate the resistance of the transmission towers and the relatively high vulnerability of substations to seismic shaking.

Keywords: Seismic vulnerability, Loss estimation Software, hazard analysis, probabilistic approach

4.2 INTRODUCTION

The prediction of the negative effects of earthquakes, referred to as seismic risk, is a complex process based on a systematic collection and analysis of three input parameters: (i) hazard, (ii) existing buildings and infrastructure (exposure) and (iii) their respective vulnerabilities [3, 4]. High-voltage electric power transmission networks are parts of the infrastructure that are vulnerable to seismic shaking and ground failures, as evidenced by recent earthquakes, e.g. the 2011 Christchurch earthquake (New Zealand) [27] and the 2023 Turkey–Syria earthquake [28]. Transmission networks consist of transmission towers that support conductive cables (conductors) and insulators, transformation substations and associated facilities. To transport power, electric towers and substations are critical for ensuring reliable electricity transmission [29]. The structural type of towers and substations varies in accordance with the electrical voltage of the line and the environment in which they are built [172]. The tower structural system can vary between lattice steel (e.g. waist-type, double circuit, guyed-V and guyed cross-rope) and tubular structures [30]. Electric installations are erected on various forms of rough terrain, including sensitive local site conditions, due to the significant length of transmission lines. They can be exposed to heavy dynamic loads from atmospheric (e.g. ice and winds) and seismic sources.

Over the past few decades, significant effort has been exerted to develop software for the accurate prediction of seismic risk [37], such as Hazard US (HAZUS) [5] and its different versions (e.g. Ergo [6]), Haz-Taiwan [7], SELENA [8], HazCan [9], InaSAFE [10], CAPRA [123], DBELA [173], OpenQuake [13] and the ER2 web application [14]. Some countries have created their customised versions of this software, whilst international projects, such as the Global Earthquake Model (GEM), are developing tools that can be used worldwide [37, 115]. These tools mostly calculate physical damage and the corresponding economic and social losses. Regardless of the significant advancements, current software packages do not adequately address specific challenges posed by the seismic vulnerability of the electric infrastructure. Simultaneously, a number of studies have analysed the effects of earthquakes on electric infrastructure and provided quantitative assessments of their vulnerability [31-33]. The preferred approach for mitigating potential negative effects relies on incorporating the latest seismic design principles recommended in the provisions of national building codes. However, most existing transmission lines were generally built with minimal consideration of seismic

effects [174]. Whilst waiting for their reinforcement and upgrade to ensure seismic resilience and simultaneously develop comprehensive decision-making and emergency response plans, the seismic risk assessment of electric transmission networks is apparently a reasonable first step towards managing and reducing the severity of potential losses.

The objective of this study is to present an innovative damage simulator for evaluating the seismic vulnerability of electrical power transmission towers and substations. This simulator consists of two major modules designed to perform specific tasks for risk analysis: (i) seismic hazard analysis that consists of probabilistic and user defined what-if event scenarios, including local site effects, and (ii) vulnerability assessment to determine the level and likelihood of damage induced in transmission installations given the seismic hazard scenario. The electrical installations are introduced with their respective coordinates and type by the user. The City of Saguenay in eastern Canada was selected as a study area due to the presence of transmission lines, past and recent seismic activities and heterogeneous surficial sediments with variable thickness that may considerably amplify earthquake transitory motion (Fig 4-1).

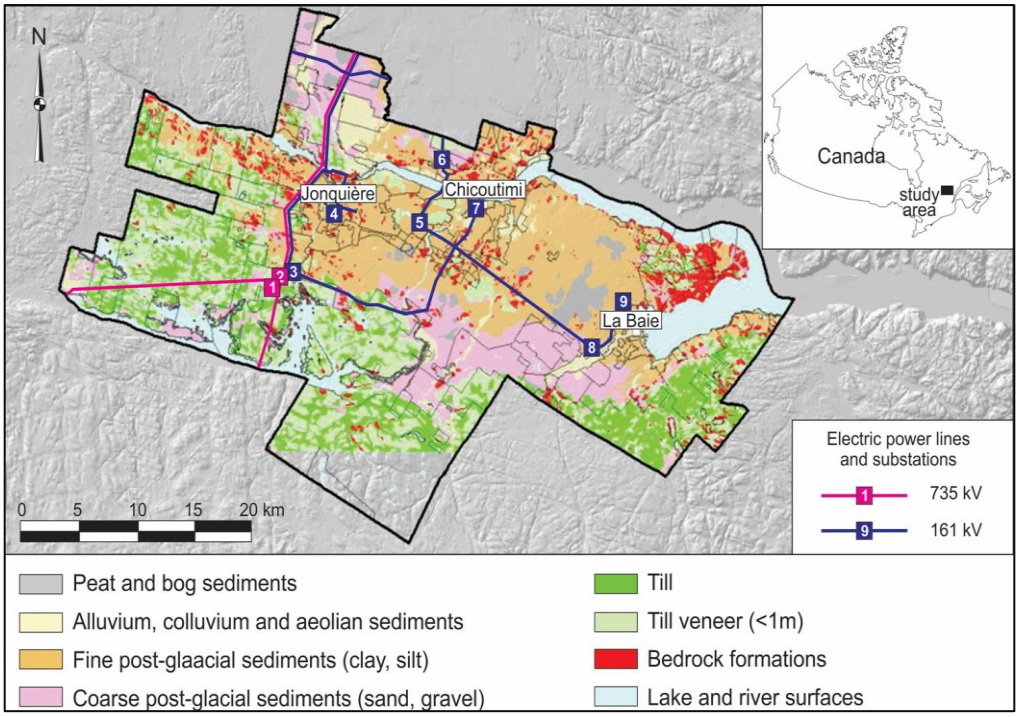

Fig 4-1. Study area of the Saguenay region with the spatial distribution of electrical installations and surficial geology map as background ([30, 170])

4.3 DEVELOPMENT OF THE SEISMIC HAZARD MODULE

The development of an efficient simulator of seismic damage to power transmission installations relies on understanding a series of interdependent tasks and variables: programming language, including method and architecture; seismic hazard at the bedrock level; site effects and inventory of assets at risk and vulnerability functions [3]. Following the decision on software architecture, the choice of programming language is a crucial factor in the development of software for seismic risk estimation. The selection of Python as the programming language for this application was based on its versatility and suitability for complex scientific calculations. Python has a large and still growing community of developers and users, and thus, it provides a wealth of resources and support for users. It also has a rich library of modules and scientific packages, (e.g. NumPy, SciPy and Matplotlib), making the implementation of various algorithms and models easy. Furthermore, Python is open-source; that is, the source code is freely available and can be modified to meet specific needs [164]. The use of Python in this application will contribute to rapidly generating more accurate and reliable results and facilitate the continued development and improvement of the software over

time. In addition, its high-level interface makes Python easy to interface with other software, improving the efficiency of the workflow.

The first step in seismic risk assessment is evaluating seismic hazard, which can be determined using probabilistic seismic hazard analysis (PSHA) or deterministic seismic hazard analysis (DSHA), and generally expressed in terms of the spatial distribution of seismic shaking intensity. The potential amplification of ground motion due to local geological and geotechnical conditions is based on the evaluation of seismic site parameters: average shear wave velocity in the top 30 m, Vs_{30} and the fundamental vibration period of the soil column on top of bedrock formations [15]. The intensity of the transitory seismic shaking is of primary focus in the present study because the simulation of induced secondary hazards site effects, such as permanent ground failure (e.g. liquefaction, landslide and lateral spread), is less accurate, time-consuming and reliant on comprehensive field measurements. The standard intensity measures (IMs) of seismic shaking are peak ground acceleration (PGA) and spectral acceleration for selected vibration periods of interest (Sa_T). A general workflow of damage simulator components including hazard module is presented in Fig 4-2.

4.3.1 Probabilistic seismic hazard scenarios

Probabilistic seismic hazard can be quantified as the likelihood of ground shaking occurring at a specific location over a given period. It represents a weighted average of the effects of all potential seismic sources that affect a location, each defined with its own fault or fault area, magnitude–frequency relationship and ground motion prediction equations (GMPEs) which account for the source-to-site attenuation of the seismic waves. Shaking intensity is typically determined for seismic bedrock with average shear wave velocity of V_s =3000 m/s or for V_s =760 m/s at the interface between engineering bedrock and surficial sediments [23]. The shaking intensity at the ground surface is implicitly calculated for the local site conditions defined by Vs_{30} of the top 30 m considering the potential amplification of the spectral accelerations. The damage simulator implements the 6th generation seismic hazard model for stable crustal conditions in eastern Canada. The model uses a multiple GMPE logic tree approach and is based on a 50/50 weighting strategy for three GMPEs from the previous 5th generation model and 13 GMPEs known as NGA-East-13 suggested for use in the 2020 National Building Code of Canada (NBCC2020), is introduced into the [175]. The objective

of this weighting strategy is to transition towards an NBCC seismic hazard model, which is fully defined only with the NGA-East-13 GMPEs. This change was necessary to incorporate site-specific amplification into each GMPE, along with epistemic uncertainty, which is impossible in the previous hazard model. The retained design return period is 2475 years, which corresponds to an exceedance probability of 2% in 50 years. To incorporate local site conditions and obtain probabilistic hazard values (PGA and Sa) at the ground surface, the user provides Vs_{30} values for the location of interest or a comma-separated values (CSV) file for the grid cells of the study area.

4.3.2 User defined what-if scenarios

The evaluation of the user defined seismic scenarios hazard is based on a point source approximation of the fault or the seismic zone of interest. The seismic source is defined with the user selected earthquake magnitude and coordinates of the epicentre and combined with GMPEs corresponding to the seismic settings of the region. In this case, the considered earthquake magnitude (M) should correspond to the magnitude–frequency relationship of the seismic source and can be determined over a realistic return period that involves the notion of likelihood. The epicentral distances (D) to the studied location or the grid cells is then automatically calculated. In the damage simulator, the source-to-site attenuation is computed with the same GMPEs from the 6th generation Canadian seismic hazard model [22, 39]. In addition, the software utilises Monte Carlo (MC) simulation to account for aleatory uncertainties in seismic IMs (e.g., PGA and Sa). To account for these uncertainties, a normal distribution with a standard deviation value from NBCC2020 is applied. The computation of the attenuation of the seismic waves with distance and the spatial distribution of the respective seismic IMs for user-provided Vs_{30} site conditions in the form of a CSV file or map is visually presented in the flowchart in Fig 4-2.

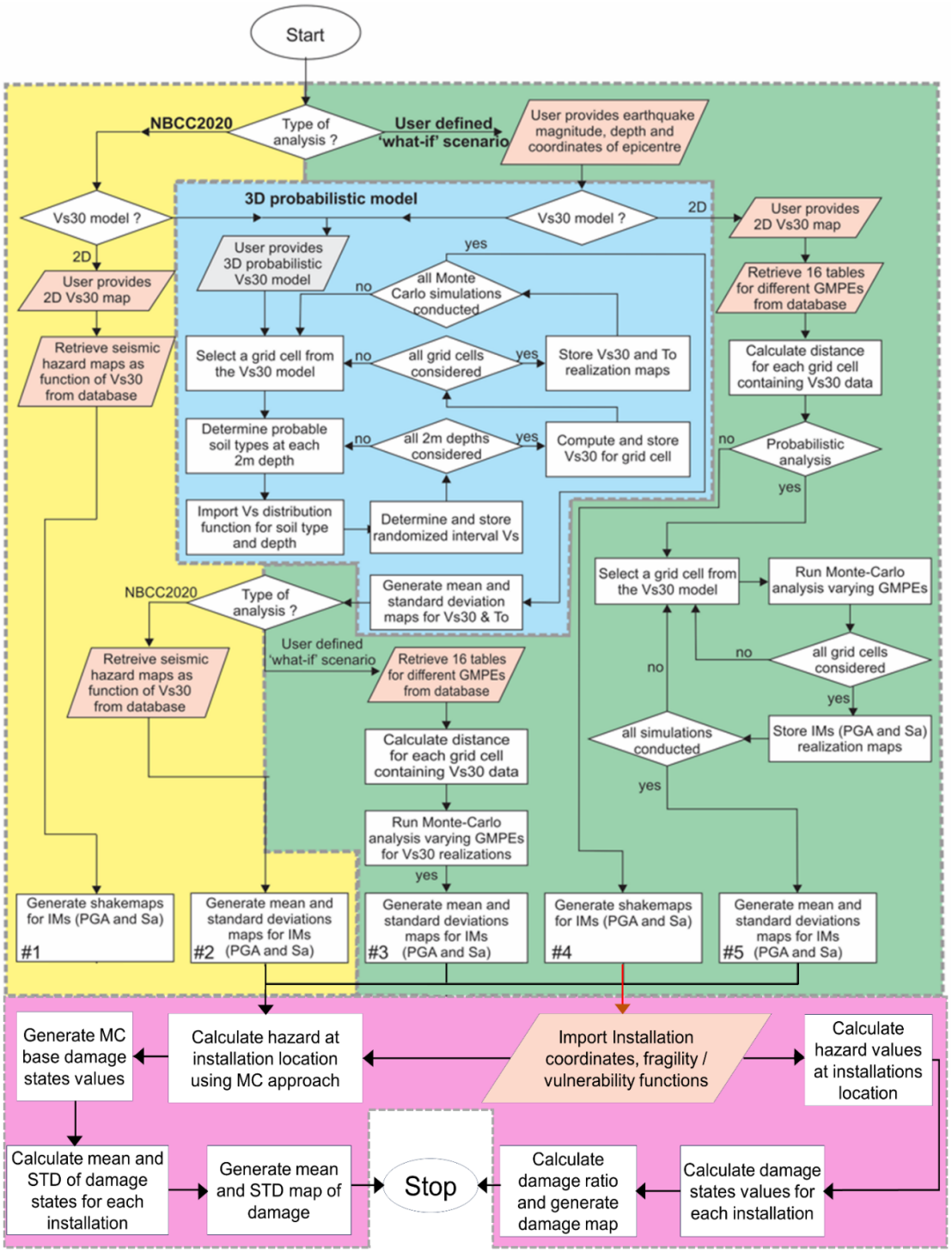

Fig 4-2.Overall flow chart of developed damage simulator.

4.3.3 Site effect parameters

The user defined event scenario also allows the integration of uncertainties in the site effect parameters into the seismic IMs at the ground surface. To this end, a MC approach is applied considering: (i) probabilistic 3D geological model represented with the probability of occurrence of a given type of surficial sediments, their thickness and depth, and (ii) probabilistic assessment of the site parameters Vs_{30} and T_0 (fundamental period of vibration) based on shear wave velocity Vs-depth correlations with non-uniform probability density functions with depth. The flowchart presented in Fig 4-2 (blue part) outlines the computations of the probabilistic site parameters and uncertainties.

The existing probabilistic 3D geological model for the Saguenay study area consisting of 75×75×2 m block elements was used was used to demonstrate this capacity [160]. The interval V_s–depth probability density functions were determined based on the considered soil types (fine clayey sediments, coarse sandy soils and glacial deposits) and depth [176]. Having stored these parameters in the temporary database, MC simulations were performed to assess the spatial and vertical variabilities of Vs_{30} and T_0 accounting for uncertainties in soil geological and geotechnical parameters. The vertical stratigraphy of each grid cell was simulated, sampling the soil type at each 2 m depth. Consequently, the corresponding best-fit V_s probability distribution function was retrieved for the given soil types and depths from the 3D geological model, and a random V_s value was generated. The number of random variables was determined by the thickness of the geological units in the stratigraphic column, and V_s estimates were sampled from the relevant distribution function based on the soil type and depth of the block. This process was repeated 15 times (for each soil block element up to 30 m depth) in each MC simulation or until the bedrock interface was reached to generate the respective Vs_{30} maps.

MC simulations were conducted until Vs_{30} values reached stability in each grid across the study area. The Vs_{30} values were computed from the average travel time through the top 30 m. The fundamental site period T_0 was obtained rom V_s through the quarter-wavelength equation [24]. The final results include spatial distribution maps of Vs_{30}, T_0 and their respective uncertainties.

4.4 VULNERABILITY ANALYSIS

The next step consists of: (1) inventory of the considered electrical installations (transmission towers and substations) exposed to the seismic hazard scenarios (exposure), and (2) selection of representative fragility functions [3]. Fragility functions correlate the probability of exceeding thresholds for different damage states ranging from none to complete damage with a given level of shaking intensity. They are defined as lognormal functions of damage with mean values at 50% damage and standard deviations generally in the order of 0.7–0.8. Fragility functions, which are intended mostly for use in urban and regional risk assessments, are representative for a group of structures with similar dynamic response characteristics. They are generated based on field observations of damage, analytical studies, expert judgment or a combination of these approaches, and the chosen method depends on the type, frequency and quality of available data, expertise, resources, and the size of the study area.

4.4.1 Transmission towers

This Although a number of studies have focused on fragility functions for most common structures (e.g. buildings and bridges), there is no existing taxonomy developed specifically for the seismic fragility of electrical installations. A comprehensive literature review was conducted to select appropriate vulnerability functions representative for transmission towers in the Saguenay region [40]. From James Bay, where electricity is produced in eight hydroelectric power plants on Grande Rivière, to the Saguenay region where it is consumed, the power transmission line extends over more than 1,000 km; hence, the potential of losing part of the initial energy is high. To reduce potential losses, voltage is increased to 735 kV, which is equivalent to four standard 315 kV lines. This increase is accompanied with higher-diameter conductors bundled in series of two to four conductors, exerting additional stress on transmission towers. To support these high-voltage conductors, Hydro-Quebec uses three types of transmission towers [40]. The waist-type tower is the most commonly used transmission tower, and it is suitable for power lines crossing rough terrain and carrying voltages between 110 kV and 735 kV. The guyed-V tower is a ‘V’-shaped lattice tower that is supported and secured by stay wires that can handle voltages between 230 kV to 735 kV. The double circuit tower is

designed for smaller footprints, and it has a height range of 25 m to 60 m, with the ability to handle voltages up to 315 kV (Fig 4-3).

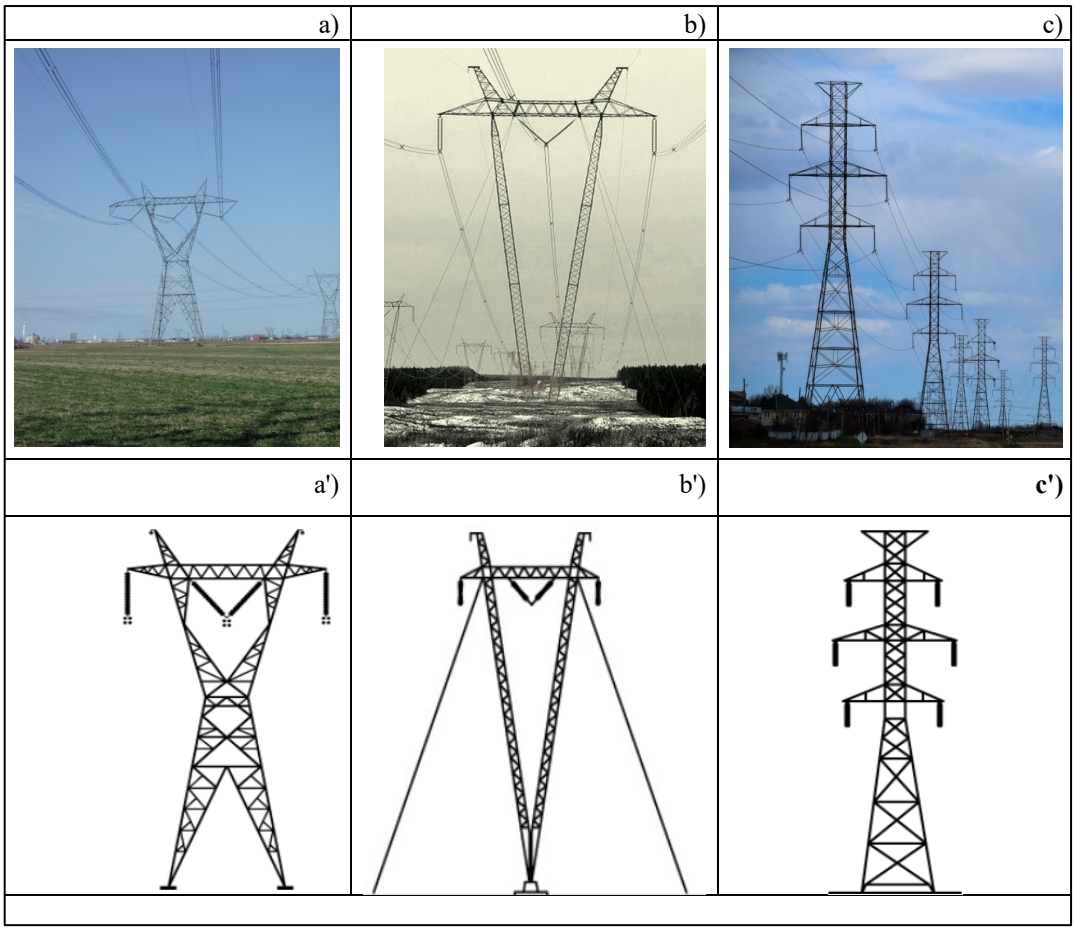

Fig 4-3. Photos and schematic presentations of : a-a') Waist-type, b-b') Guyed-V and c-c') Classic double-circuit power transmission towers *[30]*.

To describe the structural damage condition effectively, three damage states (performance levels) with three thresholds are defined using the pushover analysis [177]. In the serviceability state (SA), the tower remains in the elastic domain during an earthquake and continues to operate with minimal or no repair after the earthquake. In the damage control state (DC), the tower sustains considerable damage and plastic deformation. Depending on the extent of damage, the tower may be beyond economical repair. In the collapse prevention state (CP), the tower sustains damage, such that it can no longer support the weight of the conductors and its own weight [174]. The maximum intersegment drift ratio (ISDR), defined as the ratio

between the differential lateral displacement between two consecutive segments of a tower and their respective height, is assumed here as the response parameter that correlates best with tower damage. Similar to the seismic fragility of steel moment frames, the ISDR threshold values of the three damage states are 0.8%, 2% and 4%, respectively, of the height between consecutive segments [174]. To convert the pushover curve into a fragility function, the spectral acceleration (S_a) at the fundamental period of vibration of the tower (T) is regarded as an IM. The pushover curve and fragility functions for the classic double-circuit power transmission towers found in the study area are shown in Fig 4-4.

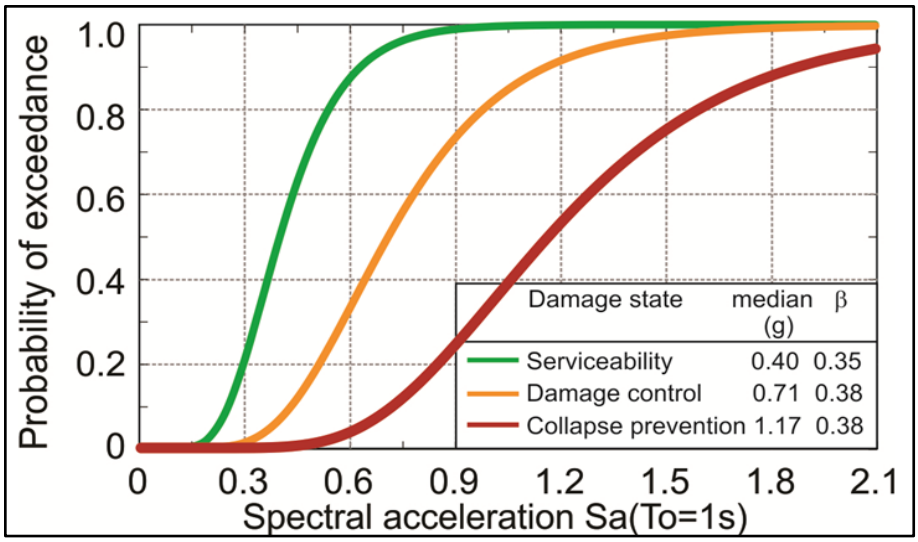

Fig 4-4. Fragility curves for a 87.3 m high Classic Double-circuit tower (Modified from [177]).

Considering the absence of established loss functions for vulnerability assessment in transmission towers, we have defined damage levels as follows: D_0=0, indicating no damage, and D_3=3, representing very severe damage or collapse. The calculation of the final damage ratio for each tower is performed using the following equation:

$$Dm = \sum P_{Ds_i} \times D_i \tag{4-1}$$

where Dm is the damage parameter that represents mean damage to the towers, P_{Ds_i} denotes the probability of each damage state and D_i corresponds to the damage value associated with each respective

damage state. Moreover, users have the option to develop their own vulnerability functions and provide them as input to the software for damage calculation.

4.4.2 Substations

Electrical substations make part of standard electric power transmission and distribution systems that transform voltage from high to low. The major components of a substation include transformers, circuit brakers and switches to isolate different parts of the electric power systems, capacitors to smooth the voltage flow, and other control devices [30]. Transformer steel structures are the largest piece of equipment in a substation structure capable of holding of several thousand Liters of mineral oil used as an insulating material. If not properly designed and anchored, this type of equipment is particularly vulnerable to seismic shaking. Due to its direct relation to inertial forces, the peak ground acceleration PGA represents a common measure of the seismic shaking intensity in stiff structures, such as substations. These types of structures basically reproduce the seismic shaking occurring at the ground surface. Therefore, the damage potential of substations is defined in terms of PGA. Herein, the fragility curves developed for HAZUS, the standard seismic risk assessment tool developed by US Federal Emergency Management Agency (reference technical manual) are used to determine the five damage states: none, slight, moderate, extensive, and complete, which can be attained during a strong seismic shaking. In case of substations, which contain many different components, these damage states determine the percentage of subcomponents that suffered damage. In Fig 4-5 are given the fragility functions for high and low voltage substations as recommended in [76]..

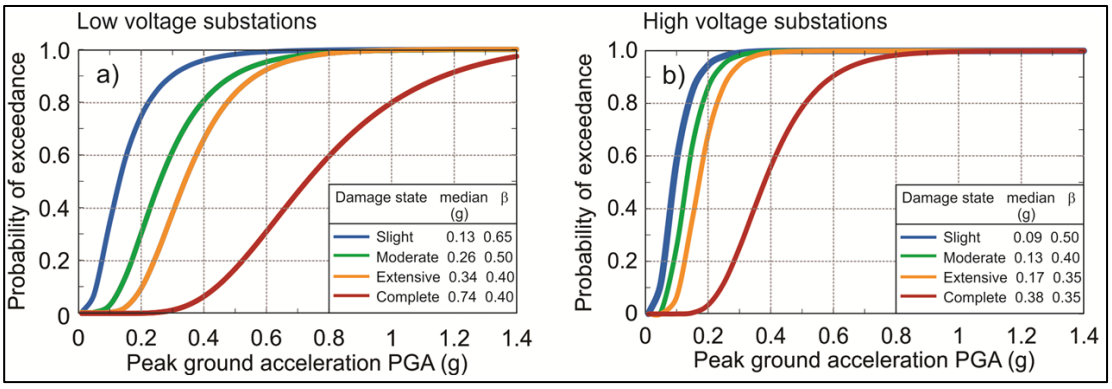

Fig 4-5. Fragility curves for high and low voltage substations with standard components ([76]).

Since the substations contain many different components, the damage states shown in Fig 4-5 actually determine the percentage of subcomponents that suffered damage: 0% (none), 5% (slight), 40% (moderate), 70% (extensive) and 100% (complete damage).

4.5 DAMAGE COMPUTATION MODULE

At present, the developed software has two distinct risk calculation workflows. The first workflow is designed to calculate damages resulting from a single user-defined seismic event. The second workflow is designed to compute seismic risk by factoring in the uncertainty associated with site parameters (V_s and T_0) and hazard parameters (PGA and Sa). In both cases, damage to transmission towers and substations is calculated for the respective IMs. As discussed earlier, damage calculation is probabilistic in nature because for the same IM, the probability of being in each of the four damage states is different.

The damage calculation workflows within the software are composed of multiple individual calculators (see Fig 4-2-pink part). Several parameters must be defined before running any of these workflows. These parameters include the geographic coordinates of the region of interest, the type of calculations being performed, the path to the input files and the specific results that must be produced. In addition, certain parameters are necessary for hazard calculations and must be specified in advance. By defining these parameters beforehand, the software can accurately and efficiently calculate seismic risks and potential damages associated with seismic events in a given region. This level of customisation and control is crucial for providing useful and reliable risk assessments for decision-making and policy planning. As such, the ability to define these parameters and run multiple workflows is a key feature of the developed software.

4.5.1 Probabilistic damage calculation workflow

The workflow for calculating damage estimates employs a probabilistic approach for incorporating uncertainties into site parameters (Vs_{30} and T_0) and hazard values, such as spectral acceleration at a period of 1 s ($Sa\ (1.0s)$). Firstly, the MC approach is applied to account for uncertainties in site parameters (Fig 4-2-blue part). In addition, another set of MC simulations is conducted to account for uncertainties in seismic IMs (e.g. PGA or Sa), applying the normal distribution and standard deviation defined in NBCC2020 GMPEs [23,

178]. The resulting values are then used to calculate the mean and standard deviation of damage states. Fig 4-2 (pink section) illustrates this probabilistic procedure for damage calculation. Furthermore, user can select NBCC2020 probabilistic maps as hazard input and run MC base site parameters to calculate damage values for installations.

4.6 RESULTS

The software generates results in three major domains: 1) site parameter analysis, 2) hazard assessment and 3) damage assessment for electric transmission towers and substations. Each of these steps includes two types of analysis: deterministic (user-defined) and probabilistic (MC based multi scenario). To evaluate the software's capabilities, geological, geotechnical and exposure data were gathered from the Saguenay region and Hydro-Quebec facilities. The detailed results of the damage simulator are presented in the following subsections.

4.6.1 Determination of site parameters and their uncertainties

The deterministic results of the site parameter analysis conducted in Saguenay are presented in Fig 4-6. This figure displays a high-resolution map of Vs_{30} and T_0, aid users to identify regions that are more susceptible and vulnerable to seismic amplification.

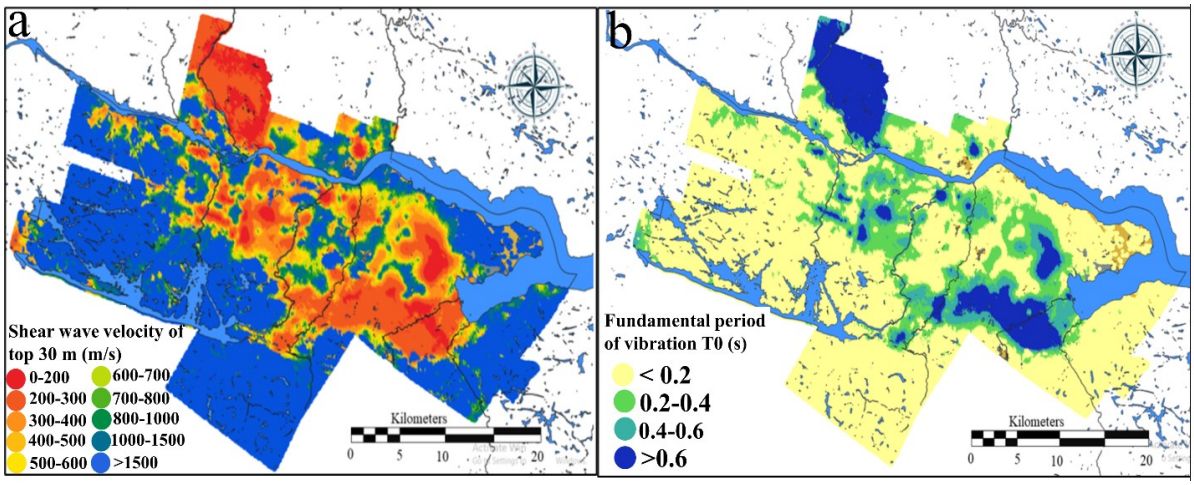

Fig 4-6. Deterministic site parameters maps: a) Vs_{30} map b) T_0 map.

Fig 4-7 presents the probabilistic maps of Vs_{30} and T_0 obtained using the MC approach described in overall flowchart of the damage simulator (Fig 4-2-blue part). These results enable users to conduct uncertainty analysis of seismic hazard and its effect on risk assessments. The results related to uncertainty of site parameters are presented in Fig 4-7-b and Fig 4-7-d. This map provides valuable insights into seismic hazard and risk in the area. These insights can be useful for various applications, such as disaster mitigation.

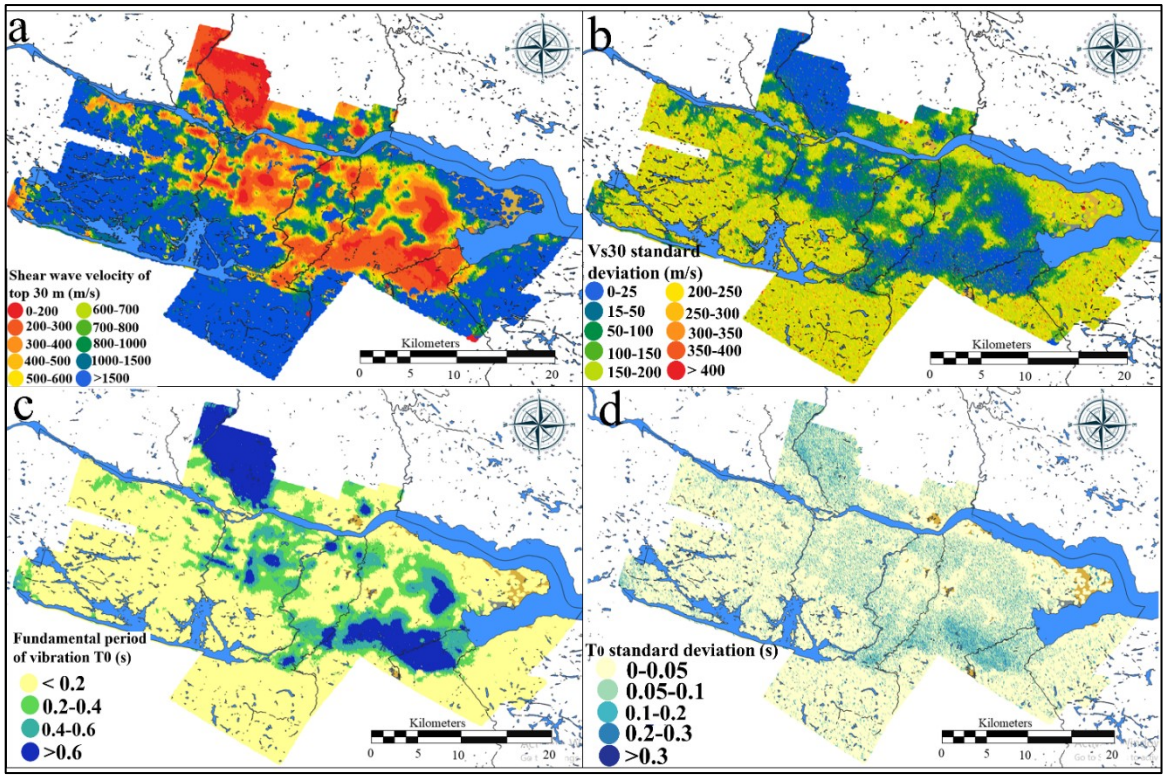

Fig 4-7. Probabilistic site parameters maps using the 3D probabilistic Vs model and MC simulations: a) Mean values of Vs_{30}, b) Standard deviations of Vs_{30}, c) Mean values of T_0 and d) standard deviations of T_0

The code for the probabilistic evaluation of the seismic site parameters developed using MC simulations was tested and validated for the geological and geotechnical settings in the Saguenay region located in eastern Canada. The study region was modelled with a grid of 155 800 2D 75 m × 75 m cells on the surface and 1 061 200 3D 2 m-thick block elements. Chi square and Q-Q statistical models were used to determine the best-fitting V_s distribution functions. The code used site-specific V_s –depth models for each of the considered uppermost surficial units: clayey silty soil and coarser sandy soil, which alternate spatially and are vertically separated with transition zones. MC simulations were used to sample the occurrence of these soil units at every 2 m deep and each with its own probability of occurrence. V_s values were then retrieved from the regression models for each block element. Fixed V_s values were assumed for the glacial till unit at the base of the Quaternary stratigraphy and bedrock formations.

4.6.2 Seismic hazard assessment with integration of uncertainty

The results obtained from the hazard analysis can be categorised into user-defined event scenarios, probabilistic hazard scenarios and seismic hazard based on MC scenarios and represented in terms of PGA and Sa.

4.6.2.1 User-defined event scenarios

To assess seismic hazard in Saguenay comprehensively, a scenario-based analysis was implemented. For this purpose, a magnitude 5.9 earthquake with a depth of 10 km was considered the hazard input parameter. The results are presented in Fig 4-8 and they provide hazard parameters in terms of PGA and spectral acceleration at a period of 1 s ($Sa\ (1.0s)$) corresponding to the fundamental vibration period of the classic double-circuit electric tower. The software also allows users to select other IMs for damage assessment. As illustrated in Fig 4-8, the software provides a spatial distribution of hazard parameters for the Saguenay region.

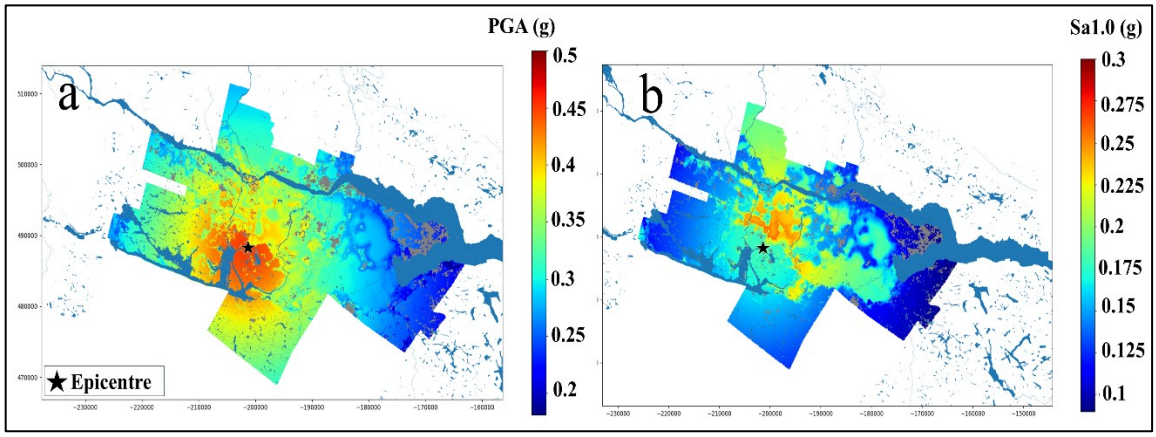

Fig 4-8. User defined scenario hazard maps for an earthquake with M=5.9 and depth of 10km; a) Peak ground acceleration b) Spectral acceleration for a period of 1.0 s.

To assess the efficacy of the newly developed software, a comparative probabilistic analysis was conducted using the ER2 software (Fig 4-10-a and Fig 4-10-b) developed for regional seismic risk assessment in eastern Canada. The results obtained from the developed software presented more precise hazard maps compared with those generated using the ER2 software. Notably, the ER2 software was

primarily designed to enable rapid hazard and damage assessments of a built environment, where uniform site conditions (site class D) are assumed for the Saguenay region.

4.6.2.2 Probabilistic hazard scenarios

The developed software exhibits the capability to generate probabilistic maps for various IMs and probabilities of exceedance. Fig 4-9 presents the $Sa\ (1.0s)$ map for the Saguenay region, with a probability of 2% over 50 years. These maps were generated using the NBCC2020 model. By integrating the site conditions model for Saguenay, the software was able to produce very detailed results, in contrast with ER2 (Fig 4-10-c and Fig 4-10-d).

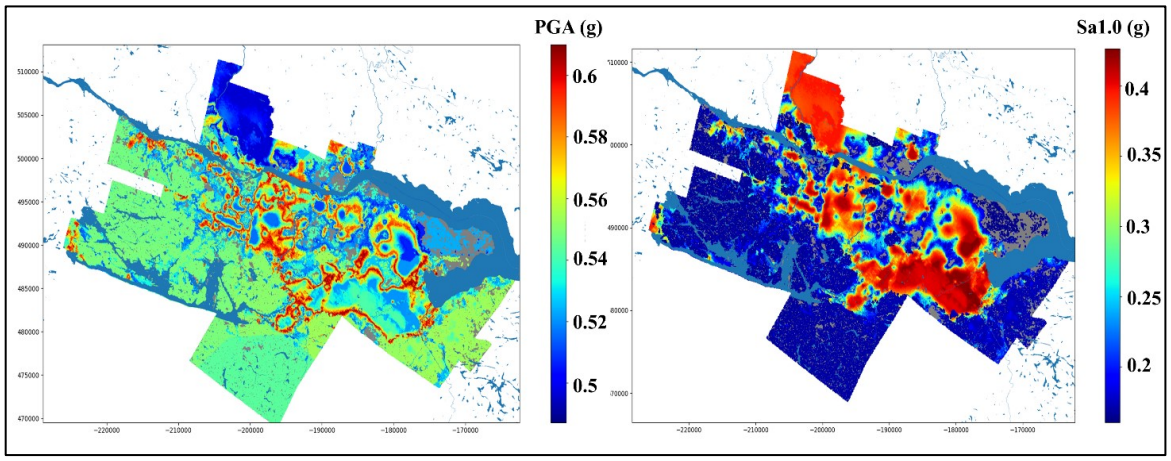

Fig 4-9. Hazard results for Saguenay region for 2% in 50 years probabilistic hazard, a) PGA map, b) Sa1.0 map.

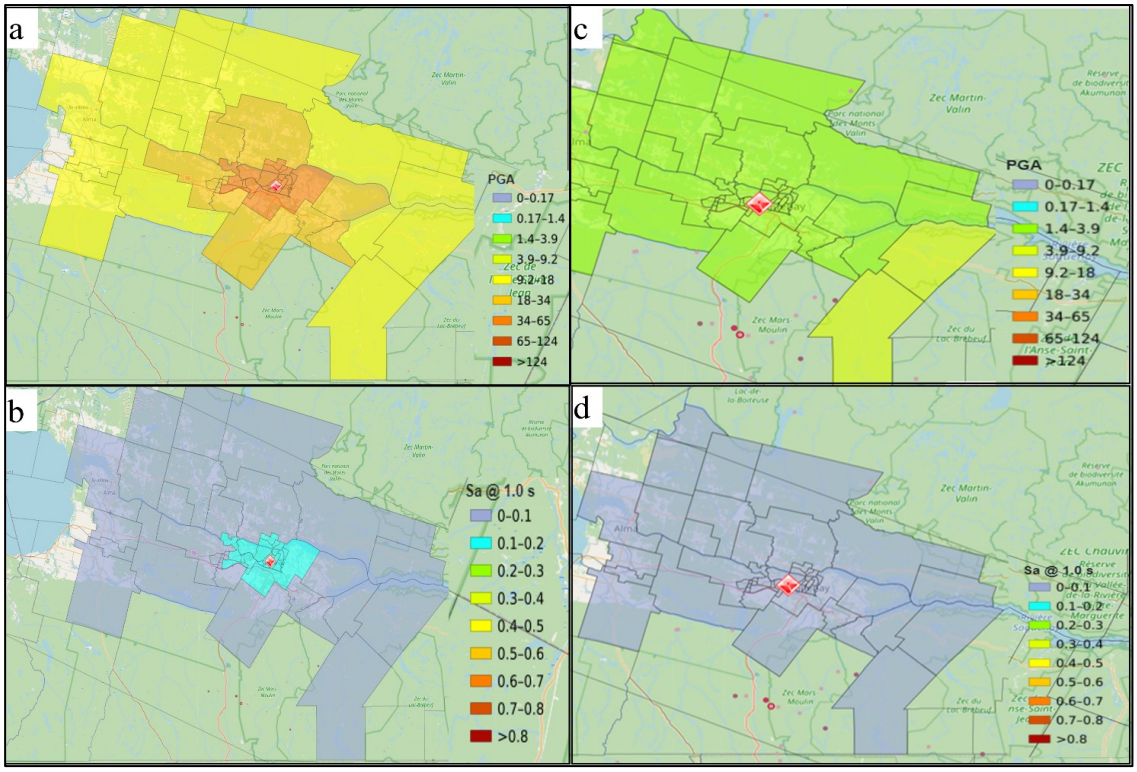

Fig 4-10. ER2 deterministic and probabilistic hazard map for the PGA and Sa1.0 parameters of the Saguenay region.

4.6.2.3 Seismic hazard scenarios based on 3d probabilistic Vs30 model and GMPEs uncertainty

As described in the methodology section, a novel aspect of the software utilised in hazard assessment is the full implementation of the MC method to generate hazard scenarios through the randomisation of site parameters and IMs. Fig 4-11-a and Fig 4-11-c display the mean PGA and $Sa\ (1.0s)$ value maps, along with their respective standard deviation (Fig 4-11-b and Fig 4-11-d). To obtain these values, 1000 MC realisations were generated for each grid cell of the mesh, and the results were subsequently averaged, and the standard deviation was assessed. These realisations may also serve as input options for the damage assessment module.

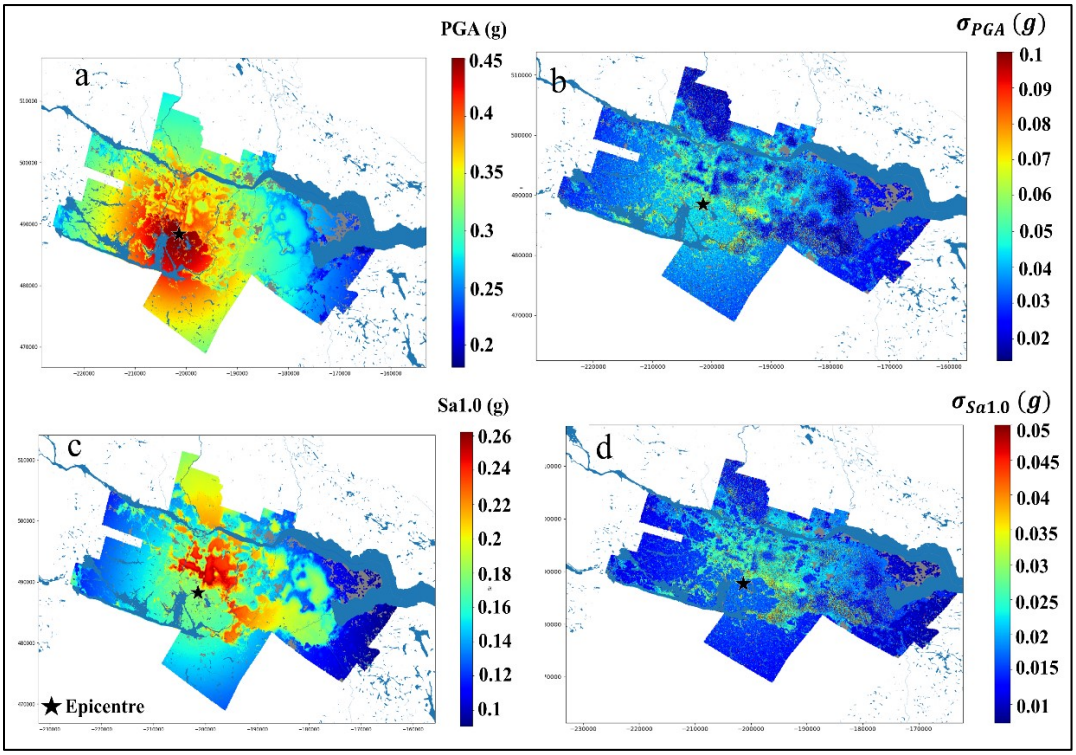

Fig 4-11. User defined scenario including uncertainties in Vs_{30} and GMPEs: a-b) mean PGA and standard deviation and c-d) mean Sa1.0 and standard deviation.

One key advantage of using the MC method in hazard assessment is the ability to model a range of potential scenarios, each with varying combinations of input parameters. This multi-scenario approach can provide a more comprehensive assessment of hazard risks, enabling users to understand the range of possible outcomes better and prepare accordingly. By incorporating the variability and uncertainty of site parameters and hazard intensities, the MC method produces a broader range of potential outcomes than a traditional deterministic analysis. Furthermore, the ability to generate multiple realisations enables users to assess the likelihood of various scenarios and their associated hazards. By providing a more detailed and probabilistic understanding of potential hazards, the MC approach offers valuable insights for hazard assessment and risk management.

4.6.3 Damage calculation results

The final results from the developed software are related to the damage assessment of electrical installations. Users can obtain results for single or multiple towers and substations by inputting deterministic or probabilistic values for site parameters and hazard intensities at the bedrock level. These results correspond to deterministic, MC-based probabilistic and NBCC2020 probabilistic scenarios.

4.6.3.1 Damage assessment for deterministic hazard scenarios

The results from this feature can be classified into two categories: deterministic fragility analysis and deterministic damage assessment. To evaluate the output of the software, fragility analysis was conducted for Saguenay 1988 earthquake scenario, with a magnitude of 5.9 and a depth of 28 km. The results are presented for two example towers and two substations in Fig 4-12 . T15 and T42 are towers number 15 and 42 which presented in Fig 4-12.

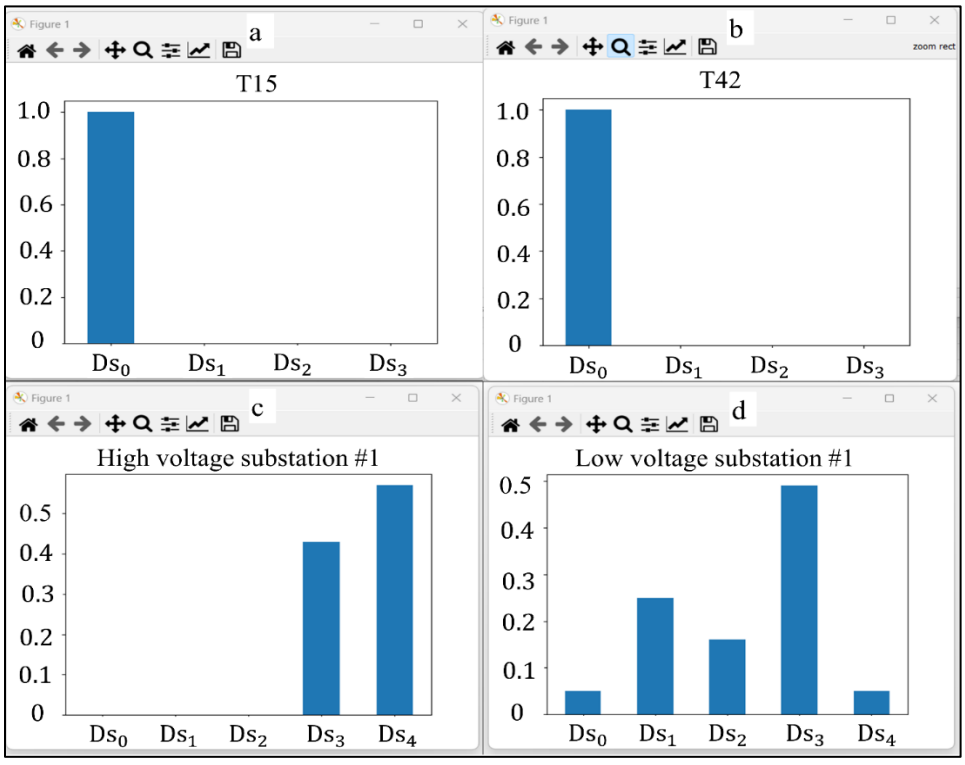

Fig 4-12. Deterministic fragility analysis of electric towers and substation for Saguenay 1988 earthquake scenario: a-b) results for two towers in region c-d) results for high voltage and low voltage substation.

The analysis of fragility for towers and substations reveals that substations are more susceptible to earthquake hazards. For towers, the fragility analysis indicates that all of them experience either no damage or only slight damage. However, when it comes to substations, the majority of them exhibit moderate to complete damage states in the fragility analysis.

In terms of deterministic damage assessment, damage analysis was conducted for the installations of the Hydro-Quebec transmission line in the Saguenay region. To this end, 95 electric towers and 6 substations were introduced with their respective coordinates. Fig 4-13 shows the damage map for Hydro-Quebec installations in a selected area. As illustrated in Fig 4-13, most of the towers in this analysis were not affected by the considered earthquake scenario but substations show relatively high vulnerability to seismic hazard. To assess the reliability of the results, we considered the hazard scenario associated with the Saguenay earthquake of 1988. The damage results generated by the developed code were consistent with the observations made during the 1988 earthquake, i.e. in accordance with the literature, electric towers were unaffected during the Saguenay earthquake.

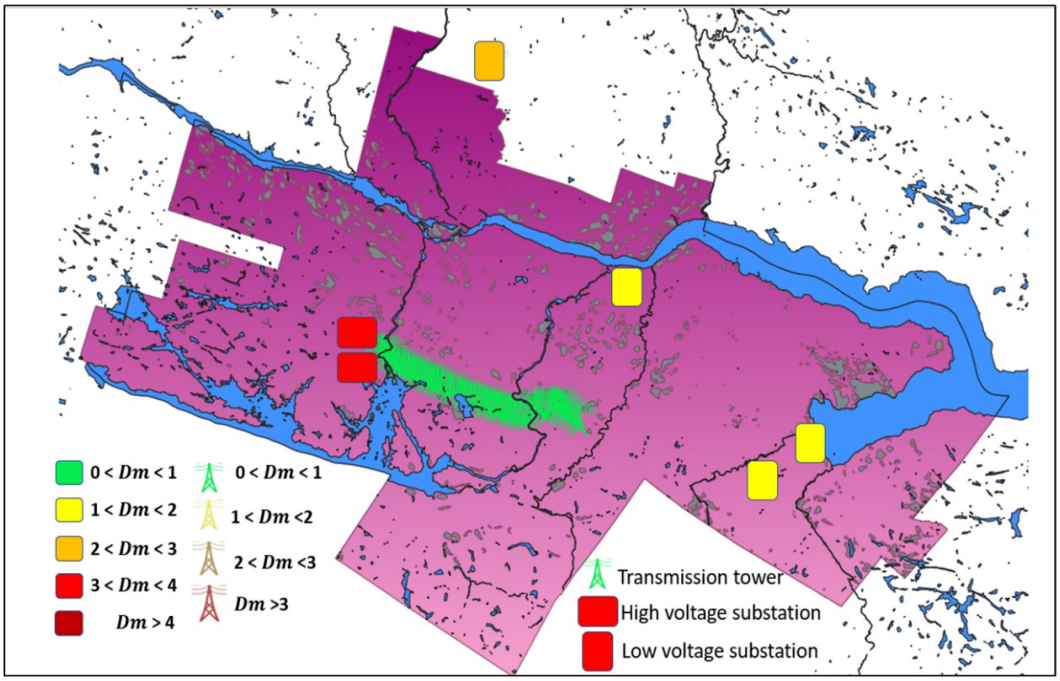

Fig 4-13. Deterministic damage assessment for the Hydro-Quebec installations in Saguenay for a scenario with M=5.9 and depth 28 km.

4.6.3.2 Damage results of electrical installations based on multiple scenario (MC method)

To evaluate the software's ability to account for uncertainties in damage assessment, we implemented a probabilistic damage analysis by using the MC method. This approach generated multiple realisations of the damage parameter with different probabilities of occurrence, enabling us to capture the effect of variability of site parameters (Vs_{30} and T_0) and hazard intensity (PGA or $Sa\ (1.0s)$).

The results of the probabilistic fragility analysis for two example towers and substations are presented in Fig 4-14. By utilizing this function, it becomes feasible to acquire the average and standard deviation for every damage state along with the damage parameter (D_m). This enables a thorough comprehension of the potential range of damage and the probabilities linked to each of them.

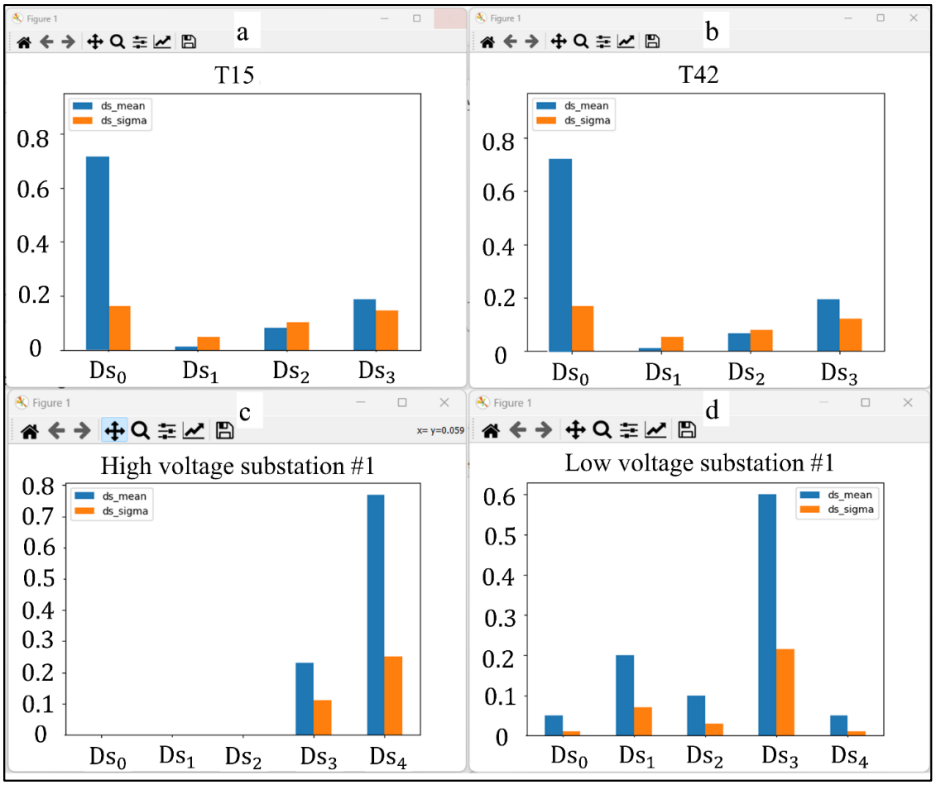

Fig 4-14. Multi-scenario fragility analysis for transmission towers and substations.

Fig 4-15 presents probabilistic damage results and uncertainties related to the damage for towers and substations. The probabilistic damage analysis demonstrated the software's ability to account for uncertainties in damage assessment, enhancing the accuracy of damage predictions and reducing associated uncertainties. This approach provides users with more precise values and a better understanding of the effect of uncertainties on final damage outcomes. By incorporating this feature, our software can empower users to make more informed decisions regarding risk mitigation and disaster management strategies, ultimately contributing to the increased resilience of critical infrastructure in hazard-prone regions.

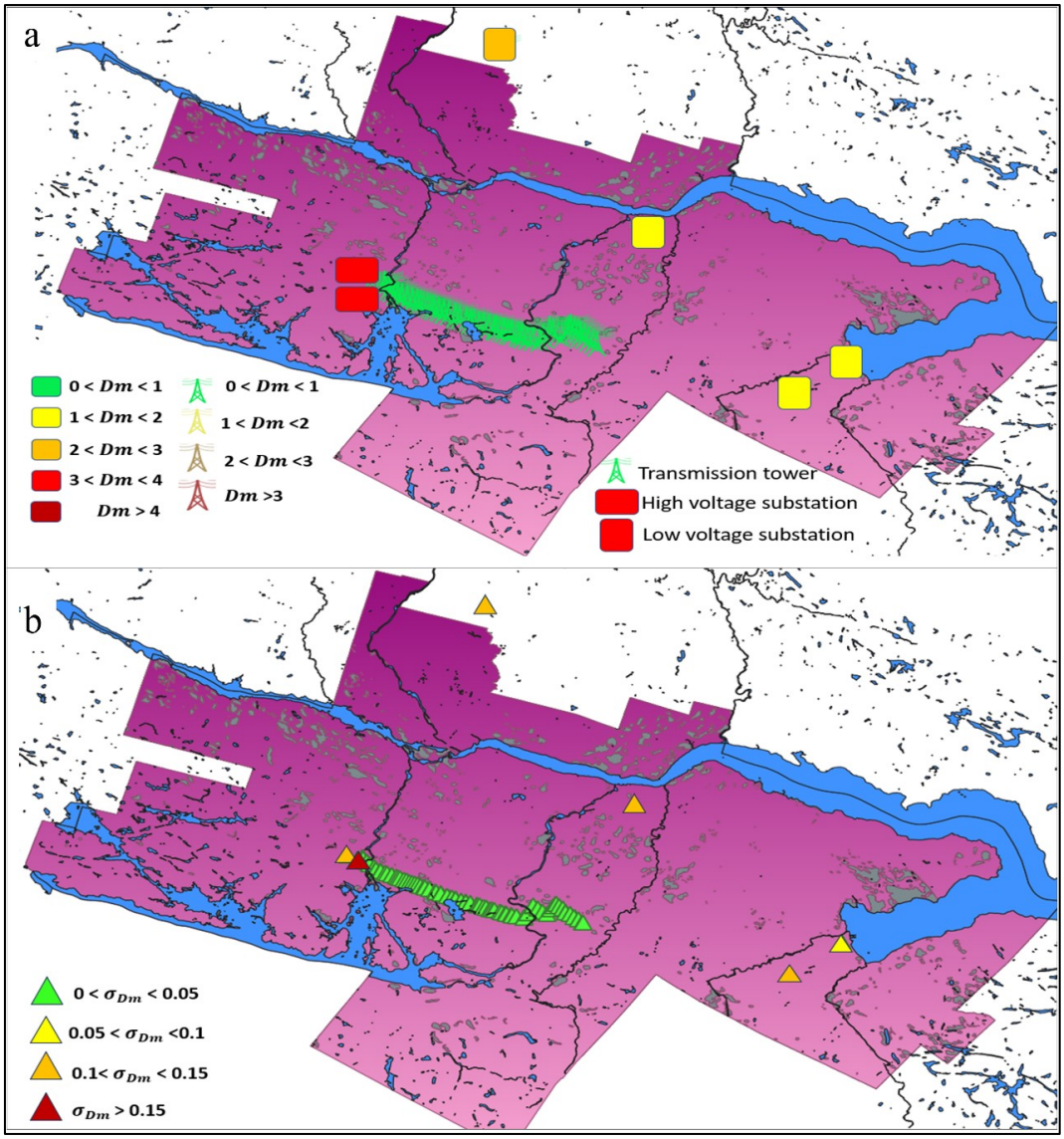

Fig 4-15.Probabilistic MC-based damage assessment for the Hydro-Quebec installations in Saguenay for a scenario with M=5.9 and depth 28 km, a) mean damage b) standard deviation of damage.

4.6.3.3 Damage results of electrical installations based on probabilistic scenarios

Moreover, for the third phase of damage assessment, we employed the probabilistic approach based on NBCC2020 with a hazard level of 2% probability of exceeding in 50 years. The analysis focused on the electric installations of the Hydro-Quebec transmission line in the Saguenay region.

The damage map in Fig 4-16 presents the outcomes for the Hydro-Quebec installations within the selected area. Notably, the majority of the towers analyzed remained unaffected by the earthquake scenario considered. However, the substations exhibited a relatively higher vulnerability to the seismic hazard, suggesting the potential for damage during events with a 2% probability of exceeding the specified hazard levels.

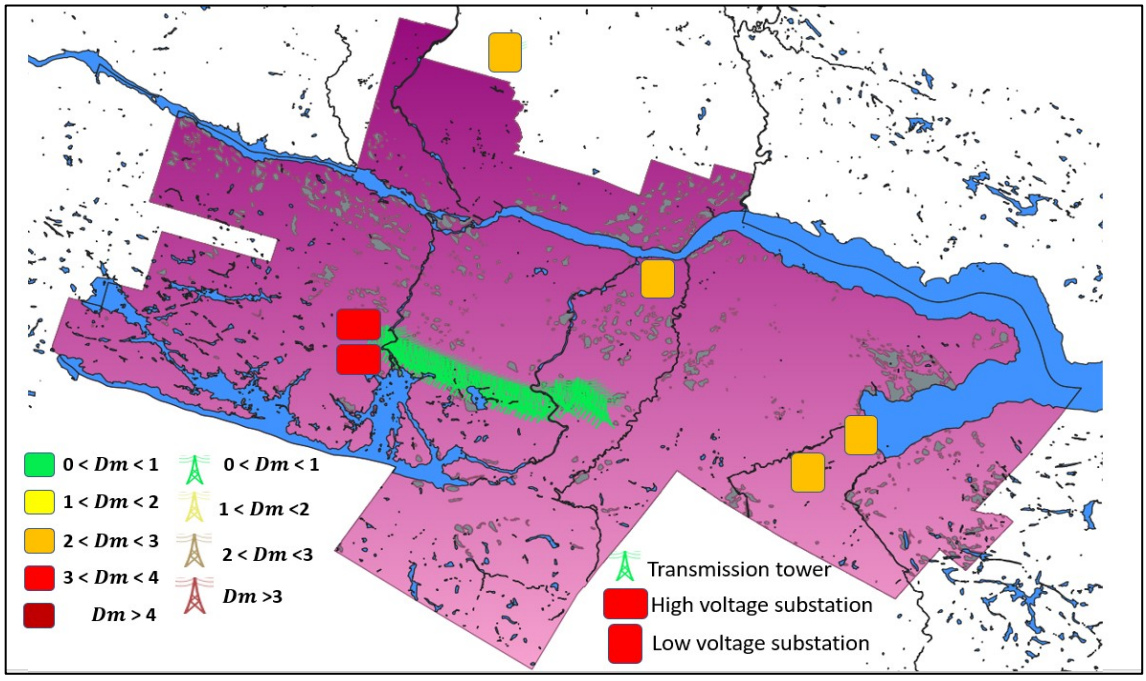

Fig 4-16. Damage calculation based on probablistic scenario of 2% probability of exceedance.

4.7 CONCLUSION

This study presents the development of a damage simulator for assessing the seismic damage of electric transmission towers and substations. The simulator was created to address the need for a user-friendly tool that could assess seismic risk for specific installations. To achieve this objective, the tool was developed to enable site parameter analysis (Vs_{30} and T_0), hazard assessment (PGA or Sa) and damage calculation modules (fragility and damage factor). Each module of the simulator employs two types of analyses, i.e. deterministic and probabilistic, to provide a variety of choices to the end user.

A novel site parameter unit (Vs_{30}, T_0) was introduced by applying a 3D block model and an MC-based V_s uncertainty incorporation algorithm. The novelty of this approach lies in recognising the irregular probability distribution of V_s with depth and accounting for specific sedimentation and erosion in determining local site parameters.

With regard to hazard assessment, the software introduced a hazard module that performs user-defined scenario, conventional probabilistic and multi-scenario probabilistic analyses. Epistemic uncertainty is captured using multiple GMPE models that were recently used in NBCC2020. Furthermore, aleatory uncertainty in this part is addressed by using a novel MC-based algorithm.

The damage assessment process employs two methodologies to provide deterministic results by considering different exposed installations and multi-scenario probabilistic analysis. In the second algorithm, uncertainties in site parameters and intensity measure (Sa 1.0) are included to provide reliable results from the software. To provide better user experience, the most advanced Python libraries are used to perform thousands of calculations in only a few minutes.

In order to assess the software's performance, a comprehensive case study was carried out utilizing the implemented code on transmission towers and substations operated by Hydro-Quebec in the Saguenay region of eastern Canada. The findings indicate that while the transmission towers remain unaffected by earthquake hazards, the substations are more vulnerable and prone to damage when exposed to seismic activity.

CHAPTER 5

CONCLUSION

In addition to the detailed conclusions in each of the scientific papers listed in Chapters 2 through 4, an overall conclusion summary obtained from the entire paper is provided herein, followed with recommendations for future work.

This thesis focuses on the aspects of seismic hazard, inventory of electric power transmission facilities and respective vulnerabilities to earthquake shaking. The development of the damage simulator aims to combine these steps in an all-in-one operation of assessment of the seismic vulnerability of electric transmission facilities. Equipped with a user-friendly interface, the simulator is intended for use by the non-expert public safety community, enabling it to identify, quantify and understand seismic risks associated with electric network components. The simulator fills the existing gap between purely building oriented seismic risk software that fail to account for the electric transmission facilities and detailed engineering studies at the scale of the facility itself. The damage simulator comprises three complementary modules for characterization of seismic site parameters, hazard assessment and damage calculation. These modules utilize deterministic and probabilistic analyses to provide the user multiple options for seismic risk assessment.

As an introductory step, a comprehensive state-of-the-art review of existing seismic risk assessment software was conducted to summarize the employed seismic risk methodologies and software components, facilitating the identification of their respective advantages and limitations. In addition to the thorough investigation of the structure of seismic risk assessment, it provided valuable insights and directions applied in the development of the damage simulator.

In the second paper, a novel approach was introduced for characterization of seismic site parameters, V_s and fundamental vibration period of surficial sediments (T_0), applying a probabilistic 3D block model together with an MC-based uncertainty incorporation algorithm. This approach accounts for the irregular probability distribution of V_s with depth, thus incorporating the region specific geological and geotechnical

conditions. The novelty of this approach is recognition of the fact that the soil stiffness properties, expressed with V_s, are functions of the specific sedimentation and erosion processes that took place during the geological age and reflected with the current local stratigraphy. This finding is accounted for by site-specific V_s vertical profiles determined at each 2 m depth for each of the considered surficial units (clayey and sandy soils).

The study region was first modelled with a grid of 155 800 2D 75×75 m grid cells on the surface. Additionally, 1 061 200 3D block elements of 75×75×2 m were included, extending all the way to the bedrock interface. A statistical model based on chi-square and Q-Q plot was developed to determine the best fit V_s probability distribution function for each 2 m depth. Ten different distribution functions were tested. The randomised V_s values were generated by applying MC simulations with the pre-determined distribution functions for each block element of the probabilistic 3D geological model. The final seismic microzonation results consist of the Vs_{30} map (V_s of the first 30 m), the Vs_{30} uncertainty map and the expected T_0 and T_0 uncertainty maps.

The hazard assessment module was developed integrating (i) user-defined scenario analysis DSHA (what-if event scenario with given magnitude, epicentre location and depth), (ii) probabilistic hazard analysis PSHA (quantification of the exceedance rate of different ground-motion intensities considering effects from all potential earthquake sources) and (iii) MC-based multiscenario probabilistic analysis. To address epistemic uncertainty, multiple GMPE models were employed. Furthermore, a novel MC-based algorithm was utilized to handle aleatory uncertainty.

The damage assessment embedded in the damage simulator encompasses two main approaches: (i) deterministic damage analysis, which calculates damage to electric towers and substations based on deterministic input parameters for local site conditions and hazard parameters, (ii) probabilistic damage analysis using probabilistic hazard values of NBCC2020 and (iii) multiscenario probabilistic analysis using the MC method, which integrates uncertainties associated with the site parameters (Vs_{30} and T_0) and the resulting shaking intensity measures ($PGA\ and\ Sa\ (1.0s)$) to ensure the accurate assessment of the expected damage values. To facilitate the use, the simulator relies on advanced Python libraries and performs multiple

calculations within minutes. To validate the software's performance, a case study was conducted with transmission towers and substations owned by Hydro-Quebec in the Saguenay region, eastern Canada.

5.1 PERSPECTIVES FOR FUTURE RESEARCHS

This PhD thesis focuses on the development of a damage simulator for assessing the seismic vulnerability of electric towers. In addition, the research team addresses previously underexplored but intriguing aspects widely applicable to the study of seismic risk assessment. In this section, recommendations for future research are provided, listing the items pertinent to the main or sub objectives of the thesis.

- To simplify the problem, this thesis relied on existing fragility and vulnerability functions, which provided a foundation for analyses of the seismic risk to electric transmission facilities. To attain even more accurate and reliable results, this thesis recommends developing vulnerability and fragility models tailored for the specific electric power installations by employing advanced numerical and analytical methods.
- To conduct a more comprehensive risk analysis, considering a wider range of infrastructure building types and infrastructure categories beyond electric transmission towers is advisable. Whilst this thesis focused on assessing the seismic vulnerability of transmission towers, expanding the scope to encompass other critical structures, such as buildings, bridges or lifeline systems, would provide a more holistic understanding of the overall seismic risk in each region. By considering multiple building types and infrastructure categories, the risk analysis can account for the diverse vulnerabilities and potential cascading effects that may arise during seismic events. This broader perspective will contribute to more effective risk management strategies, mitigation measures and emergency response planning.
- For the purpose of conducting a more comprehensive probabilistic analysis, future research could employ a multi-scenario approach that incorporates varying probabilities of occurrence for each scenario. This approach can be compared to the methodology adopted in this thesis.
- To facilitate expeditious risk assessment, an online tool can be devised for conducting a comprehensive evaluation of infrastructure's vulnerability.

References

1. Guha-Sapir, D., P. Hoyois, and R. Below, *Annual Disaster Statistical Review 2015: The numbers and trends. Centre for Research on the Epidemiology of Disasters (CRED). Institute of health and Society (IRSS) Universite catholique de Louvain–Brussels, Belgium*. 2017.
2. Porter, K., *A Beginner's guide to fragility, vulnerability, and risk. University of Colorado Boulder*. 2017.
3. Hosseinpour, V., et al., *Seismic loss estimation software: A comprehensive review of risk assessment steps, software development and limitations.* Engineering Structures, 2021. **232**: p. 111866.
4. Whitman, R.V., et al., *Development of a national earthquake loss estimation methodology.* Earthquake Spectra, 1997. **13**(4): p. 643-661.
5. Kircher, C.A., R.V. Whitman, and W.T. Holmes, *HAZUS earthquake loss estimation methods.* Natural Hazards Review, 2006. **7**(2): p. 45-59.
6. MAE Center, M.-A.E., *MAEviz software.* Urbana, IL: MAE Center, University of Illinois at Urbana-Champaign, 2006.
7. Yeh, C.-H., C.-H. Loh, and K.-C. Tsai, *Overview of Taiwan earthquake loss estimation system.* Natural hazards, 2006. **37**(1-2): p. 23-37.
8. Molina, S. and C. Lindholm, *A logic tree extension of the capacity spectrum method developed to estimate seismic risk in Oslo, Norway.* Journal of Earthquake Engineering, 2005. **9**(06): p. 877-897.
9. Ulmi, M., et al., *Hazus-MH 2.1 Canada, User and Technical Manual: Earthquake Module*. 2014: Natural Resources Canada.
10. AIFDR, *AIFDR, Australia-Indonesia Facility for Disaster Reduction, InaSafe-Eartquake tool, Available Online at: < http://inasafe.org/> (Accessed on 20 May 2020).* 2020.
11. Reinoso, E., et al. *After 10 years of CAPRA*. in *Proceedings of the 16th European Conference on Earthquake Engineering*. 2018.
12. Crowley, H., R. Pinho, and J.J. Bommer, *A probabilistic displacement-based vulnerability assessment procedure for earthquake loss estimation.* Bulletin of Earthquake Engineering, 2004. **2**(2): p. 173-219.
13. Silva, V., et al., *Development of the OpenQuake engine, the Global Earthquake Model's open-source software for seismic risk assessment.* Natural Hazards, 2014. **72**(3): p. 1409-1427.
14. Abo El Ezz, A., et al., *ER2-Earthquake: Interactive web-application for urban seismic risk assessment.* International Journal of Disaster Risk Reduction, 2019. **34**: p. 326-336.
15. Borcherdt, R.D., *Effects of local geology on ground motion near San Francisco Bay.* Bulletin of the Seismological Society of America, 1970. **60**(1): p. 29-61.
16. NEHRP, *Recommended provisions for seismic regulations of new buildings: Part I, provisions, FEMA 222A, National Earthquake Hazard Reduction Program*. 1994, Federal Emergency Management Agency Washington, DC.
17. Canadian Commission on Building and Fire Codes, *National Building Code of Canada: 2015*. 2015, National Research Council of Canada.
18. Akkar, S., M.A. Sandıkkaya, and J.J. Bommer, *Empirical ground-motion models for point-and extended-source crustal earthquake scenarios in Europe and the Middle East.* Bulletin of earthquake engineering, 2014. **12**(1): p. 359-387.
19. Borcherdt, R.D., *Estimates of site-dependent response spectra for design (methodology and justification).* Earthquake spectra, 1994. **10**(4): p. 617-653.
20. Boore, D.M., W.B. Joyner, and T.E. Fumal, *Estimation of response spectra and peak accelerations from western North American earthquakes: an interim report.* 1993.
21. European Committee for Standardization, *Eurocode 8: Design of structures for earthquake resistance-part 1: general rules, seismic actions and rules for buildings.* Brussel, 2005.
22. Canadian Commission on Building and Fire Codes, *National Building Code of Canada: 2020*. 2022, National Research Council of Canada.
23. Atkinson, G.M. and J. Adams, *Ground motion prediction equations for application to the 2015 Canadian national seismic hazard maps.* Canadian Journal of Civil Engineering, 2013. **40**(10): p. 988-998.
24. Kramer, S.L., *Geotechnical earthquake engineering*. 1996: Pearson Education India.
25. Cheng, Z., et al., *A numerical investigation of fine sediment resuspension in the wave boundary layer—Uncertainties in particle inertia and hindered settling.* Computers & Geosciences, 2015. **83**: p. 176-192.
26. Zhang, M. and H. Pan, *Application of generalized Pareto distribution for modeling aleatory variability of ground motion.* Natural Hazards, 2021. **108**(3): p. 2971-2989.

27. Reyners, M., *Lessons from the destructive Mw 6.3 Christchurch, New Zealand, earthquake.* Seismological Research Letters, 2011. **82**(3): p. 371-372.
28. Naddaf, M., *Turkey-Syria earthquake: what scientists know.* Nature, 2023.
29. Pitilakis, K., H. Crowley, and A.M. Kaynia, *SYNER-G: Typology definition and fragility functions for physical elements at seismic risk: buildings, lifelines, transportation networks and critical facilities*. Vol. 27. 2014: Springer Science & Business Media.
30. Quebec, H. *Power Transmission | Towers | Hydro-Québec*. 2023; Available from: http://www.hydroquebec.com/learning/transport/types-pylones.html.
31. Fujisaki, E., et al. *Seismic vulnerability of power supply: lessons learned from recent earthquakes and future horizons of research*. in *Proceedings of 9th international conference on structural dynamics (EURODYN 2014). European Association for Structural Dynamics, Porto, Portugal*. 2014.
32. Pires, J., A.-S. Ang, and R. Villaverde, *Seismic reliability of electrical power transmission systems.* Nuclear engineering and design, 1996. **160**(3): p. 427-439.
33. Park, H.-S., et al., *Seismic performance evaluation of high voltage transmission towers in South Korea.* KSCE Journal of Civil Engineering, 2016. **20**(6): p. 2499-2505.
34. Rodriguez-Marek, A., et al., *Capturing epistemic uncertainty in site response.* Earthquake Spectra, 2021. **37**(2): p. 921-936.
35. Atkinson, G.M., J.J. Bommer, and N.A. Abrahamson, *Alternative Approaches to Modeling Epistemic Uncertainty in Ground Motions in Probabilistic Seismic-Hazard Analysis.* Seismological Research Letters, 2014. **85**(6): p. 1141-1144.
36. Porter, K., *Cracking an open safe: uncertainty in HAZUS-based seismic vulnerability functions.* Earthquake Spectra, 2010. **26**(3): p. 893-900.
37. Hosseinpour, V., et al., *A comprehensive review of seismic hazard and loss estimation software*, in *GeoCalgary 2022 (The 75th Canadian Geotechnical Conference)*. 2022: Calgary, Alberta, Canada.
38. Foulon, T., et al., *Spatial distribution of soil shear-wave velocity and the fundamental period of vibration – a case study of the Saguenay region, Canada.* Georisk: Assessment and Management of Risk for Engineered Systems and Geohazards, 2018. **12**(1): p. 74-86.
39. Adams, J., et al., *Canada's 6th Generation Seismic Hazard Model, as Prepared for the 2020 National Building Code of Canada. 12th Can. Conf.* Earthquake Engineering, 2019.
40. Azzouz, E., *Recherche sur la vulnérabilité sismique des équipements électriques au Québec*. 2021, UQAC.
41. FEMA, *HAZUS-MH Technical Manual*. 2003, Federal Emergency Management Agency Washington, DC, USA.
42. Smolka, A., et al. *The principle of risk partnership and the role of insurance in risk mitigation*. in *Proceedings of the 13th World Conference on Earthquake Engineering, Vancouver, Canada, Paper*. 2004.
43. Kazama, M. and T. Noda, *Damage statistics (Summary of the 2011 off the Pacific Coast of Tohoku Earthquake damage).* Soils and Foundations, 2012. **52**(5): p. 780-792.
44. UNISDR, *Global Assessment Report on Disaster Risk Reduction 2015: Making Development Sustainable: the Future of Disaster Risk Management*. 2015: United Nations International Strategy for Disaster Reduction.
45. Tansey, C.M., et al., *Earthquakes to floods: a scoping review of health-related disaster research in low- and middle-income countries.* PLoS currents, 2018. **10**.
46. Chan, E.Y. and J. Kim, *Chronic health needs immediately after natural disasters in middle-income countries: the case of the 2008 Sichuan, China earthquake.* European Journal of Emergency Medicine, 2011. **18**(2): p. 111-114.
47. Smith, W., *The challenge of earthquake risk assessment.* Seismological Research Letters, 2005. **76**(4): p. 415-416.
48. UNISDR, U., *Terminology on disaster risk reduction.* Geneva, Switzerland, 2009.
49. Coburn, A.W. and R.J. Spence, *Earthquake protection*. 2002: Wiley Online Library.
50. Daniell, J., *Open source procedure for assessment of loss using global earthquake modelling software (OPAL).* Natural Hazards and Earth System Sciences, 2011. **11**(7): p. 1885-1899.
51. Bommer, J.J., *Deterministic vs. probabilistic seismic hazard assessment: an exaggerated and obstructive dichotomy.* Journal of Earthquake Engineering, 2002. **6**(spec01): p. 43-73.
52. Bird, J.F. and J.J. Bommer, *Earthquake losses due to ground failure.* Engineering geology, 2004. **75**(2): p. 147-179.

53. Porter, K., et al. *WHE-PAGER Project: a new initiative in estimating global building inventory and its seismic vulnerability*. in *Proceedings of the 14th World Conference on Earthquake Engineering*. 2008.
54. Cornell, C.A., *Engineering seismic risk analysis.* Bulletin of the seismological society of America, 1968. **58**(5): p. 1583-1606.
55. McGuire, R.K., *Seismic hazard and risk analysis*. 2004: Earthquake Engineering Research Institute.
56. National Research Council of Canada, *National Building Code of Canada, 2015*. 2015: National Research Council Canada.
57. Salsabili, M., A. Saeidi, and A. Rouleau. *Comparison of code-oriented site classification in the Saguenay region, Québec*. in *12th Canadian Conference on Earthquake Engineering, Quebec City, Canada*. 2019.
58. Dunbar, P.K., R.G. Bilham, and M.J. Laituri, *Earthquake loss estimation for India based on macroeconomic indicators*, in *Risk science and sustainability*. 2003, Springer. p. 163-180.
59. Wyss, M., et al., *Approximate model for worldwide building stock in three size categories of settlements.* Background Paper prepared for the Global Assessment Report on Disaster Risk Reduction, 2013.
60. De Bono, A. and M.G. Mora, *A global exposure model for disaster risk assessment.* International journal of disaster risk reduction, 2014. **10**: p. 442-451.
61. Mansouri, B., A. Kiani, and K. Amini-Hosseini, *A platform for earthquake risk assessment in Iran case studies: Tehran scenarios and Ahar-Varzeghan earthquake.* Journal of Seismology and Earthquake Engineering, 2014. **16**(1): p. 51-69.
62. Ploeger, S., et al., *Inventory models for regional scale natural hazards risk assessment.* Natural Resources Canada, 2018.
63. Dell'Acqua, F., P. Gamba, and K. Jaiswal, *Spatial aspects of building and population exposure data and their implications for global earthquake exposure modeling.* Natural hazards, 2013. **68**(3): p. 1291-1309.
64. Cooke, R., *Experts in uncertainty: opinion and subjective probability in science*. 1991: Oxford University Press on Demand.
65. Wieland, M., et al., *Towards a cross-border exposure model for the Earthquake Model Central Asia.* Annals of Geophysics, 2015. **58**(1).
66. Calvi, G., et al., *Development of seismic vulnerability assessment methodologies over the past 30 years.* ISET Journal of Earthquake Technology, 2006. **43**.
67. Clementi, F., et al., *Assessment of seismic behaviour of heritage masonry buildings using numerical modelling.* Journal of Building Engineering, 2016. **8**: p. 29-47.
68. Wesson, R.L., et al., *Losses to single-family housing from ground motions in the 1994 Northridge, California, earthquake.* Earthquake Spectra, 2004. **20**(3): p. 1021-1045.
69. Rais, A., S. Giovinazzi, and A. Palermo, *Pipelines at Bridge Crossings: Empirical-Based Seismic Vulnerability Index*, in *Pipelines 2015*. 2015. p. 1642-1654.
70. Banerjee, S. and M. Shinozuka, *Experimental verification of bridge seismic damage states quantified by calibrating analytical models with empirical field data.* Earthquake Engineering and Engineering Vibration, 2008. **7**(4): p. 383-393.
71. Bender, J. and A. Farid, *Seismic vulnerability of power transformer bushings: complex structural dynamics and seismic amplification.* Engineering structures, 2018. **162**: p. 1-10.
72. Rossetto, T., et al., *Evaluation of existing fragility curves*, in *SYNER-G: Typology definition and fragility functions for physical elements at seismic risk*. 2014, Springer. p. 47-93.
73. Kwon, O.-S. and A. Elnashai, *The effect of material and ground motion uncertainty on the seismic vulnerability curves of RC structure.* Engineering structures, 2006. **28**(2): p. 289-303.
74. Calvi, G.M., et al., *Development of seismic vulnerability assessment methodologies over the past 30 years.* ISET journal of Earthquake Technology, 2006. **43**(3): p. 75-104.
75. D'ayala, D., et al., *Guidelines for analytical vulnerability assessment of low/mid-rise Buildings—Methodology. Vulnerability Global Component project*. 2014, DOI.
76. FEMA, *Hazus-MH 2.1 technical manual*. 2012, FEMA Washington, DC.
77. Miranda, E., *Approximate seismic lateral deformation demands in multistory buildings.* Journal of Structural Engineering, 1999. **125**(4): p. 417-425.
78. D'Ayala, D. and E. Speranza, *Definition of collapse mechanisms and seismic vulnerability of historic masonry buildings.* Earthquake Spectra, 2003. **19**(3): p. 479-509.
79. Fajfar, P., *Capacity spectrum method based on inelastic demand spectra.* Earthquake Engineering & Structural Dynamics, 1999. **28**(9): p. 979-993.
80. Council, A.T., *ATC-13 earthquake damage evaluation data for California (Technical Report).* 1985.

81. Jaiswal, K., et al. *Use of expert judgment elicitation to estimate seismic vulnerability of selected building types*. in *Proc. 15th World Conference on Earthquake Engineering, Lisbon, Portugal, 24-28 Sep 2012*. 2012.
82. Bal, İ.E., et al., *Detailed assessment of structural characteristics of Turkish RC building stock for loss assessment models.* Soil Dynamics and Earthquake Engineering, 2008. **28**(10-11): p. 914-932.
83. HAZUS, *HAZUS-MH MR5, Advanced Engineering Building Module (AEBM), Technical and User's Manual*. 2013, FEMA Washington, DC.
84. Mileti, D., *Disasters by design: A reassessment of natural hazards in the United States*. 1999: Joseph Henry Press.
85. Perry, R.W., M.K. Lindell, and K.J. Tierney, *Facing the unexpected: Disaster preparedness and response in the United States*. 2001: Joseph Henry Press.
86. Spence, R., et al., *Earthquake disaster scenario prediction and loss modelling for urban areas.* 2007.
87. Daniell, J., et al., *Review of open source and open access software packages available to quantify risk from natural hazards.* Washington, DC: World Bank and Global Facility for Disaster Reduction and Recovery, 2014.
88. Daniell, J., A. Vervaeck, and F. Wenzel. *A timeline of the Socio-economic effects of the 2011 Tohoku Earthquake with emphasis on the development of a new worldwide rapid earthquake loss estimation procedure*. in *Australian Earthquake Engineering Society 2011 Conference, Nov*. 2011.
89. Kircher, C.A., et al., *Development of building damage functions for earthquake loss estimation.* Earthquake spectra, 1997. **13**(4): p. 663-682.
90. ATC, *Seismic evaluation and retrofit of concrete buildings.* Report No. SSC 96-01: ATC-40, 1996. **1**.
91. Krawinkler, H. and G. Seneviratna, *Pros and cons of a pushover analysis of seismic performance evaluation.* Engineering structures, 1998. **20**(4-6): p. 452-464.
92. Hamburger, R., et al. *FEMA P58: Next-generation building seismic performance assessment methodology*. in *15th World Conference on Earthquake Engineering*. 2012.
93. Lu, X., et al., *A coarse-grained parallel approach for seismic damage simulations of urban areas based on refined models and GPU/CPU cooperative computing.* Advances in Engineering Software, 2014. **70**: p. 90-103.
94. Bommer, J., et al., *Development of an earthquake loss model for Turkish catastrophe insurance.* Journal of Seismology, 2002. **6**(3): p. 431-446.
95. Yeh, C.-H., W.-Y. Jean, and C.-H. Loh. *Building damage assessment for earthquake loss estimation in Taiwan*. in *Twelfth World Conference on Earthquake Engineering*. 2000.
96. Nastev, M., *Adapting Hazus for seismic risk assessment in Canada.* Canadian geotechnical journal, 2013. **51**(2): p. 217-222.
97. Mouroux, P., et al. *The European RISK-UE project: an advanced approach to earthquake risk scenarios*. in *Proc. of the 13th World Conference on Earthquake Engineering*. 2004.
98. Mouroux, P. and B. Le Brun, *Risk-UE project: an advanced approach to earthquake risk scenarios with application to different European towns*, in *Assessing and managing earthquake risk*. 2008, Springer. p. 479-508.
99. Robinson, D., G. Fulford, and T. Dhu, *EQRM: Geoscience Australia's Earthquake Risk Model: Technical Manual: Version 3.0, GA Record 2005/01.* Geoscience Australia, Canberra, Australia, 2005.
100. NORSAR, *NORSAR, Risk Analysis Software—The SELENA-RISe Open Risk Package. Kjeller, Norway. Available online:*

selena.sourceforge.net (accessed on 21 May 2020). 2020.
101. Molina-Palacios, S., et al., *A next-generation open-source tool for earthquake loss estimation.* 2017.
102. Molina, S., et al., *'SELENA v6.5–User and Technical Manual v2. 0.* NORSAR, Kjeller, Norway, 2015.
103. Lang, D.H. and F.V.G. Corea, *RISe: illustrating georeferenced data of seismic risk and loss assessment studies using Google Earth.* Earthquake Spectra, 2010. **26**(1): p. 295-307.
104. Applied Technology Council, *Improvement of nonlinear static seismic analysis procedures*. 2005: FEMA Region II.
105. Molina, S., D.H. Lang, and C.D. Lindholm, *SELENA–An open-source tool for seismic risk and loss assessment using a logic tree computation procedure.* Computers & Geosciences, 2010. **36**(3): p. 257-269.
106. European, S., *Eurocode 8: Design of structures for earthquake resistance—Part 1: General rules, seismic actions and rules for buildings.* European Standard NF EN, 1998. **1**: p. 2005.

107. Gruppo di Lavoro, M. *Indirizzi e criteri per la microzonazione sismica*. in *Conferenza delle Regioni e delle Provincie autonome. Dipartimento della protezione civile, Roma*. 2008.
108. Molina, S., et al., *Topographic amplification effects - towards their inclusion in ELE Studies (State-of-the-art report)*. 2015.
109. Robinson, D., T. Dhu, and P. Row, *EQRM: An open-source event-based earthquake risk modeling program.* AGU Fall Meeting Abstracts, 2007.
110. Robinson, D., G. Fulford, and T. Dhu, *EQRM: Geoscience Australia's Earthquake Risk Model: Technical Manual: Version 3.0*. 2005.
111. Patchett, A., et al., *Investigating earthquake risk models and uncertainty in probabilistic seismic risk analyses*. 2005.
112. Dhu, T., et al., *EVENT-BASED EARTHQUAKE RISK MODELLING*. 2008.
113. GEM, G.E.M., *GEM, Global Earthquake Model, Openquake Platform. Pavia, Italy. Available online: https://github.com/gem/oq-platform (accessed on 21 May 2020).* 2020.
114. GEM, *The OpenQuake-engine User Manual.* Global Earthquake Model (GEM) Technical Report, 2017. **201710**: p. 187.
115. Silva, V., et al., *Development of an open-source platform for calculating losses from earthquakes.* University of Aveiro, Portugal, 2014.
116. Chiou, B.-J. and R.R. Youngs, *An NGA model for the average horizontal component of peak ground motion and response spectra.* Earthquake spectra, 2008. **24**(1): p. 173-215.
117. QGIS Association, *QGIS Association, QGIS Geographic Information System, QGIS.org, Available Online at: < http://www.qgis.org> (Accessed on 12 December 2020).* 2020.
118. Abo El Ezz, A., M. Nollet, and M. Nastev, *Methodology for rapid assessment of seismic damage to buildings in Canadian settings.* Geological Survey of Canada, 2014.
119. Porter, K., *Cracking an Open Safe: More HAZUS Vulnerability Functions in Terms of Structure-Independent Intensity.* 2009. **25**(3): p. 607-618.
120. Nollet, M.-J., et al., *Earthquake magnitude and shaking intensity dependent fragility functions for rapid risk assessment of buildings.* Geosciences, 2018. **8**(1): p. 16.
121. Boore, D.M. and G.M. Atkinson, *Ground-motion prediction equations for the average horizontal component of PGA, PGV, and 5%-damped PSA at spectral periods between 0.01 s and 10.0 s.* Earthquake Spectra, 2008. **24**(1): p. 99-138.
122. ERN-AI, E., *ERN-Al, Capra tool, Available Online at: < http://ecapra.org/> (Accessed on 20 April 2020).* 2020.
123. Reinoso, E., et al., *AFTER 10 YEARS OF CAPRA*. 2018.
124. Bernal, G.A. and O.-D. Cardona. *Next generation CAPRA software*. in *Proceedings of the 16th European Conference on Earthquake Engineering*. 2018.
125. Aguilar Meléndez, A., et al., *Development and Validation of Software CRISIS to Perform Probabilistic Seismic Hazard Assessment with Emphasis on the Recent CRISIS2015.* Computación y Sistemas, 2017. **21**(1).
126. Crowley, H., et al., *GEM1 seismic risk report: part 1.* GEM Foundation, Pavia, Italy, GEM Technical Rep, 2010. **5**: p. 2010.
127. NCSA, N., *National Center for Supercomputing Applications (NCSA), Multi-hazard assessment Software, Available Online at: < http://ergo.ncsa.illinois.edu/> (Accessed on 20 April 2020).* 2020.
128. Elnashai, A.S., et al., *Overview and Applications of Maeviz-Hazturk 2007.* Journal of Earthquake Engineering, 2008. **12**(sup2): p. 100-108.
129. Elnashai, A.S. and J.F. Hajjar. *Mid-America Earthquake Center Program in Consequence-Based Seismic Risk Management*. in *8th US National Conference on Earthquake Engineering 2006*. 2006.
130. Karaman, H., M. Şahin, and A.S. Elnashai, *Earthquake Loss Assessment Features of Maeviz-Istanbul (Hazturk).* 2008. **12**(sup2): p. 175-186.
131. Schäfer, D., M. Pietsch, and H. Wenzel. *EQvis: a consequence based risk management software tool*. in *Proceedings of the 5th international conference on structural engineering, mechanics and computation, University of Cape Town*. 2013.
132. Pranantyo, I.R., M. Fadmastuti, and F. Chandra. *InaSAFE applications in disaster preparedness*. in *AIP Conference Proceedings*. 2015. AIP Publishing.
133. Vecere, A., R. Monteiro, and W.J. Ammann, *Comparative analysis of existing tools for assessment of post-earthquake short-term lodging needs.* Procedia engineering, 2016. **161**: p. 2217-2221.

134. Sengara, I.W., et al., *Empirical fatality model for Indonesia based on a Bayesian approach.* Geological Society, London, Special Publications, 2017. **441**(1): p. 179-187.
135. Jaiswal, K., D. Wald, and M. Hearne, *Estimating casualties for large worldwide earthquakes using an empirical approach.* US Geological Survey Open-File Report, 2009. **1136**: p. 78.
136. OOFIMS, *OOFIMS, Object-Oriented Framework for Infrastructure Modeling and Simulation. Available online: https://sites.google.com/a/uniroma1.it/oofims/download (accessed on 21 May 2020).* 2020.
137. Franchin, P. and F. Cavalieri, *Seismic vulnerability analysis of a complex interconnected civil infrastructure*, in *Handbook of seismic risk analysis and management of civil infrastructure systems*. 2013, Elsevier. p. 465-514e.
138. Cavalieri, F., P. Franchin, and P.E. Pinto, *Application to selected transportation and electric networks in Italy*, in *SYNER-G: Systemic Seismic Vulnerability and Risk Assessment of Complex Urban, Utility, Lifeline Systems and Critical Facilities*. 2014, Springer. p. 301-330.
139. Esposito, S., et al., *Simulation-based seismic risk assessment of gas distribution networks.* Computer-Aided Civil and Infrastructure Engineering, 2015. **30**(7): p. 508-523.
140. Crowley, H. and J.J. Bommer, *Modelling seismic hazard in earthquake loss models with spatially distributed exposure.* Bulletin of Earthquake Engineering, 2006. **4**(3): p. 249-273.
141. Silva, V., *Critical issues on probabilistic earthquake loss assessment.* Journal of Earthquake Engineering, 2018. **22**(9): p. 1683-1709.
142. Bommer, J., R. Spence, and R. Pinho. *Earthquake loss estimation models: time to open the black boxes*. in *First European Conference on Earthquake Engineering and Seismology. Geneva*. 2006.
143. Jaiswal, K.S., et al., *Estimating annualized earthquake losses for the conterminous United States.* Earthquake Spectra, 2015. **31**(S1): p. S221-S243.
144. Sousa, L., et al., *Epistemic Uncertainty in Hazard and Fragility Modelling for Earthquake Engineering*. 2018.
145. Silva, V., *Critical issues in earthquake scenario loss modeling.* Journal of Earthquake Engineering, 2016. **20**(8): p. 1322-1341.
146. Crowley, H., *Earthquake risk assessment: present shortcomings and future directions*, in *Perspectives on European earthquake engineering and seismology*. 2014, Springer, Cham. p. 515-532.
147. Braganza, S. and G.M. Atkinson, *A model for estimating amplification effects on seismic hazards and scenario ground motions in southern Ontario.* Canadian Journal of Civil Engineering, 2017. **44**(6): p. 441-451.
148. Pitilakis, K., et al., *Towards the revision of EC8: proposal for an alternative site classification scheme and associated intensity dependent spectral amplification factors.* Soil Dynamics and Earthquake Engineering, 2019. **126**: p. 105137.
149. Molnar, S., et al., *Overview of local site effects and seismic microzonation mapping in Metropolitan Vancouver, British Columbia, Canada.* Engineering Geology, 2020. **270**: p. 105568.
150. Wibowo, A., et al., *InaSAFE: Preparing Communities to Be a Step Ahead*. 2014. p. 172-176.
151. Kalakonas, P., et al., *Exploring the impact of epistemic uncertainty on a regional probabilistic seismic risk assessment model.* Natural Hazards, 2020. **104**(1): p. 997-1020.
152. Yilmaz, C., V. Silva, and G. Weatherill, *Probabilistic framework for regional loss assessment due to earthquake-induced liquefaction including epistemic uncertainty.* Soil Dynamics and Earthquake Engineering, 2021. **141**: p. 106493.
153. Talukder, M.K. and L. Chouinard, *Probabilistic methods for the estimation of seismic F a and F v maps—application to Montreal.* Bulletin of Earthquake Engineering, 2016. **14**(2): p. 345-372.
154. Rosset, P., M. Bour-Belvaux, and L. Chouinard, *Microzonation models for Montreal with respect to VS 30.* Bulletin of Earthquake Engineering, 2015. **13**(8): p. 2225-2239.
155. Nastev, M., et al., *Regional VS30 model for the St. Lawrence Lowlands, Eastern Canada.* Georisk: Assessment and Management of Risk for Engineered Systems and Geohazards, 2016. **10**(3): p. 200-212.
156. Motazedian, D., et al., *Seismic site period studies for nonlinear soil in the city of Ottawa, Canada.* Soil Dynamics and Earthquake Engineering, 2020. **136**: p. 106205.
157. Bazzurro, P. and C.A. Cornell, *Ground-motion amplification in nonlinear soil sites with uncertain properties.* Bulletin of the Seismological Society of America, 2004. **94**(6): p. 2090-2109.
158. Toro, G., *Probabilistic models of site velocity profiles for generic and site-specific ground-motion amplification studies.* Technical Rep, 1995. **779574**.

159. Sun, Q., X. Guo, and D. Dias, *Evaluation of the seismic site response in randomized velocity profiles using a statistical model with Monte Carlo simulations.* Computers and Geotechnics, 2020. **120**: p. 103442.
160. Salsabili, M., et al., *3D Probabilistic Modelling and Uncertainty Analysis of Glacial and Post-Glacial Deposits of the City of Saguenay, Canada.* Geosciences, 2021. **11**(5): p. 204.
161. Salsabili, M., et al., *Development of empirical CPTu-Vs correlations for post-glacial sediments in Southern Quebec, Canada, in consideration of soil type and geological setting.* Soil Dynamics and Earthquake Engineering, 2022. **154**: p. 107131.
162. Rathje, E.M., A.R. Kottke, and W.L. Trent, *Influence of input motion and site property variabilities on seismic site response analysis.* Journal of geotechnical and geoenvironmental engineering, 2010. **136**(4): p. 607-619.
163. Motazedian, D., et al., *Development of a VS30 (NEHRP) map for the city of Ottawa, Ontario, Canada.* Canadian Geotechnical Journal, 2011. **48**(3): p. 458-472.
164. Virtanen, P., et al., *SciPy 1.0: fundamental algorithms for scientific computing in Python.* Nature methods, 2020. **17**(3): p. 261-272.
165. Law, A.M. and W.D. Kelton, *Simulation modeling and analysis*. Vol. 3. 2000: McGraw-Hill New York.
166. NRCan. *Earthquake zones in Eastern Canada*. 2021 [cited 2022 15/12/2022]; Available from: https://www.seismescanada.rncan.gc.ca/zones/eastcan-en.php#CSZ.
167. Somerville, P.G., et al., *The 25 November 1988 Saguenay, Quebec, earthquake: source parameters and the attenuation of strong ground motion.* Bulletin of the Seismological Society of America, 1990. **80**(5): p. 1118-1143.
168. Globensky, Y., *Géologie des Basses-Terres du Saint-Laurent, Quebec*. 1987, Ministère des richesses naturelles du Quebec.
169. Walter, J., et al., *Characterization of general and singular features of major aquifer systems in the Saguenay-Lac-Saint-Jean region.* Canadian Water Resources Journal/Revue canadienne des ressources hydriques, 2018. **43**(2): p. 75-91.
170. Daigneault, R.-A., et al., *Rapport Final sur les Travaux de Cartographie des Formations Superficielles Réalisés dans le Territoire Municipalisé du Saguenay-Lac-Saint-Jean*. 2011, Ministère des Ressources naturelles et de la Faune du Québec: Quebec City, QC, Canada.
171. CERM-PACES, *Résultat du Programme d'Acquisition de Connaissances sur les Eaux Souterraines de la Région Saguenay-Lac-Saint-Jean. Chicoutimi: Centre d'Études sur les Ressources Minérales*. 2013, Université du Québec à Chicoutimi.
172. Ghazal, T., E. Elkassas, and M.I. El-Masry, *Conductive Cables Vibrations Effect On Lattice Steel Transmission Towers.* Journal of Steel Structures and Construction 2019. **5**(151): p. 7.
173. Crowley, H., et al., *Development of a displacement-based method for earthquake loss assessment.* European School for Advanced Studies in Reduction of Seismic Risk, Pavia, Research Report No. ROSE-2006, 2006. **1**.
174. Tian, L., X. Gai, and B. Qu, *Shake table tests of steel towers supporting extremely long-span electricity transmission lines under spatially correlated ground motions.* Engineering Structures, 2017. **132**: p. 791-807.
175. Kolaj, M., et al. *Ground-motion models for the 6th Generation Seismic Hazard Model of Canada*. in *12th Canadian Conference on Earthquake Engineering*. 2019.
176. Vahid Hosseinpour, et al. *A Monte-Carlo based Vs30 microzonation map for*

Saguenay, QC. in *8th Canadian Conference on Geotechnique and Natural Hazards*. 2022. Quebec City, Canada: Canadian Geotechnical Society.
177. Pan, H., et al., *Sensitivities of the seismic response and fragility estimate of a transmission tower to structural and ground motion uncertainties.* Journal of Constructional Steel Research, 2020. **167**: p. 105941.
178. Kolaj, M., J. Adams, and S. Halchuk. *The 6th generation seismic hazard model of Canada*. in *17th World Conference on Earthquake Engineering, Sendai, Japan, Paper 1c-0028*. 2020.

PUBLICATIONS

JOURNAL ARTICLES

Seismic loss estimation software: A comprehensive review of risk assessment steps, software development and limitations. *Engineering Structures*, 232, 111866, https://doi.org/10.1016/j.engstruct.2021.111866

Development of a probabilistic seismic microzonation software considering geological and geotechnical uncertainties, *Georisk* (Accepted with revision)

Development of a damage simulator for probabilistic assessment of seismic vulnerability of electrical installation**,** *Engineering Structures*, (Submitted)

CONFERENCE PAPERS

A Monte-Carlo based $Vs30$ microzonation map for Saguenay, QC, *Geohazards 8 Conference*, June 2022, Quebec City, Canada

A comprehensive review of seismic hazard and loss estimation software, *GeoCalgary Conference*, October 2022, Calgary, Canada

A Monte-Carlo based microzonation model for application in seismic hazard studies, *8th international conference on earthquake geotechnical engineering,* May 2024, Osaka, Japan (Accepted)

APPINDEX: GUIDE TO USE THE CODE

1.REQUIREMENTS:

1.1.Install Python:

Downlaod the latest version of Python for different OS using link below:

https://www.python.org/downloads/

Installing Python on Windows:

1. **Download Python:**
    - Visit the official Python website at python.org.
    - Click on the "Downloads" tab.
    - Choose the latest version of Python (it's recommended to use the latest stable version) for Windows.
    - Download the executable installer (**.exe** file).
2. **Run the Installer:**
    - Locate the downloaded installer and double-click on it to run.
    - Check the box that says "Add Python X.X to PATH" during installation. This will make it easier to run Python from the command line.
3. **Install Python:**
    - Click "Install Now" and the installer will install Python on your system.
4. **Verify Installation:**
    - Open a command prompt and type **python --version** or **python -V** to check if Python is installed successfully.
    - You can also run **python** to enter the Python interactive shell.

Installing Python on macOS:

1. **Download Python:**
    - Visit the official Python website at python.org.
    - Click on the "Downloads" tab.
    - Choose the latest version of Python (it's recommended to use the latest stable version) for macOS.
    - Download the macOS installer package (**.pkg** file).
2. **Run the Installer:**
    - Locate the downloaded installer and double-click on it to run.
    - Follow the on-screen instructions. Make sure to check the box that says "Add Python X.X to PATH" during installation.
3. **Install Python:**
    - Click "Install Now" and the installer will install Python on your system.
4. **Verify Installation:**
    - Open a terminal and type **python3 --version** or **python3 -V** to check if Python is installed successfully.
    - You can also run **python3** to enter the Python interactive shell.

1.2.Libraries used for development:

1. **NumPy:**
    - **Description:** NumPy is a powerful library for numerical computing in Python. It provides support for large, multi-dimensional arrays and matrices, along with mathematical functions to operate on these arrays.
    - **Download Link:** NumPy
    - **Documentation:** NumPy Documentation
2. **Pandas:**
    - **Description:** Pandas is a data manipulation and analysis library. It provides easy-to-use data structures like Series and DataFrame for efficient data manipulation, cleaning, and analysis in Python.
    - **Download Link:** Pandas
    - **Documentation:** Pandas Documentation
3. **GeoPandas:**
    - **Description:** GeoPandas extends the data manipulation capabilities of Pandas to allow spatial operations on geometric types. It simplifies working with geospatial data by integrating with Shapely and Fiona libraries.
    - **Download Link:** GeoPandas
    - **Documentation:** GeoPandas Documentation
4. **Matplotlib:**
    - **Description:** Matplotlib is a 2D plotting library for Python. It enables the creation of static, animated, and interactive visualizations in Python. Matplotlib is often used in combination with NumPy for data visualization.
    - **Download Link:** Matplotlib
    - **Documentation:** Matplotlib Documentation
5. **ArcPy:**
    - **Description:** ArcPy is a Python site package that provides a useful and productive way to perform geographic data analysis, data conversion, data management, and map automation with ArcGIS software.
    - **Download Link:** ArcGIS
    - **Documentation:** ArcPy Documentation
6. **Shapely:**
    - **Description:** Shapely is a Python library for manipulation and analysis of geometric objects. It is often used in conjunction with GeoPandas and other geospatial libraries to handle geometric operations.

- **Download Link:** Shapely
- **Documentation:** Shapely Documentation

7. SciPy:

- **Description:** SciPy is an open-source library used for scientific and technical computing. It builds on NumPy and provides modules for optimization, integration, interpolation, eigenvalue problems, signal and image processing, and more.
- **Download Link:** SciPy
- **Documentation:** SciPy Documentation

2.Site parameters analysis module:

2.1.Distribution fitting:

1. Open *distribution fitting-with_std.py* file using Python.
2. Load the measured Vs data by giving the path of your data to following part of the code:
   ```
   df = pd.read_csv("C:/Desktop/Vs-data (1)/SCPTu-UQAC-MTQ-Total.csv")
   ```
   The csv or excel file should contain data of with the label of Depth (m) and Vs (m/s).
3. Run the code to obtain best fitted distrubtions and their parameters to provided data.
4. Run the code for each soil type separately if want to have distribution for each soil type.

2.2.Deterministic site parameters:

Inorder to generate deterministic Vs30 map follow following steps:

1. Open *Vs30 -Conventional measured regression.py* file using Python.
2. Load 3D geological block model file using following part of the code:
   ```
   df_sgc=pd.read_csv('c/DataforDevelop/Damage_Simulator/blk_sgc_final2.csv')
   ```
   Replace the path of your geological model file with the path showed in the code.
3. Provide your Vs-depth regression formula in following section of the code:

```
group.loc[group['Zone'] == 2,'vs_gravel'] = (162.531)*((group['Z1'])**0.161)
group.loc[group['Zone'] == 1,'vs_sand'] = (162.531)*((group['Z1'])**0.161)
group.loc[group['Zone'] == 0,'vs_clay'] = (109.709*(group['Z1'])**0.246)
group.loc[group['Zone'] == 4,'vs_till'] = 580
```

4. Run code to generate Vs_{30} map.

Inorder to generate deterministic T_0 map follow following steps:

1. Open *T0 -Conventional measured regression.py* file using Python.

2. Load 3D geological block model file using following part of the code:
   `df_sgc=pd.read_csv('c/DataforDevelop/Damage_Simulator/blk_sgc_final2.csv')`
   Replace the path of your geological model file with the path showed in the code.

3. Provide your Vs-depth regression formula in following section of the code:

```
group.loc[group['Zone'] == 2,'vs_gravel'] = (162.531)*((group['Z1'])**0.161)
group.loc[group['Zone'] == 1,'vs_sand'] = (162.531)*((group['Z1'])**0.161)
group.loc[group['Zone'] == 0,'vs_clay'] = (109.709*(group['Z1'])**0.246)
group.loc[group['Zone'] == 4,'vs_till'] = 580
```

4. Run code to generate T_0 map.

2.3.Probablisitic site parameters:

Inorder to generate MC-based Vs30 map follow following steps:

1. Open *Vs30-mont carlo based-edited for sigma.py* file using Python.

2. Load 3D geological block model file using following part of the code:
   `df_sgc=pd.read_csv('c/DataforDevelop/Damage_Simulator/blk_sgc_final2.csv')`
   Replace the path of your geological model file with the path showed in the code.

3. Determine the MC realizations you want in following parameter:
   `mont_size = 1000`

4. Provide distribution parameters from distribution fitting code in following section of the code:

```
#Vs for 0 < Z < 2
     try:
         group.at[group.loc[((group['Zone'] == 1) | (group['Zone'] == 2)) &
( (group['Z1'] == 1.0))].index[0], 'Vs'] = norm.rvs(167.29,
51.14,size=(1,mont_size))
     except:
          try:
              group.at[group.loc[( group['Zone'] == 0) & ( (group['Z1'] ==
1.0))].index[0], 'Vs'] = invgauss.rvs(1.1261363076163105, 86.13499308802449,
31.936641403334185,size=(1,mont_size))
          except:
               try:
                    group.at[group.loc[( group['Zone'] == 4) & ( (group['Z1']
== 1.0))].index[0], 'Vs'] = norm.rvs(580, 174,size=(1,mont_size))
               except:
                     pass
```

Repeat this process for all depths.

5. Run code to generate probablistic Vs_{30} map and its uncertainty.

Inorder to generate MC-based T_0 map follow following steps:

1. Open *T0-mont carlo based-edited for sigma.py* file using Python.

2. Load 3D geological block model file using following part of the code:
   ```
   df_sgc=pd.read_csv('c/DataforDevelop/Damage_Simulator/blk_sgc_final2.csv')
   ```
   Replace the path of your geological model file with the path showed in the code.

3. Determine the MC realizations you want in following parameter:
   ```
   mont_size = 1000
   ```

4. Provide distribution parameters from distribution fitting code in following section of the code:

```
#Vs for 0 m < Z < 2 m
     try:
         group.at[group.loc[((group['Zone'] == 1) | (group['Zone'] == 2)) &
( (group['Z1'] == 1.0))].index[0], 'Vs'] = norm.rvs(167.29,
51.14,size=(1,mont_size))
     except:
          try:
              group.at[group.loc[( group['Zone'] == 0) & ( (group['Z1'] ==
1.0))].index[0], 'Vs'] = invgauss.rvs(1.1261363076163105, 86.13499308802449,
31.936641403334185,size=(1,mont_size))
          except:
               try:
                   group.at[group.loc[( group['Zone'] == 4) & ( (group['Z1']
== 1.0))].index[0], 'Vs'] = norm.rvs(580, 174,size=(1,mont_size))
               except:
                     pass
```

Repeat this process for all depths.

5. Run code to generate probablistic T_0 map and its uncertainty.

3.Hazard analysis module:

3.1.User defined scenario analysis:

1. Open *Deterministic hazard.py* file using Python.
2. Define the path of the GMPE:

```
gmpe_1= pd.read_excel("C:/Users/ Desktop/Testhazard/NGA13-w-f.xlsx")
gmpe_2=pd.read_excel("C:/Users/ Desktop/Testhazard/AA13-w-f.xlsx")
```

3. Enter Magnitude and coordinate of epiceter in excel file (M= magnitude, X-epi and Y-epi)

4. Define path of the Vs30 value generated in previous step:

```
dff=pd.read_csv('c:/Users//Desktop/Testhazard/Vs30_Mp_Measurerd_Vsdata_Till=580-2022-03-03.csv')
```

5. Select parameter of interest (e.g. PGA, Sa 1.0, …)

6. Define your study area shape files in following part of the code:

```
saguenay_map=gpd.read_file('C:/Users/GISSaguenay/Depots_de_surface_saguenay.shp')
ville_saguenay_map=gpd.read_file('C:/Users/ /GIS-Saguenay/ville_du_saguenay.shp')
hydro_saguenay_map=gpd.read_file('C:/Users/ /GIS-Saguenay/hydro/hydro.shp')
```

7. Run code to generate deterministic hazard maps

3.2.Probablisitic hazard analysis (2% in 50 years):

1. Open *2%maps based on NBCC2020.py* file using Python.
2. Define the path of the GMPE:

```
gmpe_1=pd.read_excel("C:/Users/Desktop/Testhazard/probmiro.xlsx")
```

3. Define path of the Vs30 value generated in previous step:

```
dff=pd.read_csv('c:/Users//Desktop/Testhazard/Vs30_Mp_Measurerd_Vsdata_Till=580-2022-03-03.csv')
```

4. Select parameter of interest (e.g. PGA, Sa 1.0).

5. Define your study area shape files in following part of the code:

```
saguenay_map=gpd.read_file('C:/Users/GISSaguenay/Depots_de_surface_saguenay.
shp')
ville_saguenay_map=gpd.read_file('C:/Users/ /GIS-Saguenay/
ville_du_saguenay.shp')
hydro_saguenay_map=gpd.read_file('C:/Users/ /GIS-Saguenay/hydro/hydro.shp')
```

6. Run code to generate 2% maps.

3.3.MC-based hazard analysis:

1. Open *Mc-based- hazard.py* file using Python.
2. Define the path of the GMPE:

```
gmpe_1= pd.read_excel("C:/Users/ Desktop/Testhazard/NGA13-w-f.xlsx")
gmpe_2=pd.read_excel("C:/Users/ Desktop/Testhazard/AA13-w-f.xlsx")
```

3. Enter Magnitude and coordinate of epiceter in excel file (M= magnitude, X-epi and Y-epi).

4. Define path of the Vs30 value generated in previous step:

```
dff=pd.read_csv('c:/Users//Desktop/Testhazard/Vs30_Mp_Measurerd_Vsdata_Ti
ll=580-2022-03-03.csv')
```

5. Select parameter of interest (e.g. PGA, Sa 1.0, …).
6. Enter number of MC realizations and STD of hazard parameter:

```
mont_size = 1000
mont_STD_for_HazParam = 0.6
```

7. Define your study area shape files in following part of the code:

```
saguenay_map=gpd.read_file('C:/Users/GISSaguenay/Depots_de_surface_saguenay.
shp')
ville_saguenay_map=gpd.read_file('C:/Users/ /GIS-Saguenay/
ville_du_saguenay.shp')
hydro_saguenay_map=gpd.read_file('C:/Users/ /GIS-Saguenay/hydro/hydro.shp')
```

8. Run code to generate MC based probablistic hazard maps and STD of hazard parameter**.**

4.Damage analysis:

4.1.Deterministic damage analysis:

1. Open *Deterministic-damage.py* file using Python.
2. Define the path of the GMPE:

```
gmpe_1= pd.read_excel("C:/Users/ Desktop/Testhazard/NGA13-w-f.xlsx")
gmpe_2=pd.read_excel("C:/Users/ Desktop/Testhazard/AA13-w-f.xlsx")
```

3. Enter Magnitude and coordinate of epiceter in excel file (M= magnitude, X-epi and Y-epi)
4. Enter the coordinate of installations in excel file.
5. Define fragility parameters in excel fil for each type of the installations
   Tower type = 1 , High voltage substation type = 2 and Low voltage substation type = 3.
6. Select parameter of interest for each type of installations (PGA for substations, Sa 1.0 for towers).

7. Define path of the Vs30 value generated in previous step:

```
dff=pd.read_csv('c:/Users//Desktop/Testhazard/Vs30_Mp_Measurerd_Vsdata_Till=580-2022-03-03.csv')
```

8. Define your study area shape files in following part of the code:

```
saguenay_map=gpd.read_file('C:/Users/GISSaguenay/Depots_de_surface_saguenay.shp')
ville_saguenay_map=gpd.read_file('C:/Users/ /GIS-Saguenay/ville_du_saguenay.shp')
hydro_saguenay_map=gpd.read_file('C:/Users/ /GIS-Saguenay/hydro/hydro.shp')
```

9. Run code to generate deterministic fragility analysis and damage results

4.2.MC-based damage analysis:

1. Open *MC-based-damage.py* file using Python.
2. Define the path of the GMPE:

```
gmpe_1= pd.read_excel("C:/Users/ Desktop/Testhazard/NGA13-w-f.xlsx")
gmpe_2=pd.read_excel("C:/Users/ Desktop/Testhazard/AA13-w-f.xlsx")
```

3. Enter Magnitude and coordinate of epiceter in excel file (M= magnitude, X-epi and Y-epi).
4. Enter the coordinate of installations in excel file.
5. Define fragility parameters in excel fil for each type of the installations
   Tower type = 1 , High voltage substation type = 2 and Low voltage substation type = 3.
6. Select parameter of interest for each type of installations (PGA for substations, Sa 1.0 for towers).
7. Enter MC realizations number:
   `mont_size = 1000`

8. Define path of the Vs30 value generated in previous step:

```
dff=pd.read_csv('c:/Users//Desktop/Testhazard/Vs30_Mp_Measurerd_Vsdata_Till=580-2022-03-03.csv')
```

9. Define your study area shape files in following part of the code:

```
saguenay_map=gpd.read_file('C:/Users/GISSaguenay/Depots_de_surface_saguenay.
shp')
ville_saguenay_map=gpd.read_file('C:/Users/ /GIS-Saguenay/
ville_du_saguenay.shp')
hydro_saguenay_map=gpd.read_file('C:/Users/ /GIS-Saguenay/hydro/hydro.shp')
```

10. Run code to generate fragility analysis and damage results and STD of damage states and damage.